# Pathological and cognitive alterations in mouse models of traumatic brain injury and hypoperfusion

**Aisling Spain BA MSc**

**Doctor of Philosophy**
**The University of Edinburgh**
**2010**

# Table of Contents

# Acknowledgements

Firstly, I would like to thank my supervisors, Dr. Jill Fowler and Dr. Karen Horsburgh, for all their guidance, advice and support in the last 3 years. I've also been very fortunate in being able to call on Dr. Stephanie Daumas, Dr. Emma Wood and Prof. Jim McCulloch for their assistance and expertise.

During my Ph.D. I've been extremely lucky to work with a great group of people in the Horsburgh and McCulloch labs. There is no one in the group who I couldn't turn to for help, advice or good laugh when I needed. I have to give a special mention to Robin Coltman, my partner in crime in Ph.D. studentship, for keeping things in perspective and knowing when the best cure is the liberal application of alcohol.

I'd also like to thank the BRR staff for technical support and a bit of craic during a long day's behavioural testing.

I also want to thank my parents, grandparents and sisters for their support and for putting up having to tell people that, yes I am still at university 9 years later. Finally I have to thank all my friends in both Ireland and Scotland, particularly Maura for fielding late-night phone calls and braving the cold to pay visits.

# Declaration

I declare that this thesis comprises my own original work and has not been submitted previously for any degree. The work comprising this thesis was carried out by myself, except where acknowledged in the text. All sources of data and information have been specifically referenced.

Aisling Spain

# List of Figures

# List of Tables

# Abstract

Intact white matter is critical for normal cognitive function. In traumatic brain injury (TBI), chronic cerebral hypoperfusion and Alzheimer's disease (AD) damage to white matter is associated with cognitive impairment. However, these conditions are associated with grey matter damage or with other pathological states and the contribution of white matter damage in isolation to their pathogenesis is not known. Furthermore, TBI is a risk factor for AD and cerebral hypoperfusion is an early feature of AD. It is hypothesised that white matter damage following TBI or chronic cerebral hypoperfusion will be associated with cognitive deficits and that white matter changes after injury contribute to AD pathogenesis. To investigate this, this thesis examined the contribution of white matter damage to cognitive deficits after TBI and chronic cerebral hypoperfusion and furthermore, investigated the role of white matter damage in the relationship between TBI and AD. Three studies addressed these aims. In the first, mild TBI was induced in wild-type mice and the effects on axons, myelin and neuronal cell bodies examined at time points from 4 hours to 6 weeks after injury. Spatial reference learning and memory was tested at 3 and 6 weeks after injury. Injured mice showed axonal damage in the cingulum, close to the injury site in the hours after injury and at 6 weeks, damage in the thalamus and external capsule were apparent. Injured and sham animals had comparable levels of neuronal damage and no change was observed in myelin. Injured animals showed impaired spatial reference learning at 3 weeks after injury, demonstrating that selective axonal damage is sufficient to impair cognition. In the second study mild

TBI was induced in a transgenic mouse model of AD and the effects on white matter pathology and AD-related proteins examined 24 hours after injury. There was a significant increase in axonal damage in the cingulum and external capsule and parallel accumulations of amyloid were observed in these regions. There were no changes in tau or in overall levels of AD-related proteins. This suggests that axonal damage may have a role in mediating the link between TBI and AD. The third study used a model of chronic cerebral hypoperfusion in wild type mice and investigated white matter changes after one and two months of hypoperfusion as well as a comprehensive assessment of learning and memory. Chronic cerebral hypoperfusion resulted in diffuse myelin damage in the absence of ischaemic neuronal damage at both 1 and 2 months after induction of hypoperfusion. Hypoperfused animals also showed minimal axonal damage and microglial activation. Cognitive testing revealed a selective impairment in spatial working memory but not spatial reference or episodic memory in hypoperfused animals, showing that modest reductions in blood flow have effects on white matter sufficient to cause cognitive impairment. These results demonstrate that selective damage to white matter components can have a long-term impact on cognitive function as well as on the development of AD. This suggests that minimisation of axonal damage after TBI is a target for reducing subsequent risk of AD and that repair or prevention of white matter damage is a promising strategy for rescuing cognitive function in individuals who have experienced mild TBI or chronic cerebral hypoperfusion.

# List of Abbreviations

| | |
|---|---|
| 3xTg | Mice transgenic for human $APP_{Swe}$, $PS1_{M146V}$ and $tau_{P301L}$ |
| Aβ | Amyloid β |
| AD | Alzheimer's disease |
| AICD | APP intracellular domain |
| APP | Amyloid precursor protein |
| CBF | Cerebral blood flow |
| CCI | Controlled cortical impact |
| CT | Computed tomography |
| Cdk5 | Cyclin dependent kinase 5 |
| DTI | Diffusion tensor imaging |
| EDTA | Ethylenediaminetetraacetic acid |
| EGTA | Ethylene glycol tetraacetic acid |
| FJC | Fluorojade C |
| FPI | Fluid percussion injury |
| GAPDH | Glyceraldehyde 3-phosphate dehydrogenase |
| GSK-3β | Glycogen synthase kinase 3β |
| H&E | Haematoxilyn and eosin |
| IL-1α | Interleukin-1α |
| IL-1β | Interleukin-1β |
| IL-6 | Interleukin-6 |
| MAG | Myelin associated glycoprotein |
| MBP | Myelin basic protein |
| MCI | Mild cognitive impairment |
| MES | 2-(N-morpholino)ethanesulfonic acid |
| MRI | Magnetic resonance imaging |
| PBS | Phosphate buffered saline |
| PVDF | Polyvinylidene fluoride |
| ROD | Relative optical density |
| sAPP | Soluble extracellular APP domain |

| | |
|---|---|
| SDS | Sodium dodecyl sulfate |
| SDS-PAGE | Sodium dodecyl sulfate polyacrylamide gel electrophoresis |
| SPECT | Single photon emission computed tomography |
| TBI | Traumatic brain injury |
| TNFα | Tumor necrosis factor-α |

# 1 Introduction

## 1.1 White matter

Alterations in white matter are implicated in the development of cognitive deficits in pathological states. The role of white matter in maintaining communication between brain regions underlies its importance in normal cognitive function. Damage to any or all of the multiple components that comprise white matter may disrupt communication between grey matter regions, resulting ultimately in impairments in cognition and behaviour. Throughout this thesis the role of white matter changes in response to insult and their effect on cognition will be a recurring theme.

### *1.1.1 Components of white matter*

White matter comprises myelinated axons and glial cells, including astrocytes, microglia and the oligodendrocytes which produce the myelin sheath and blood vessels (Figure 1.1). Myelination of axons allows for rapid propagation of action potentials along the axons' length by means of saltatory conduction. The multiple layers of myelin enclosing sections of axons are formed in the central nervous system by oligodendrocyte processes wrapping around the axon (Bunge et al., 1961). Not only do these layers of myelin increase the efficiency of signal conduction along axons but they also protect axons from insults such as nitric oxide released by

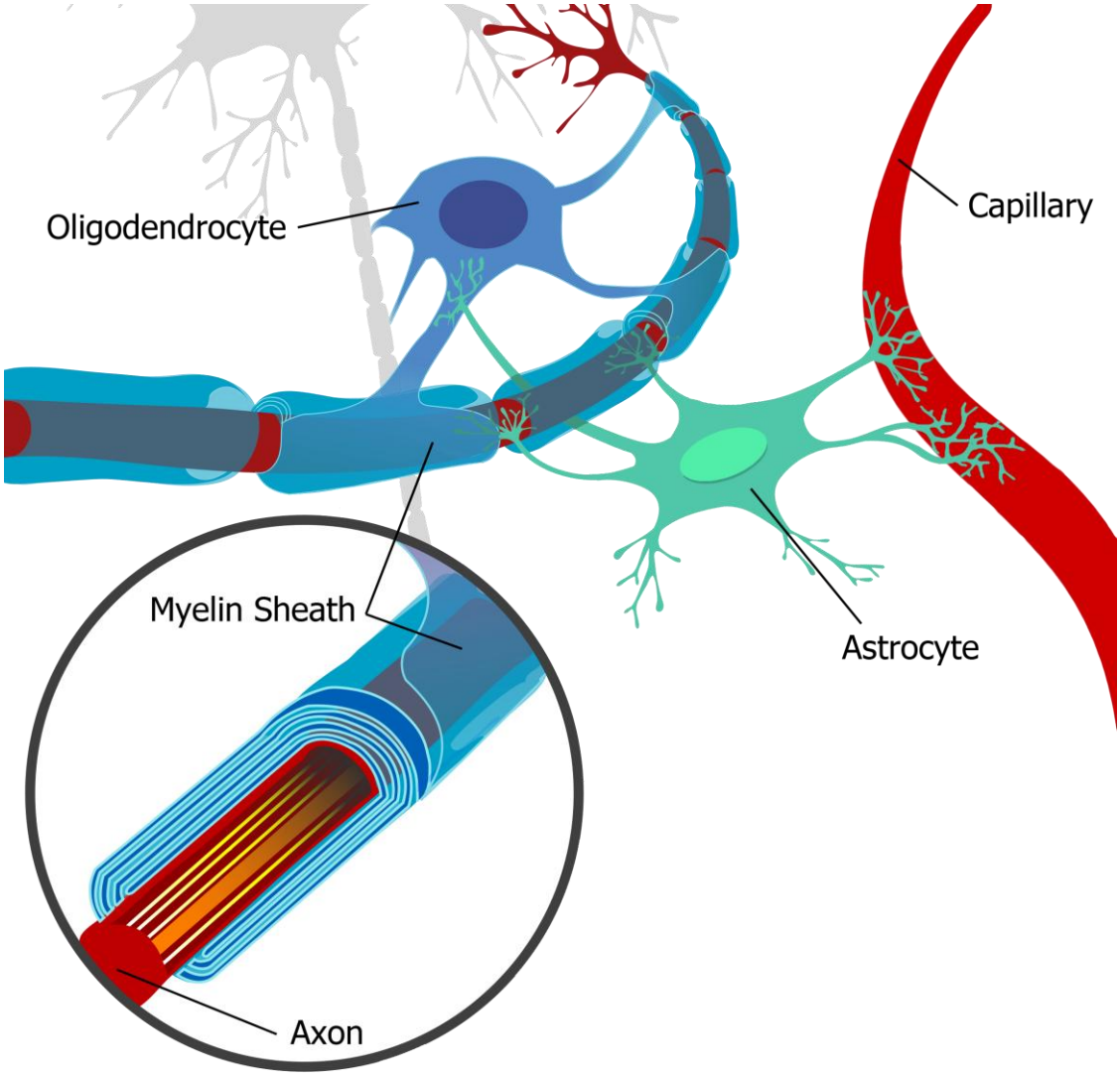


**Figure 1.1: Components of white matter**

White matter is comprised of axons, their myelin sheaths, glial cells and capillaries. The myelin sheath is formed by oligodendrocyte processes which wrap around the axon multiple times. Each oligodendrocyte can form multiple segments of myelin. Astrocytes have points of contact with oligodendrocytes, axons and the blood brain barrier and may aid in transfer of metabolites to and from axons and oligodendrocytes as well as the transfer of glucose from capillaries to oligodendrocytes (Nave, 2010).

activated microglia under inflammatory conditions and may also provide metabolic support (Nave, 2010). Astrocytes provide trophic support for oligodendrocytes, by linking oligodendrocytes to capillaries (Paspalas and Papadopoulos, 1998) as well as stimulating the formation of the myelin sheath (Franklin and ffrench-Constant, 2008). Myelin sheath formation is a prolonged process, continuing in some regions to the sixth decade of life (Benes et al., 1994) and generally proceeding from the most caudal to the most rostral regions of the brain (Baumann and Pham-Dinh, 2001).

### *1.1.2 Role of white matter in cognition*

White matter structure has been observed to vary in conjunction with variations in normal cognitive abilities (Fields, 2008; Schmithorst et al., 2005). However the importance of white matter in cognition is perhaps most obvious in instances where changes in cognitive performance are associated with damage to white matter. For instance, in both Alzheimer's disease (AD) and vascular dementia deficits in cognitive ability have been demonstrated to correlate with lesions of white matter (Gootjes et al., 2004) and even in normal aging decreases in cognitive ability are associated with disruption of white matter tracts (O'Sullivan et al., 2001). Disruption of white matter tracts may affect cognition by outright disconnection of regions crucial for normal function (e.g. Salat et al., 2010) although the complete severance of connections to or from a particular region is an extreme example. In less severe cases, changes in signal conduction velocity due to myelin disruption or interruption of conduction along individual axons due to damage can disturb the synchronous

firing necessary for the successful function of networks of regions involved in cognitive processes (Fell et al., 2001).

## 1.2 Traumatic brain injury

### *1.2.1 Traumatic brain injury*

Approximately 1 million people present each year at U.K. accident and emergency departments with a traumatic brain injury (TBI) (Headway, 2010). It is the most common cause of death and disability in the under 45 age group and can lead to persistent long-term cognitive impairment (Bruns and Hauser, 2003; Masel and Dewitt, 2010). Typically, Glasgow Coma Scale (Teasdale and Jennett, 1974) score is used to categorise injuries as mild, moderate and severe; with a score of 13 to 15 being considered mild, 9 to 12 moderate and less than 9 defined as severe (Bruns and Hauser, 2003). The score is determined by measuring patients' motor responsiveness, verbal performance and eye opening (Teasdale and Jennett, 1974). Mild injury is estimated to account for 80% of all TBI (Bruns and Hauser, 2003).

Injury mechanisms in TBI fall into primary and secondary categories. Primary mechanisms of injury are those due to direct mechanical trauma and can be further subdivided into focal and diffuse injuries (Figure 1.2). Focal injuries involve local damage to specific regions of the brain due to causes such as contusions and lacerations following an impact. Diffuse injuries appear throughout the brain and are

not necessarily associated with an injury site and include diffuse axonal injury. Secondary damage has a delayed onset and occurs as a consequence of primary injury and induces excitotoxicity, oxidative stress, activation of inflammatory signalling, brain swelling and increased intracranial pressure and alterations in cerebral blood flow and metabolism leading to cell death by necrosis or apoptosis, or to damage to axons and exacerbation of primary injuries (Werner and Engelhard, 2007).

Large, primary focal lesions are frequently observed in moderate to severe injuries and involve extensive tissue damage and cell death in addition to diffuse injury (Maas et al., 2008). In cases of moderate to severe injury focal damage may be the most clinically significant pathology immediately after injury, unlike mild TBI, where diffuse injury, particularly to axons, may have a more important role (Sterr et al., 2006). Secondary damage after injury arises from a number of causes. These include the deleterious effects of some pro-inflammatory cytokines following injury (Morganti-Kossmann et al., 2007) and excessive release of glutamate following injury, leading to excitotoxic intracellular influx of $Ca^{2+}$ and subsequent damage to the neuronal cytoskeleton and membrane (Gennarelli, 1997). Cerebral blood flow may also be altered following injury, resulting in both hyper- and hypoperfusion (Martin et al., 1997).

This thesis will focus primarily on mild TBI, where evidence suggests that the long-term persistence of cognitive symptoms after injury is related to diffuse damage to white matter regions (Kraus et al., 2007; Niogi et al., 2008). The high incidence of

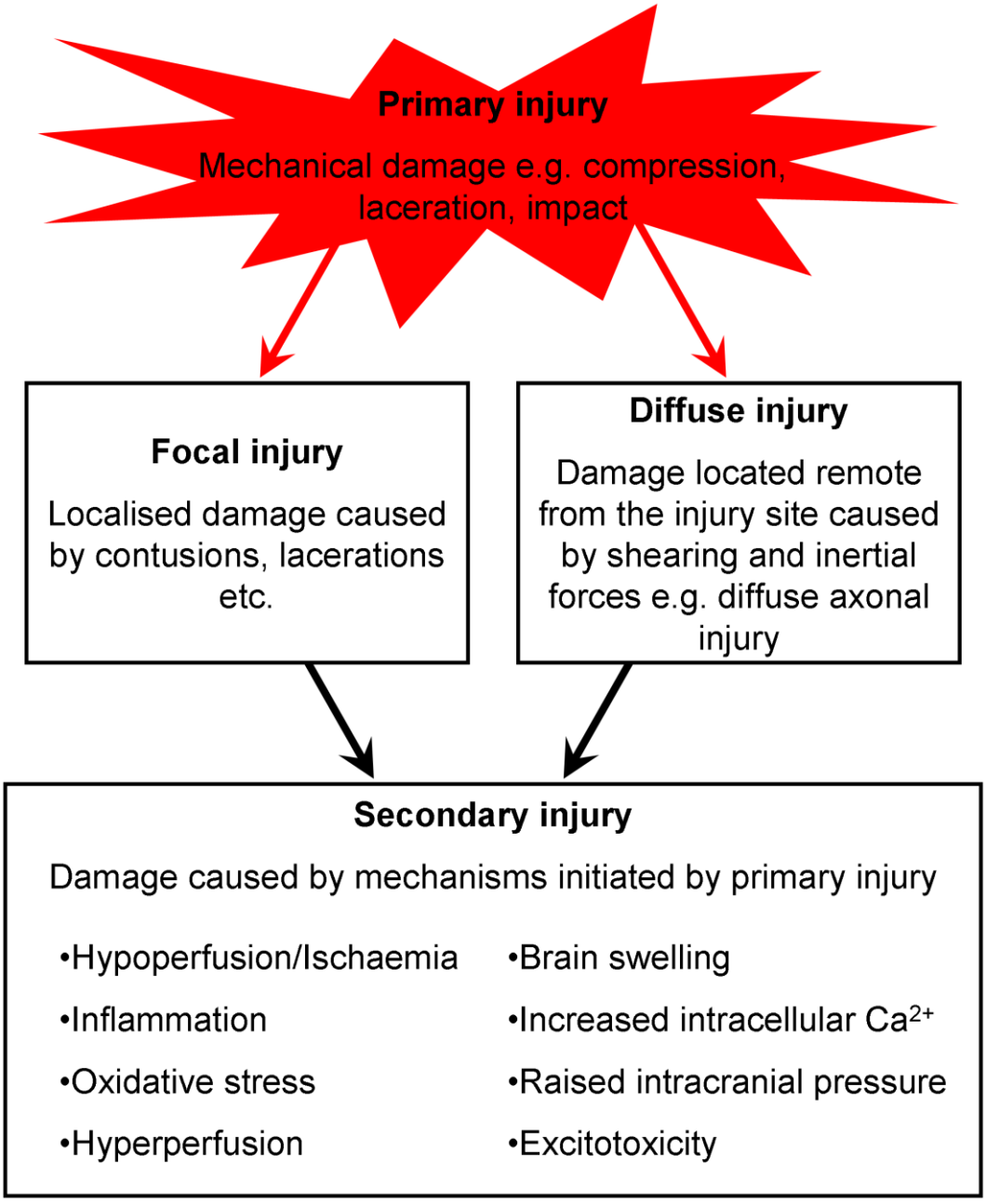


**Figure 1.2: Mechanisms and types of injury in traumatic brain injury** In TBI damage results from primary, mechanical causes which are an immediate result of the injury event as well as from secondary, delayed onset mechanisms initiated by primary injury events. Primary injury can be further subdivided into focal and diffuse injury types. Focal injuries have a restricted location, close to the site of the initial injury event, while diffuse injuries occur in locations remote from the injury site.

mild TBI combined with its low mortality rate (af Geijerstam and Britton, 2003) and sustained cognitive deficits after injury means that a substantial number of people live with a chronic impairment as the result of an apparently minor injury (Arciniegas et al., 2005).

### *1.2.2 White matter damage in mild traumatic brain injury*

Mild TBI may not always produce damage that is easily visualised by magnetic resonance imaging (MRI) or computed tomography (CT) scans as are normally used to identify structural changes after TBI (Inglese et al., 2005; Kraus et al., 2007) and the high survival rates for this level of injury mean that opportunities for studying the pathological consequences of mild TBI post-mortem are limited. The development of diffusion tensor imaging (DTI) MRI technique for imaging white matter (Basser, 1994) has proven useful in studying white matter changes after mild TBI. Changes in indices of white matter integrity are typically observed in a variety of regions and at time points ranging from days to years after injury (Inglese et al., 2005; Kraus et al., 2007; Messé et al., In press). Changes in white matter integrity also coexist with long-term deficits in short-term and working memory as well as attention (Kraus et al., 2007). Imaging studies are, however, limited by the difficulty in identifying which components of white matter are affected in mild TBI, meaning they are unsuitable for identifying cellular targets for clinical intervention.

### *1.2.3 Cerebral hypoperfusion after traumatic brain injury*

Cerebral hypoperfusion or a reduction in cerebral blood flow (CBF) is frequently observed secondary injury following TBI and is predictive of poor recovery following TBI (Overgaard and Tweed, 1983). A number of mechanisms can give rise to cerebral hypoperfusion: damage to cerebral blood vessels due to shearing forces during injury, failure of cerebrovascular autoregulation, alterations in levels of cholinergic neurotransmitters and increased vasoconstriction due to prostaglandins (Werner and Engelhard, 2007). Cerebral hypoperfusion also reduces the amount of oxygen and glucose being delivered to cells and results in cell death due to failures in ATP production followed by disruptions in ionic homeostasis and subsequent excitotoxicity. This is in addition to excitotoxic events caused by TBI itself, exacerbates the damage caused by this mechanism. Other secondary injuries that can be induced by severe hypoperfusion as well as by TBI include generation of reactive oxidative species and inflammation (Bramlett and Dietrich, 2004). As well as inducing reductions in CBF, excitotoxicity following TBI can cause increased metabolic demand in injured tissue which can increase the vulnerability of cells to ischaemic insult, meaning that ischaemic tissue damage may occur with smaller reductions in blood flow than in otherwise healthy tissue (Bramlett and Dietrich, 2004). Cerebral hypoperfusion may also have a role in long-term impairment after mild TBI, as suggested by reports of hypoperfusion in the frontal, pre-frontal, temporal cortices and sub-cortical structures detected 2 years after mild TBI in a group of patients with persistent cognitive deficits (Bonne, 2003). Reduced CBF has been observed in the hours following lateral FPI in rats (Yamakami and McIntosh,

1989;1991). Regional reductions in CBF have been found to persist up to 9 months after lateral FPI (Hayward et al., In press).

### *1.2.4 Models of traumatic brain injury*

Given the diversity of injury types in human TBI it is not surprising that there are a number of rodent models of TBI. Frequently used models include weight drop, controlled cortical impact (CCI) and fluid percussion injury (FPI) (Cernak, 2005; Morales et al., 2005 for review). In the CCI model the injury is produced by the impact of a pneumatic cylinder on the exposed, intact dura (Dixon et al., 1991; Smith et al., 1995). Progressive cell loss in the cortex, hippocampus and thalamus has been reported, along with damage to the afferent connections from these regions. This makes this technique suitable for modelling injury types with focal mechanical trauma to the brain. In the weight drop model a guided weight is dropped on to either the exposed skull or dura of the animal (Feeney et al., 1981; Tang et al., 1997a;b). A modified version of this technique called the impact acceleration model involves attachment of a metal plate to the skull to avoid skull fracture. There is the risk of a second, uncontrolled injury if the weight bounces on the skull after being dropped. Focal damage to the injury site can be modelled using this technique at severe injury levels (Feeney et al., 1981) and lower impact levels are capable of producing cell loss and diffuse axonal damage (Lewen et al., 1995; Tang et al., 1997b), while the impact acceleration version is useful for inducing selective diffuse axonal injury. In models of mild TBI, weight drop injury has been demonstrated to produce a learning deficit that persists to 90 days after injury in the absence of

structural changes visible using MRI (Zohar et al., 2003). Other studies modelling mild TBI have demonstrated learning and memory impairments up to 3 weeks after injury in conjunction with cortical and hippocampal cell loss (Tang et al., 1997a) but there has been a lack of investigation of white matter pathology following mild TBI in conjunction with behavioural assessment.

In FPI a fluid pulse applied to the intact dura through an opening in the skull produces the injury (McIntosh et al., 1989). There are two varieties of FPI which are distinguished by the location of the injury site. In midline FPI the injury site is located over the midline, whereas in the lateral model it is placed lateral to the midline between bregma and lambda. This difference in injury position results in less brainstem involvement and lower mortality rates than in the midline version of the model, making it more suitable for modelling mild injuries (McIntosh et al., 1989). Increased focal cortical cell loss after lateral FPI is associated with increasing injury severity and has been observed to progress up to 1 year after severe injury in conjunction with diffuse hippocampal and thalamic cell loss (Pierce et al., 1998). Diffuse axonal degeneration continuing after injury also occurs in a range of regions including the brainstem, caudate/putamen, corpus callosum and external capsule up to 35 days after injury in mice (Carbonell and Grady, 1999) and 1 year in rats (Pierce et al., 1998). Lateral FPI also results in deficits in working memory, spatial learning and spatial memory, measured at time points from 2 days to 1 year after injury and is associated with cell loss in the cortex, hippocampus and thalamus as well as diffuse axonal damage (Hicks et al., 1993; Lyeth et al., 2001; Pierce et al., 1998).

Rats and mice are the species most commonly used to model TBI but the lissencephalic brain structure of rodents, combined with the relatively small mass of the rodent brain means that there are significant mechanical differences between TBI in rodents and humans (Morales et al., 2005). Primates, cats and pigs have gyrencephalic brains and have been used to model TBI. In cats, FPI has been shown to produce axonal damage, detectable between 1 and 6 hours after injury (Erb and Povlishock, 1988) as well as damage to neurons in hindbrain regions (Sullivan et al., 1976). In miniature pigs and primates rotational forces induced by acceleration of the head produce diffuse white matter damage (Gennarelli et al., 1982; Ross et al., 1994; Smith et al., 1997) as well as neuronal damage in the hippocampus (Smith et al., 1999; Smith et al., 1997).

## 1.3 Chronic cerebral hypoperfusion

### *1.3.1 Chronic cerebral hypoperfusion*

Modest long-term reductions in blood flow are linked to white matter pathology (Pantoni and Garcia, 1997). CBF decreases with age (Stoquart-ElSankari et al., 2007) while white matter damage is also observed with greater frequency with advancing age (de Leeuw et al., 2001). In addition, chronic hypoperfusion and linked white matter damage are associated with impaired cognitive function in aging (Appelman et al., 2010) and reductions in CBF correlate with cognitive impairment (Tiehuis et al., 2008). The mechanism of the link between chronic hypoperfusion

and white matter damage is not clear as minor reductions in CBF, such as the 20 to 25% decrease observed in aging, are not sufficient to cause cell death (Stoquart-ElSankari et al., 2007). Examination of the effects of these relatively modest reductions in CBF is complicated in aging humans by the fact that they are caused by a diversity of pathological states such as hyper- and hypotension, atherosclerosis, and diabetes. This renders development of animal models of pure chronic hypoperfusion necessary for establishing the impact of chronically reduced CBF on white matter and cognition.

### *1.3.2 Models of chronic cerebral hypoperfusion*

Modelling chronic hypoperfusion in animals allows isolation of its pathological and cognitive effects. The most frequently used model of chronic cerebral hypoperfusion is bilateral occlusion of the common carotid arteries in the rat. This model shows neuronal damage, notably in the hippocampus and widespread damage to white matter, both of which increase with increasing duration of hypoperfusion (Ohtaki et al., 2006; Wakita et al., 2002). The white matter damage observed is characterised by loss of myelination and rarefaction and vacuolisation of the corpus callosum and the optic tract, which appears to be particularly vulnerable in this model (Farkas et al., 2004a; Wakita et al., 2002). A variety of cognitive deficits have also been observed in this model, including spatial and nonspatial learning impairments, working memory deficits and increased anxiety (de Bortoli et al., 2005; Farkas et al., 2004b; Murakami et al., 2000). These deficits have been observed to worsen over time following the induction of hypoperfusion (Liu et al., 2005; Sopala and Danysz,

2001). However, interpretation of behavioural results in this model is complicated by preferential damage to the optic tract as well as the presence of other visual system defects, a major confound in the use of behavioural tasks which are heavily reliant on intact vision, such as the Morris water maze and the radial arm maze.

In gerbils, where complete occlusion of the common carotid arteries results in a more severe pathology than in the rat, owing to vascular differences between the species (Mayevsky and Breuer, 1992), stenosis of the common carotid arteries produces damage to white matter and a deficit in learning (Kurumatani et al., 1998). Stenosis is achieved by placing wire coils of a specified diameter around the arteries. Adaptation of this technique to the mouse has resulted in a model with diffuse white matter lesions appearing 14 days after the induction of hypoperfusion and persisting at 30 days (Shibata et al., 2004). Assessment of behavioural abilities revealed a deficit in working memory while spatial reference learning, associative learning and levels of locomotor activity remained normal (Shibata et al., 2007). Damage in this model is selectively to white matter and damage in the optic tract is not reported to be higher than in other regions, meaning that the observed behavioural changes are most likely due to diffuse damage to white matter. There are a number of elements of this model that require further investigation, including parallel assessment of behaviour and pathology in the same animals and determination of whether chronic hypoperfusion has differential effects on the different components of white matter.

## 1.4 Alzheimer's disease

### *1.4.1 Alzheimer's disease pathology*

AD is a common neurodegenerative disorder that results in profound cognitive disability. The disease is defined by progressive cognitive impairment and by the post-mortem detection of insoluble extracellular plaques containing aggregated amyloid β (Aβ) protein and intracellular fibrillar aggregations of hyperphosphorylated tau protein. Areas particularly affected include the cortex, hippocampus, entorhinal cortex and amygdala (Wenk, 2003). AD is estimated to affect 35 million people worldwide and incurs considerable healthcare costs and places a large burden on those who care for sufferers (Alzheimer's Disease International, 2010; Querfurth and LaFerla, 2010). There are a variety of risk factors for AD, including apolipoprotein E4 genotype (Corder et al., 1993), TBI (Heyman et al., 1984) and vascular factors including stroke, hypertension and cerebrovascular disease (Qiu et al., 2007 for review). The majority of cases occur in people aged over 65 and have no known cause, the rest (~1%) are due to heritable mutations in genes encoding either the amyloid precursor protein (APP); from which Aβ is derived or the presenilins; elements of the APP cleaving enzyme γ – secretase. The identification of these heritable mutations affecting Aβ production that lead to AD, in the absence of tau mutations which lead to AD, lead to the amyloid cascade hypothesis (Hardy and Higgins, 1992) which gives primacy to the role of Aβ in AD pathogenesis. This hypothesis states that Aβ deposition is the causal factor in AD

and that other pathological characteristics of AD; neurofibrillary tangles, cell loss and cognitive impairment result directly from this deposition. Although some questions have been answered as to the processes involved in the generation of Aβ, how it may interact with tau to produce hyperphosphorylated aggregates and how both these proteins exert their neurotoxic effects, it is not known what precipitates these events. The amyloid cascade hypothesis has proven useful for framing questions about the progression of AD pathology but does not make predictions regarding initiating factors. Recently, Hardy (2009) has updated the hypothesis to incorporate a vascular element to the development of AD; this updated hypothesis posits that vascular damage may be caused by Aβ deposition while also initiating Aβ damage.

Aβ is formed by sequential cleavage of APP by β – and γ – secretases (Figure 1.3). APP is a transmembrane protein of unknown normal function although it is thought to be involved in axonal transport, cell adhesion, cholesterol metabolism and gene transcription (Turner et al., 2003). Cleavage of APP by β – secretase in the extracellular domain produces a 99 residue C-terminal fragment that is cleaved in the transmembrane domain by the protein complex γ – secretase to form the Aβ peptide, which is 36 to 43 amino acids in length. Alternatively cleavage by α – secretase occurs within the Aβ domain of APP and precludes the formation of Aβ (Goedert and Spillantini, 2006). The principle products of amyloidogenic cleavage are Aβ peptides that are 40 or 42 amino acids long ($A\beta_{40}$ and $A\beta_{42}$, respectively). Aβ tends to form aggregates of multiple peptides with the solubility and toxicity of these peptide molecules changing with increasing numbers of peptides. Ultimately,

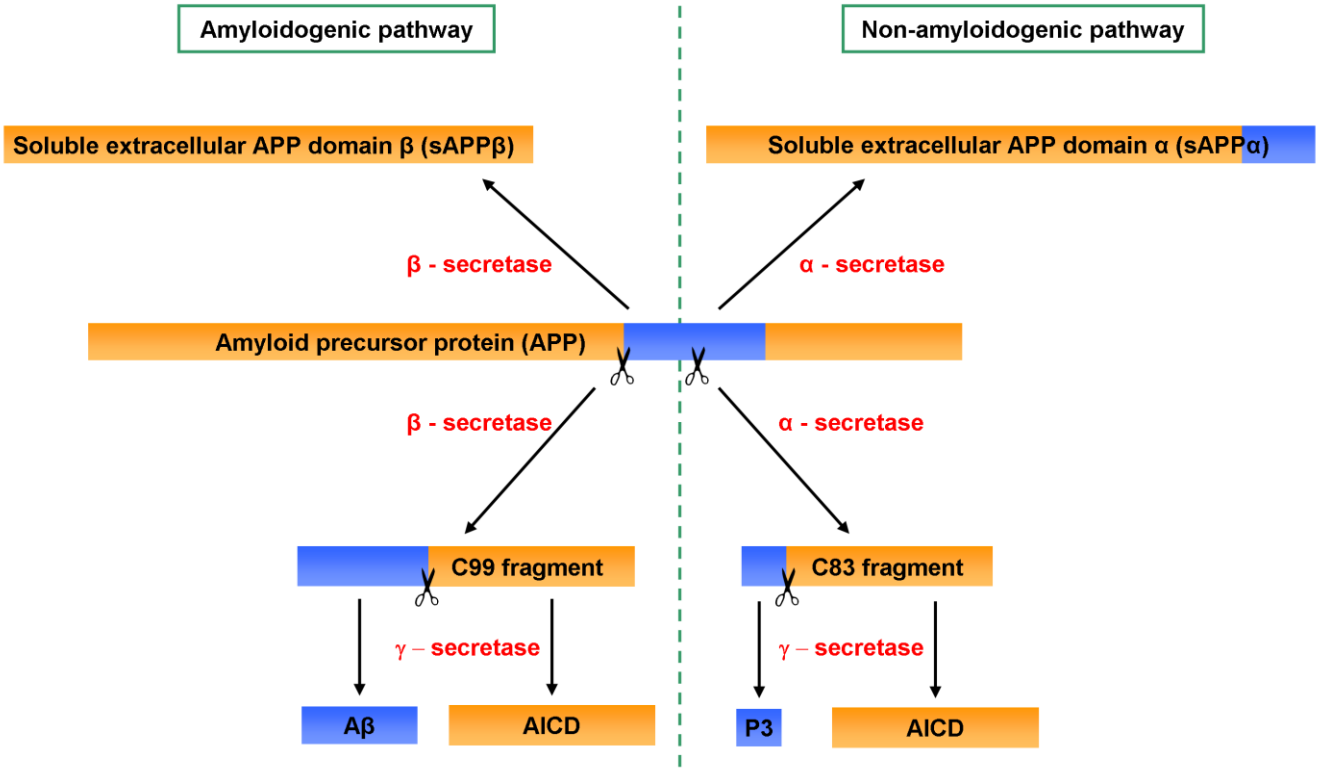


**Figure 1.3: Amyloidogenic and non-amyloidogenic cleavage of amyloid precursor protein (APP)** Non-amyloidogenic cleavage of APP is by α – secretase with in the Aβ region of APP in the first instance to produce soluble extracellular APP domain α (sAPPα) and an 83 amino acid long C-terminal fragment. This is then cleaved by γ – secretase to produce a P3 fragment and an APP intracellular domain (AICD). The first step in amyloidogenic cleavage of APP is by β – secretase which produces sAPPβ and a 99 amino acid C-terminal fragment that is cleaved by γ – secretase to produce Aβ and AICD.

aggregation of Aβ results in the formation of protofibrils and then fibrils which are deposited extracellularly as insoluble plaques (LaFerla et al., 2007). $A\beta_{42}$ is the more aggregation prone form of the protein and is more neurotoxic than $A\beta_{40}$ (Findeis, 2007). Soluble oligomers of Aβ show greater levels of neurotoxicity than the insoluble plaques of Aβ that are deposited in the brains of AD patients (Finder and Glockshuber, 2007). Levels of soluble Aβ oligomers also correlate with cognitive impairment better than either total levels of Aβ or numbers of Aβ plaques, further suggesting an important role for these formations of Aβ (Tomic et al., 2009). The mechanism of the neurotoxic effects of Aβ is unclear although it has been shown to have a deleterious effect on oxidative phosphorylation (Rhein et al., 2009; Yao et al., 2009), induce inflammation (Apelt and Schliebs, 2001; Richards et al., 2003) and apoptosis (Nelson and Alkon, 2007), impair fast axonal transport (Pigino et al., 2009) and alter intracellular calcium homeostasis (Zempel et al., 2010). There is also evidence that toxicity of Aβ may be mediated by tau (Findeis, 2007; Wilcock et al., 2009; Zempel et al., 2010).

Tau is a microtubule associated protein, involved in stabilisation of the axonal cytoskeleton. The hyperphosphorylation of tau reduces its affinity for microtubules and promotes its aggregation into paired helical filaments, which are the main component of the neurofibrillary tangles observed in AD (Alonso et al., 1996). The amount of neurofibrillary tangles observed also correlates with the cognitive status of AD patients (Goedert and Spillantini, 2006). Hyperphosphorylated tau is also neurotoxic, with a number of hypothesised mechanisms of action including sequestration of normal microtubule associated proteins, disruption of microtubule

dynamics and disruption of intracellular trafficking (Wang and Liu, 2008). Aβ and tau have been demonstrated to act in a synergistic way to cause defects in oxidative phosphorylation (Rhein et al., 2009), suggesting that the progression of pathology in AD may not be as linear in fashion as suggested by the amyloid cascade hypothesis. Evidence from animal models of AD (see below) shows that the presence of pathological forms of tau does not lead to the development of Aβ pathology, while tau pathology may be prevented by clearance of Aβ, confirming this prediction of the amyloid cascade hypothesis. How Aβ affects tau phosphorylation status is unknown but inflammatory cytokines induced by Aβ are known to affect tau phosphorylation (Li et al., 2003). Aβ also activates tau kinases such as cyclin dependent kinase 5 (Cdk5) and glycogen synthase kinase 3β (GSK-3β) (Blurton-Jones and LaFerla, 2006).

### *1.4.2 White matter in Alzheimer's disease*

In addition to the well characterised Aβ and hyperphosphorylated tau pathology changes in white matter are also associated with AD (e.g. Bartzokis et al., 2003; Brun and Englund, 1986a; Englund et al., 1988; Yoshita et al., 2006). White matter alterations are an early event in the development of AD (Stokin et al., 2005) and in at least one transgenic model precede the development of classic AD plaque and tangle pathology (Desai et al., 2009).

Pathological investigation (Brun and Englund, 1986a, b; Englund et al., 1988) has shown loss of myelin, axons and oligodendrocytes in post-mortem AD brains as well as astrocytic gliosis. These findings have been confirmed in studies using magnetic resonance imaging (MRI) (Bartzokis et al., 2003; Targosz-Gajniak et al., 2009; Yoshita et al., 2006) and although the evidence for a direct correlation between disease progression and volume of white matter abnormalities observed is mixed it is clear that volume of white matter damage is related to age (Bartzokis et al., 2003; Targosz-Gajniak et al., 2009). Individuals with mild cognitive impairment (MCI), a high proportion of whom go on to develop AD (Landau et al., 2010) also show white matter changes in MRI scans (DeCarli et al., 2001) and these changes may be predictive of later conversion to AD (Davatzikos et al., In press). Also, higher levels of white matter damage have been reported in individuals with AD, compared to those with MCI, suggesting that there may be a relationship between white matter damage and severity of cognitive impairment (Targosz-Gajniak et al., 2009; Wu et al., 2002). As with white matter lesions in normal aging populations, white matter changes in AD are also linked to cerebral hypoperfusion (Fernando et al., 2006; Meyer et al., 2008; Ruitenberg et al., 2005). Cerebral hypoperfusion is an early event in AD and has been detected in temporal and parietal regions before the onset of cognitive decline (Farkas and Luiten, 2001). In individuals with MCI, hypoperfusion, as well as the presence of white matter lesions is detectable prior to the development of AD (Farkas and Luiten, 2001; Matsuda et al., 2007).

Bartzokis (2004; 2009) has suggested that myelin damage is a primary pathological event in AD where homeostatic responses to age-related loss of vulnerable late-

myelinating oligodendrocytes are responsible for the classic plaque and tangle pathology of AD. Direct validation of this theory in animal models is required, however it is known that oligodendrocytes are vulnerable to Aβ related toxicity (Desai et al., 2010; Xu et al., 2001) and that axonal damage can be induced by expression of mutant human tau in oligodendrocytes, due to disruption of axonal transport (Higuchi et al., 2005). Alternatively, it has also been proposed that deficits in axonal transport may lead to the synaptic and neuronal loss observed in AD and also to increased processing of APP to Aβ and increased phosphorylation of tau. However, Aβ can also have effects on axonal transport, making it unclear whether it is a cause or result of impaired axonal transport (Muresan and Muresan, 2009). The direction of the relationship between AD and white matter damage may not be clear but it is evident that white matter pathology is a prominent feature of AD.

### *1.4.3 Models of Alzheimer's disease*

The discovery of genes responsible for early onset, familial AD has allowed the generation of transgenic mouse models of AD. A variety of mutations in genes encoding APP and presenilin 1 and 2 are responsible for the heritable forms of the disease in humans. Mutations in the *APP* gene can result in increased production of total Aβ or an increase in the proportion of the long form of $A\beta_{42}$ relative to $A\beta_{40}$ (Findeis, 2007; Goedert and Spillantini, 2006). Mutations in either of the *presenilin* genes also increase relative levels of $A\beta_{42}$, owing to altered cleavage of APP by γ - secretase.

Although aging mice do not normally display abnormalities in Aβ or tau like those seen in AD (Selkoe, 1991), introduction of mutant versions of human genes into the mouse genome results in models recapitulating some of the Aβ-related pathological features of AD (McGowan et al., 2006 for review). Lines transgenic for *APP* with one or more mutations develop amyloid plaques and cognitive deficits in an age-dependent manner (e.g. Dodart et al., 1999; Games et al., 1995; Mucke et al., 2000). For instance, the PDAPP line, characterised by Games (1995) display Aβ plaques beginning at 6 to 9 months of age and increasing in density as the animals age. Deficits in recognition and episodic memory have been reported from 3 months old and progressing to 18 to 21 months of age (Chen et al., 2000; Dodart et al., 1999). The timing and location of amyloid pathology is variable between transgenic lines due to differences in the promoter under which the transgene is expressed and in levels of transgene expression. Mice expressing mutant *presenilin* transgenes in addition to the mutant *APP* gene show a similar pattern of pathology and cognitive deficits to those transgenic only for *APP* but with an accelerated rate of development (Borchelt et al., 1997; Holcomb et al., 1998). Expression of mutant *presenilin* is itself sufficient to increase levels of $A\beta_{42}$ (Duff et al., 1996). Unlike human AD however, neuronal loss is not a feature of these models and tau pathology is also absent. Despite these limitations, transgenic mouse models of AD have allowed identification of the importance of oligomeric forms of Aβ in cognitive deterioration owing to the presence of a behavioural deficit prior to the onset of amyloid plaque pathology (Borchelt et al., 1997; Cleary et al., 2005; Lesné et al., 2006; Westerman et al., 2002).

Modelling of the tau pathology observed in human AD has necessitated the use of transgenics expressing genes not related to AD as there are no tau-related mutations linked to AD. Expression of human *tau* with a mutation causing frontotemporal dementia and parkinsonism linked to chromosome 17 in mice leads to development of hyperphosphorylated tau throughout the brain, along with massive neuronal degeneration and cognitive changes but without changes in Aβ (Lewis et al., 2000). As noted by Allen et al. (2002) the formations of hyperphosphorylated tau seen in these models do not necessarily correspond to the forms observed in AD. Additionally, the presence of extensive motor deficits in these models renders attribution of behavioural changes to neuronal loss or the presence of pathology difficult (e.g. Lewis et al., 2000; Ramsden et al., 2005). Similar to findings in models of amyloid pathology the link between the classic neurofibrillary tangle pathology of AD has not been shown to be clearly linked to cognitive decline in these models. Suppression of mutant *tau* expression has been found to reverse the memory deficits observed and halt neuronal death without halting the increase in amount of neurofibrillary tangles (SantaCruz et al., 2005), indicating that neurofibrillary tangles are not necessarily neurotoxic themselves but that destabilisation of microtubules and impairment of axonal transport may be the basis for this (Sun et al., 2008; Zhang et al., 2004).

Recapitulation of both of the characteristic pathological features of AD in a single model has led to the development of transgenic lines containing combinations of *APP*, *presenilin* and *tau* transgenes. These models, such as those characterised by Oddo et al. (2003a, b) and Lewis et al. (2001) have demonstrated the temporal order

of progression of these features of AD with Aβ deposits appearing prior to neurofibrillary tangles and acceleration of neurofibrillary tangles appearance relative to single transgenics, demonstrating an interaction between Aβ and tau pathology. Interestingly accumulation of endogenous mouse tau in mice transgenic for mutant human *APP* has been induced by knockout of *NO synthase 2*, giving further evidence of the role of Aβ in the development of tau pathology even in the absence of non-AD relevant *tau* mutations (Colton et al., 2006; Wilcock et al., 2008; 2009). These models displaying multiple pathologies also exhibit synaptic dysfunction (Oddo et al., 2003b) and behavioural changes (Martinez-Coria et al.), similar to transgenic lines displaying only Aβ pathology but in the case of the Wilcock et al. (2008) study at least, the presence of tau abnormalities exacerbated the behavioural deficits observed in single *APP* transgenics. Administration of antibodies against Aβ to the triple transgenic model developed by the LaFerla group demonstrated that clearance of Aβ pathology in this model also led to a reduction in tau pathology (Oddo et al., 2004), further demonstrating the link between Aβ and tau pathology in AD.

White matter abnormalities are also a feature of transgenic mouse models of AD (e.g. Desai et al., 2009; 2010; Wirths et al., 2007). Reductions in myelination in the hippocampus and entorhinal cortex of triple transgenic mice as well as reductions in oligodendrocyte markers have been recorded prior to the age at which pathology typically begins in these animals (Desai et al., 2009). This reduced myelination is progressive and is associated with abnormalities in axonal morphology at up to 6 months of age. Similarly, progressive axonopathy has been observed in the brains of APP/PS1 transgenic mice by Wirth et al (2007). The use of DTI in APP transgenic

mice from 8 to 18 months of age suggested the presence of axonal damage after 8 months of age and myelin damage from 15 months (Song et al., 2004; Sun et al., 2005). Cerebral hypoperfusion is another early event in AD that is recapitulated in transgenic models, with reduced blood flow having been recorded prior to the appearance of Aβ plaques (Niwa et al., 2002).

As has been noted above mutations in the *APP* and *PS1* genes account for only 1% of cases of AD in humans, also AD in humans is not associated with mutations in genes encoding tau. This is a factor that places some restrictions on extrapolation of findings from transgenic mice into humans, however other species have been reported to develop AD-like pathology and cognitive deficits in an age-dependent manner. Primate species, such as the rhesus macaque, develop Aβ plaques with aging (Ichinohe et al., 2009; Uno et al., 1996)) although, in contrast to humans, the main Aβ species found in plaques is $A\beta_{40}$ (Sani et al., 2003). Rhesus macaques also display neuronal loss and axonal loss associated with the presence of Aβ plaques (Shah et al., 2010). Deposition of Aβ is also observed in aged dogs and the anatomical distribution of Aβ deposition is similar to that observed in humans, with the prefrontal and entorhinal cortices showing particularly high levels of Aβ deposition (Head et al., 2000) as in humans, the primary form of Aβ deposited is $A\beta_{42}$ (Nakamura et al., 1997). Intraneuronal aggregations of hyperphosphorylated tau are also observed with aging (Pugliese et al., 2006). Dogs also display cognitive deficits associated with Aβ pathology (Head et al., 1998). Aging cats also show Aβ and hyperphosphorylated tau pathology as well as age-related cognitive changes (Gunn-Moore et al., 2006; Gunn-Moore et al., 2007). The long time required for the

development of pathology in these species (~9 years in dogs and ~25 years in rhesus macaques) has meant that although these models replicate features of human sporadic AD their use has been somewhat limited

## 1.5 Traumatic brain injury and Alzheimer's disease

### *1.5.1 Traumatic brain injury as a risk factor for Alzheimer's disease*

Although AD has no known cause a number of risk factors have been identified with the chief environmental one being a history of TBI. Epidemiological studies show increased incidence of AD in individuals with a history of TBI (Fleminger et al., 2003; Graves et al., 1990; Guo et al., 2000; Mortimer et al., 1991; Schofield et al., 1997), even at intervals up to 50 years after TBI (Plassman et al., 2000). These studies have mainly focused on moderate to severe injuries which are readily verifiable owing to the existence of medical records meaning that the picture concerning the more common mild TBI is not as clear. Work carried out in populations of athletes, who may experience multiple mild TBIs suggests that mild TBI can also have a significant impact on the likelihood of developing cognitive impairment in later life (De Beaumont et al., 2009; Guskiewicz et al., 2005; Lipton et al., 2008; Matser et al., 1999).

As well as observed increases in the rate of AD observed following TBI AD-type pathology has also been noted. Studies of individuals who have died as a result of

TBI have found Aβ plaques to be present regardless of age (Graham et al., 1995; Horsburgh et al., 2000; Roberts et al., 1994). Analysis of tissue removed from the brains of severely brain injured patients hours after injury also showed deposited Aβ in one third of patients (Ikonomovic et al., 2004). Plaques composed of the more aggregation prone $A\beta_{42}$ have also been demonstrated to be more frequent than those composed of $A\beta_{40}$ (Horsburgh et al., 2000; Ikonomovic et al., 2004). However, post-mortem studies of patients who survived for several days to years after TBI do not show persistent Aβ plaque pathology (Chen et al., 2009; Macfarlane et al., 1999). TBI-induced microglial activation may be responsible for clearance of Aβ plaques (Hickman et al., 2008; Koenigsknecht and Landreth, 2004). While Aβ plaques have not been shown to be a long-term feature of pathology after TBI intra-axonal accumulation of Aβ in damaged axons has been demonstrated to persist for up to 3 years after TBI (Chen et al., 2009). The cognitive status of these long-term survivors of TBI is indeterminate, precluding investigation of links between the presence of pathology in the brain and deficits in cognition.

Neurofibrillary tau pathology and Aβ deposition are characteristic of dementia pugilistica, a dementia primarily observed in boxers and other athletes who have received multiple TBIs (Schmidt et al., 2001; Toth et al., 2005). Behaviourally, this syndrome is defined by cognitive and motor impairments and the composition of the neurofibrillary tangles is similar to that observed in AD (Schmidt et al., 2001). After acute head injury however, evidence of increased numbers of neurofibrillary tangles was not present although tau immunoreactivity was present (Smith et al., 2003a). The absence of neurofibrillary tangle pathology in acute studies may reflect either a

necessity for multiple injuries to result in tau pathology as in dementia pugilistica or the temporal order of development of AD pathology as demonstrated in transgenic models.

### *1.5.2 Alzheimer's disease pathology in animal models of traumatic brain injury*

While investigation of TBI on the presence of AD-related pathology in humans generally shows that TBI produces AD-type changes, particularly in Aβ, the evidence from animal studies is more equivocal. Acute increases in total Aβ levels in the brains of mice transgenic for mutant human *APP* have been observed but not linked to an increase in Aβ pathology (Smith et al., 1998). In fact, reductions in the levels of Aβ plaques have been observed following severe injury in similar models (Nakagawa et al., 1999; 2000). In contrast to these studies of severe injury mild TBI has been demonstrated to induce increased Aβ at 16 weeks after injury and this increase in deposition is accelerated when animals are subjected to multiple mild TBI (Uryu et al., 2002). Importantly, studies in transgenic mice are using animals that either already display Aβ plaques or will go on to develop them, owing to their genotype. This means that modelling TBI in this fashion introduces a further insult into an already pathological system, something which is unlikely to be the case in humans, particularly in young sufferers of TBI.

Work on non-transgenic rats has failed to show extracellular deposition of Aβ in response to TBI but it has demonstrated persistent accumulation of Aβ in damaged axons, similar to human studies (Iwata et al., 2002) as well as increased levels of Aβ

in cells at 6 months after injury (Hoshino et al., 1998). In pigs extracellular deposition of Aβ has been reported in addition to accumulation of Aβ in injured axons (Chen et al., 2004; Smith et al., 1999). These changes were found to persist up to 6 months after injury and were in addition to increases in overall levels of Aβ in the first 7 days after injury (Chen et al., 2004).

Accumulation of hyperphosphorylated tau following TBI has been less frequently investigated in animals. In mice already displaying hyperphosphorylated tau TBI produces a transient increase in tau hyperphosphorylation at 4 hours after injury (Genis et al., 2000). At 9 months after repeated TBI mice transgenic for human tau do not show changes in tau phosphorylation (Yoshiyama et al., 2005). Investigations of tau-related changes in other species do not agree with these studies, however. Accumulation of tau in damaged axons as well as in neurons has also been observed in pigs from 3 to 10 days after injury (Smith et al., 1999) while rats show increases in the levels of hyperphosphorylated tau observed in neurons over time up to 6 months after injury (Hoshino et al., 1998). The low number of studies investigating tau pathology following TBI in animal models makes generalisations in this area difficult, although it does appear that there is some impact of TBI on tau while the timing of changes remains to be elucidated.

### *1.5.3 Potential mechanisms of traumatic brain injury influence on Alzheimer's disease*

Pathological studies of the development of Aβ or tau pathology following TBI have demonstrated some ways in which TBI can influence the development of AD-type pathology. In particular, co-accumulation of APP, Aβ and proteins necessary for production of Aβ from APP in the damaged axons of both pigs and humans after TBI (Chen et al., 2004; Uryu et al., 2007) points towards a role for damaged axons as localised reservoirs of substrate for secretases to cleave to Aβ. Accumulation of APP in injured axons is likely due to interruptions in anterograde axonal transport caused by damage to the neuronal cytoskeleton, a source of tau alterations due to disruption of microtubule assembly (Geddes et al., 1999). In addition to accumulation of proteins involved in the generation of Aβ in axons, overall levels of APP have been shown to be increased following TBI at time points ranging from hours to days after injury (Szczygielski et al., 2005), providing another potential pool of APP from which the Aβ pathology observed in grey matter could be derived. Pro - inflammatory cytokines including interleukin-1α (IL-1α), IL-1β, IL-6 and tumour necrosis factor-α (TNFα) induced by TBI have also been demonstrated to regulate processing of APP to Aβ (Ge and Lahiri, 2002; Goldgaber et al., 1989; Schmitz and Chew, 2008) and to influence tau phosphorylation via their effects on tau kinases (Kitazawa et al., 2005; Quintanilla et al., 2004).

## 1.6 Summary

The importance of white matter in cognitive function is highlighted by situations in which damage to white matter results in cognitive impairment. TBI, chronic hypoperfusion and AD are all associated with damage to white matter and cognitive impairment. However the contribution of white matter damage in isolation to the pathogenesis of each of these conditions is not known. It is hypothesised that white matter damage following TBI or chronic cerebral hypoperfusion will be associated with a cognitive deficit and that white matter changes after injury will result in the development of AD related pathology. To investigate this, this thesis will examine the effects of TBI and hypoperfusion on white matter and associated cognitive deficits as well as examining the role of white matter damage in the relationship between TBI and AD.

## 1.7 Thesis aims and hypotheses

*Chapter 3: Effect of mild traumatic brain injury on pathology and cognition in wild-type mice*

It was hypothesised that mild TBI would cause selective damage to axons at short and long-term time points after injury as well as inducing a persistent deficit in learning and memory.

To investigate the impact of mild TBI on white matter damage as well as cognitive deficits in mice, a detailed examination of axons, myelin and neuronal cell bodies was undertaken at time points ranging from 4 hours to 6 weeks as well as an investigation of learning and memory 3 and 6 weeks after injury.

*Chapter 4: Effect of mild traumatic brain injury on white matter and Alzheimer's disease pathology in an Alzheimer's disease model*

In a transgenic model of AD it was hypothesised that mild TBI would cause axonal damage as well as deposition of Aβ and in white matter in the hours after injury as well as increases in intracellular levels of Aβ and tau. It was also predicted that overall levels of APP, Aβ and normal and hyperphosphorylated tau would be increased.

To investigate the effect of mild TBI on Aβ, tau and white matter pathology in a transgenic mouse model of AD, axons, myelin, Aβ and tau as well as the levels of axonal and AD-related proteins were examined at 24 hours after mild TBI.

*Chapter 5: Effect of chronic cerebral hypoperfusion on white matter and cognition in mice*

Chronic cerebral hypoperfusion was hypothesised to cause damage to elements of white matter as well as a deficit in spatial learning, memory, serial spatial learning or working memory.

To investigate the effects of chronic cerebral hypoperfusion on cognition and white matter pathology in wild-type mice, axonal and myelin damage as well as a number of cognitive domains were investigated after one or two months of hypoperfusion.

# 2 Materials and methods

## 2.1 Animals and surgical techniques

All animals were housed on a 12 hour light/dark cycle and had access to food and water ad libitum, except during radial arm maze testing, where food intake and the weights of individual mice were monitored continuously. All animals were kept on a 12 hour light/dark cycle. All experiments were carried out under a UK Home Office licence and adhered to regulations specified in the Animals (Scientific Procedures) Act (1986).

The wild-type strain used in both mild traumatic brain injury (TBI) and hypoperfusion studies was C57Bl/6J (Charles River, UK). In the study of the effects of mild TBI on white matter and Alzheimer's disease (AD) pathology a triple transgenic (3xTg) mouse model of AD as described by Oddo (2003). These mice express human $APP_{Swe}$, and $tauP_{301L}$ transgenes under a Thy1.2 promoter as well as the M146V mutation knocked into murine PS1. Mice were originally derived by microinjection of the transgenes into single-cell embryos from homozygous $PS1_{M146V}$ knockin mice and backcrossed onto the $PS1_{M146V}$ knockin strain. Breeding was carried out in-house, breeding pairs having been originally obtained from the Department of Neurosciences, University of Manchester.

### *2.1.1 Induction of mild TBI*

Mild TBI was modelled using lateral fluid percussion injury (FPI; McIntosh, 1989) surgery and was carried out by Dr. Jill Fowler as previously described by Lifshitz (2008). Wild-type animals were anaesthetized with 250 mg/kg avertin. 3xTg animals were anaesthetised in an anaesthesia chamber with 5% isoflurane in 30:70 mixture of oxygen and nitrous oxide for 5 minutes and maintained with 1.5% isoflurane anaesthesia via a nose cone while the craniotomy was drilled. A 3mm craniotomy was drilled between bregma and lambda over the right parietal cortex, leaving the underlying dura intact. Animals in which the dura was breached were excluded from the study. A modified Luer-Lok hub (BD Biosciences, Oxford, UK) was placed over the craniotomy site and secured with cyanoacrylate glue and methyl methacrylate cement. After recovery (24 hours for avertin anaesthetised animals and at least 1 hour for isoflurane anaesthetised animals) mice were reanaesthetised in a chamber using 5% isoflurane in 30:70 mixture of oxygen and nitrous oxide for 5 minutes. Once anaesthetised, animals were connected to the fluid percussion device (McIntosh et al., 1989) via high pressure tubing and a fluid pressure pulse was delivered. Sham control animals underwent the same procedure, including connection to the fluid percussion device but did not receive a fluid pressure pulse. The injury hub was then removed. Following this animals were placed on their backs and the righting time recorded, as a measure of injury severity. Animals were then reanaesthetised as before and maintained with 1.5% isoflurane anaesthesia via a nose cone briefly while the scalp incision was sutured.

*2.1.2 Induction of chronic cerebral hypoperfusion*

Chronic cerebral hypoperfusion was induced as described previously (Shibata et al., 2004) and surgery was carried out by Dr. Karen Horsburgh. Animals were anaesthetised in a chamber with 5% isoflurane in a mixture of 30:70 oxygen:nitrous oxide and maintained with 1.5% isoflurane anaesthesia via a nose cone. The common carotid arteries were exposed via midline cervical incision. Microcoils of 0.18 mm diameter (Sawane Spring Co., Hamamatsu, Japan) were placed around the common carotid arteries with a 30 minute interval between the insertion of the first and second microcoils. Sham animals underwent the same surgical procedure as hypoperfused animals, with the exception of the placement of microcoils. At the end of the surgical procedure the incision was sutured.

## 2.2 Behavioural testing

Prior to surgery all animals designated for behavioural testing were handled for 5 minutes per day for 5 consecutive days to minimise stress resulting from handling. All behavioural testing was carried out by pairs of experimenters blinded to the experimental status of the animals.

### *2.2.1 Morris water maze*

All water maze testing was carried out in a 2m diameter tank filled with water to a depth of 50cm, at a temperature of 25 ± 1°C and rendered opaque by the addition of liquid latex. The experimental room was painted white and equipped with a variety of 3D and 2D cues in contrasting colours to improve their salience (Figure 2.1). Timing of latencies to the platform, tracking of swim patterns in all versions of the water maze task and control of the submerged platform in the probe tests was done using the *WaterMaze* video tracking system (v 2.6, ActiMetrics Software).

### *2.2.2 Cued platform testing in the Morris water maze*

Animals were trained on a cued version of the water maze task for 1 day prior to surgery in order to exclude animals that showed an abnormal stress response to the task. In this task the target platform was 20cm in diameter and was marked by a 20 cm high cue and was located in a different quadrant for each trial on a given day. The platform was submerged 1cm below the surface of the water. A white curtain was drawn around the pool to preclude the use of any extramaze cues to find the platform in this task.

Training on the cued version of the water maze task was repeated for four days, beginning 1 week after surgery. Each animal was trained for 4 trials per day, with 20 minutes between trials. Training in the cued version of the water maze task was

carried out to establish the presence of gross motor or visual impairments and to train the animals to swim to and climb on to a submerged platform. At the start of each trial the animal was placed in the pool, facing the wall and allowed to swim until finding a platform centred in one of the quadrants of the pool or until 90 seconds had expired. Mice were placed in the pool at one of the four cardinal points (north, south, east and west), with the start position varying for each trial so that the no starting position was repeated on any day.

### *2.2.3 Spatial reference learning and memory in the Morris water maze*

Spatial reference memory training began 3 days after the end of the cued platform water maze task. The 13cm diameter platform was not visible to animals in this task; being submerged 1cm below the surface of the water and uncued. Animals were trained over 5 days for 4 trials per day and the platform remained in a constant location for each animal throughout testing, while the start location varied. The platform locations and start positions used were counterbalanced across groups. Prominent extra maze cues were available throughout the room. Probe tests were carried out 10 minutes after the final trial of spatial reference training and again, 24 hours later.

*2.2.4 Episodic memory in the Morris water maze*

Episodic memory was tested using a trials to criterion protocol as described by Chen et al. (2000). Testing began 3 days after the end of the cued platform water maze task. The platform used in this task was the same as used during spatial reference memory testing. Animals learned a series of platform locations to a criterion of performance. Trials were conducted in the same way as in the spatial reference memory protocol. The criterion used was an average latency to reach the platform of less than 20 seconds over 3 consecutive trials. Animals were permitted a maximum of 32 trials to reach this criterion, except for the first platform location, where the maximum number of trials permitted was 40. The maximum number of trials per day was 8. After reaching criterion or 32 trials, training on that platform location ended and memory for the platform location probed as described below at 10 minutes and 3 hours after the end of training. On the next day training began on a new platform location. Animals continued to learn a sequence of platform locations for a minimum of 10 days or until 5 platform locations had been learned. Probe tests were carried out only after the first 5 platform locations. Platform locations and start positions used were counterbalanced across groups.

*2.2.5 Probe testing in the Morris water maze*

During probe testing the 13cm diameter platform was submerged at the bottom of the pool for 60 seconds while the mouse searched in the pool. After 60 seconds the

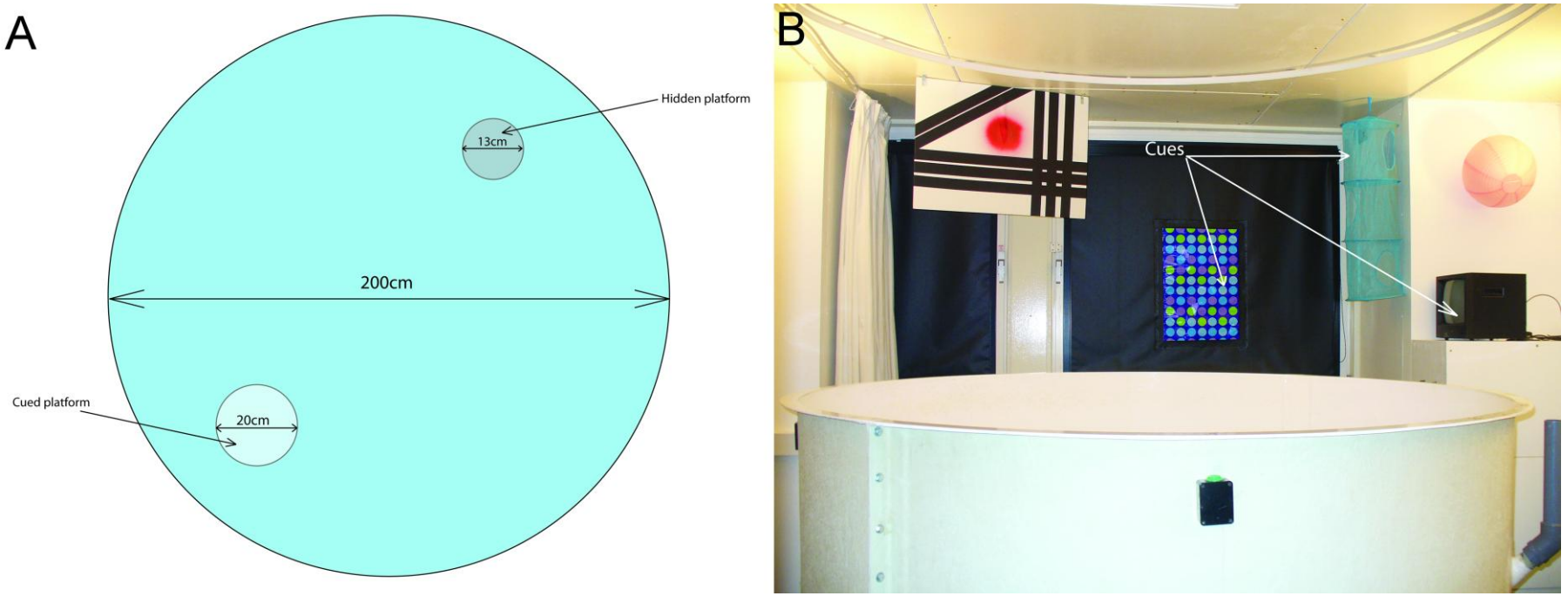


**Figure 2.1: Water maze dimensions and cues**

The water maze (A) had a diameter of 200cm. The diameter of the platform in the cued version of the water maze task was 20cm and the diameter of the platform in the spatial reference memory task had a diameter of 13cm. There were numerous 3D and 2D extramaze cues in contrasting colours in the room the maze was housed in (B).

platform was made available in the same position as it had been in the preceding training period and the mouse allowed a further 30 seconds to locate it, in order to minimise extinction of the platform finding behaviour.

### *2.2.6 Working memory testing in the radial arm maze*

Working memory was tested using an 8-arm radial maze protocol adapted from Shibata et al. (2007). The maze and its dimensions are shown in Figure 2.2. Doors at the proximal end of each arm were controlled remotely using Any-Maze software (Stoelting, Dublin, Ireland). Each arm was enclosed by a 20cm high transparent perspex wall. Tracking of the animals in the maze was carried out using the same software. The experimental room was equipped with both 2D and 3D cues in colours that contrasted with the white walls of the room. Food deprivation began 3 weeks after surgery and animals were maintained at 85 – 90% of initial bodyweight throughout testing. Pre-testing was carried out both to acclimatise animals to the maze environment and to train the animals to retrieve food pellets from the plastic food wells located at the end of each arm. On the first pre-training day food pellets (Bio-Serv, USA) were scattered about the maze and the animal allowed to explore freely for 5 minutes. On the second pre-training day food pellets were placed in each of the food wells and the animal placed in the central platform. The animal was allowed to retrieve the food pellet from each arm in turn.

For each trial of the spatial working memory task all 8 arms were baited with food pellets. Each training trial began with the animal being placed in the central platform

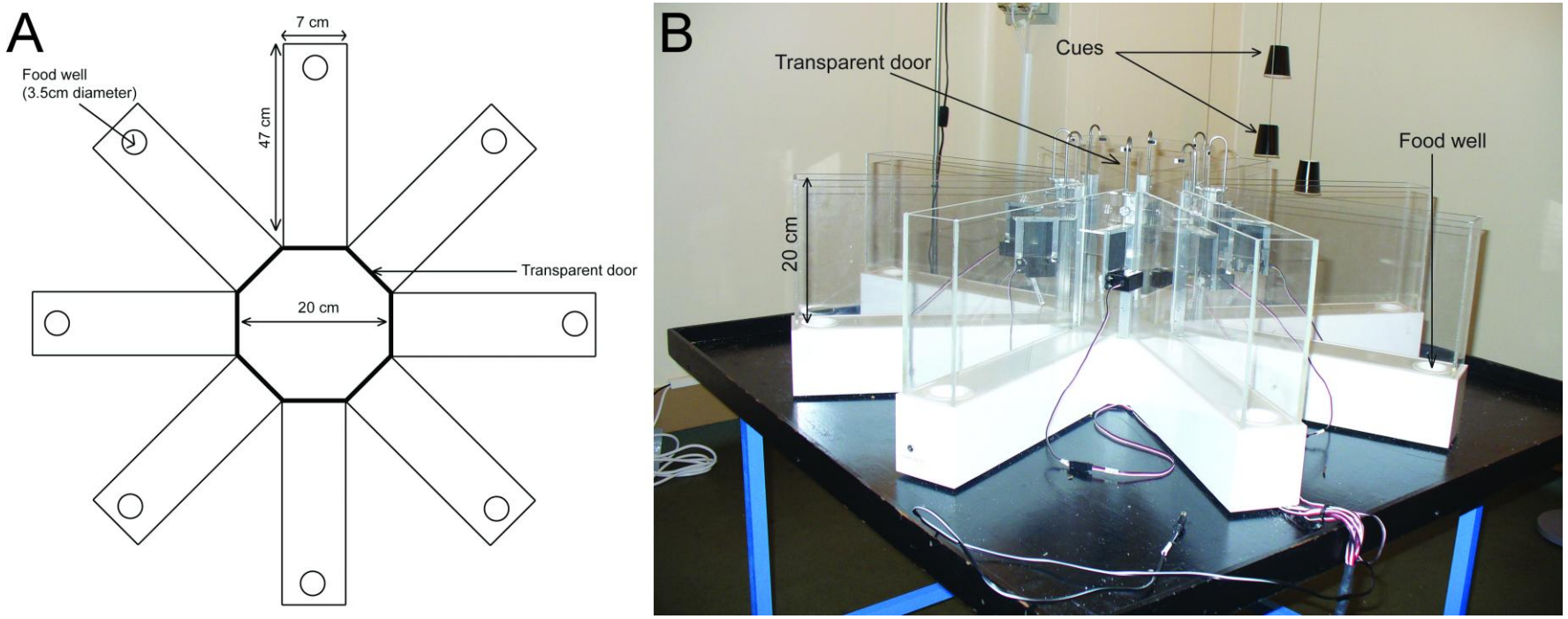


**Figure 2.2: Radial arm maze dimensions and cues**

The central reservation of the radial arm maze (A) had a diameter of 20cm while the arms of the maze were 47cm long and 7cm wide. A food well of 3.5cm diameter was located at the end of each arm. Each arm was enclosed by a 20cm high transparent wall and could be opened and closed by means of remotely operated transparent doors (B). The room in which the maze was housed was equipped with 3D and 2D extramaze cues in contrasting colours (B).

with all doors open. An arm choice was recorded when the centre of the mouse had travelled 5cm along the arm. An arm choice triggered closure of the doors to the other 7 arms. When the animal returned to the central platform it was confined there for 5 seconds before being allowed to make another arm choice. The trial ended when the animal had retrieved all 8 food pellets or when 25 minutes had elapsed. Each animal completed 1 training trial per day. After 16 days of training a 2 minute delay was introduced after the fourth arm choice. This assessed the effects of increasing the load on working memory in the task. Training on this protocol continued for 4 further trials

## .2.3. Perfusion fixation

Animals selected for histological or immunohistochemical analysis were terminated by transcardiac perfusion. Animals were deeply anaesthetised with 5% isoflurane in an anaesthetic chamber. Depth of anaesthesia was assessed by presence or absence of reaction to hindpaw pinch. Once animals showed no reaction to this test they were moved to a mask for maintenance of anaesthesia during the procedure. The thoracic cavity was opened and the diaphragm exposed. The diaphragm was cut through to expose the heart, which was gently freed of connective tissue. A needle was inserted into the left ventricle and clamped in place and an incision was made in the right atrium. Animals were perfused with 20mL of heparinised 0.9% saline in phosphate buffer via the clamped needle; fixation was achieved by perfusion with 4% paraformaldehyde in phosphate buffer (pH = 7.4). The animals were decapitated

and the scalp cut back to expose the skull and the entire head placed in 4% paraformaldehyde in phosphate buffer overnight. The following day the brain was removed from the skull and returned to the paraformaldehyde solution for 2 hours before removal to phosphate buffer for storage up to 2 days prior to paraffin embedding. In cases where the quality of perfusion was sub-optimal (as determined by the rigidity of the limbs) the brain was removed from the skull immediately following decapitation and placed directly into 4% paraformaldehyde solution overnight before removal to phosphate buffer solution.

## 2.4 Paraffin embedding and sectioning

Brains of C57Bl/6J mice in the initial FPI studies were divided into 3mm thick coronal sections prior to paraffin embedding. Sections were placed in embedding cassettes and dehydrated through successive alcohols and xylene into paraffin in the sequence described in Table 2.1

In studies using 3xTg mice whole brains were dehydrated and prepared for paraffin embedding in a Tissue Tek VIP 2 (Sakura Finetek Europe, Alphen aan den Rijn, The Netherlands) automatic tissue processor in the sequence described in Table 2.2

Following processing brains were embedded in fresh paraffin, mounted on a plastic cassette and allowed to set at room temperature. Paraffin embedded tissue blocks were cut at 6μm on a microtome prior to mounting on poly-L-lysine coated slides

| Solution | Duration | Temperature |
|---|---|---|
| 70% Ethanol | 2 x 30 mins | Room temperature |
| 90% Ethanol | 2 x 30 mins | Room temperature |
| 100% Ethanol | 2 x 30 mins | Room temperature |
| Xylene | 2 x 30 mins | Room temperature |
| Paraffin wax | 3 x 30 mins | 65°C |
| Paraffin wax | Overnight | 65°C |

**Table 2.1: Manual processing of brains for paraffin embedding** Sequence of solutions used and time spent in each for manual preparation of brains for paraffin embedding

| Solution | Duration | Temperature |
|---|---|---|
| 50% Ethanol | 60 mins | 35ºC |
| 80% Ethanol | 60 mins | 35ºC |
| 95% Ethanol | 60 mins | 35ºC |
| 100% Ethanol | 60 mins | 35ºC |
| 100% Ethanol | 90 mins | 35ºC |
| 100% Ethanol | 120 mins | 35ºC |
| 100% Ethanol | 60 mins | 35ºC |
| Xylene | 3 x 60 mins | 35ºC |
| Paraffin wax | 3 x 60 mins | 60ºC |
| Paraffin wax | Hold for at least 60 mins | 60ºC |

**Table 2.2: Automatic processing of brains for paraffin embedding** Sequence of solutions used and time spent in each for automatic preparation of brains for paraffin embedding

(SuperFrost, Menzel-Gläser, Braunschweig, Germany) or charged slides (SuperFrost Plus, VWR International, Lutterworth, UK).

## 2.5 Histology

Slides containing sections from the level corresponding to -1.94mm from bregma according to Franklin and Paxinos (1997) were selected for staining with haematoxylin and eosin (H&E) and fluoro-jade C (FJC) to determine the presence of neuronal damage. All analyses were carried out by a single blinded experimenter

### *.2.5.1 Haematoxylin and eosin staining*

Sections were deparaffinised in an oven at 60°C for 30 minutes and then in xylene for 15 minutes. They were then rehydrated through graduated alcohol solutions and running tap water. Sections were immersed in Gill's haematoxylin solution (Thermo Fisher, Loughborough, UK) for 35 seconds and then rinsed briefly in running tap water. Staining was differentiated in a solution of 1% HCl in 70% ethanol for 8 seconds and sections were then washed in running tap water for 2 minutes. Immersion in Scott's tap water solution (2% $MgSO_4$, 0.35% $NaHCO_3$) for 2 minutes achieved blueing of the nuclei, this was followed by a two minute wash in running tap water. Sections were then placed in eosin Y solution (Surgipath, Cambridgeshire, UK.) for 2 minutes and washed again for 2 minutes in running tap water before dehydration in graduated alcohols and xylene. Sections were then

mounted and coverslipped using DPX mounting medium (Thermo Fisher, Loughborough, UK)

### *2.5.2 Fluoro-jade C staining*

The fluoro-jade C (FJC) staining protocol was adapted from Schmued et al. (2005). Sections were deparaffinised and rehydrated as described for haematoxylin and eosin (H&E) staining. Sections were washed for 2 minutes in distilled water followed by transfer to 0.06% potassium permanganate solution for 15 minutes. After three 1 minute washes in distilled water, sections were placed in a 0.0001% solution of FJC (Millipore, Watford, UK) in 0.1% acetic acid for 10 minutes. Sections were again given three one minute washes in distilled water and dried in an oven at 60°C before clearing in xylene and coverslipping and mounting in DPX.

### *2.5.3 Quantification of neuronal damage*

Damage to neuronal perikarya was assessed using FJC or H&E stained sections in the cortex, hippocampus and dorsal thalamus.

In H&E stained sections the presence or absence of damaged eosinophilic neurons was recorded. Damaged neurons appeared pyknotic and were distinguishable from dark cell change by their eosinophilic appearance (e.g. Figure 3.4, arrowheads; Jortner, 2006).

In FJC stained sections the presence or absence of fluorescent, damaged neurons was noted. Damaged neuronal cell bodies were identifiable as green fluorescently labelled cells against a dark background.

## 2.6 Immunohistochemistry

One section adjacent to those used for histological staining was selected from each animal for each of the immunohistochemical stains used. All analyses were carried out by a single blinded experimenter.

*2.6.1 Immunohistochemistry*

Sections were deparaffinised and rehydrated as described for H&E staining. Endogenous peroxidase activity was blocked by immersion of sections in a solution of 3% $H_2O_2$ in methanol for 30 minutes. Sections were then washed for 10 minutes. Antigen retrieval was performed at this stage as necessary (see Table 2.3). Two ten minute washes in phosphate buffered saline (PBS) preceded incubation for 1 hour at room temperature in a solution of 0.5% bovine serum albumin and 10% normal serum in PBS to block non-specific binding. After incubation the blocking solution was drained off and primary antibody solution made in blocking solution was applied and sections incubated overnight at 4°C. Sections were then washed twice for ten minutes in PBS before application of the appropriate biotinylated secondary antibody made in PBS at a dilution of 1:100 for 1 hour at room temperature. Following two

further 10 minute washes in PBS sections were incubated for 1 hour in an avidin-biotin-peroxidase complex solution (Vector Labs, Peterborough, UK) then given two washes in PBS for 10 minutes. Sections were developed by incubation with 3,3'-diaminobenzidine (Vector Labs, Peterborough, UK) for 3 minutes before washing for 10 minutes in running water and dehydration through graduated alcohol solutions as described for haematoxylin and eosin staining. Sections were mounted and coverslipped with DPX. Prior to dehydration sections stained against myelin associated glycoprotein (MAG) were counterstained with haematoxylin using the same procedure as described for H&E staining. Sections were dehydrated and mounted following the blueing step.

Details of the primary antibodies used, along with their corresponding secondary antibodies, normal sera and antigen retrieval protocols are listed in Table 2.3. Optimal concentrations for primary antibody use were determined by testing a range of dilutions in sections from the same animals in which staining was to be carried out.

In the case of staining sections from 3xTg mice with primary antibodies raised in mouse, a high level of non-specific staining from the anti-mouse secondary was found, possibly due to an elevated inflammatory response to injury in these animals. In these instances a “Mouse on Mouse” kit (Vector, Peterborough, UK) was used to decrease undesirable staining. This necessitated the following changes to the staining protocol. After antigen retrieval or blocking of endogenous peroxidases the mouse on mouse blocking reagent was applied for 30 minutes at room temperature.

| Primary antibody | Clone | Supplier | Dilution | Antigen retrieval | Normal serum | Secondary antibody |
|---|---|---|---|---|---|---|
| Amyloid precursor protein (APP) | 22C11 | Millipore, Watford, UK | 1:5000 (wild-type study)<br>1:1000 (3xTg study) | Microwaved for 10 minutes in 0.01mol/L and left to cool for 30 minutes | Horse | Anti mouse |
| Amyloid β | 4G8 | Millipore, Watford, UK | 1:250 | 10 minutes in 80% formic acid | Horse | Anti mouse |
| | | Cambridge Bioscience, Cambridge UK | 1:1000 | | | |
| Myelin basic protein (MBP) | 12 | Millipore, Watford, UK | 1:5000 | N/A | Rabbit | Anti rat |
| Myelin associated glycoprotein (MAG) | L-20 | Santa Cruz Biotechnology, Heidelberg, Germany | 1:500(wild-type study)<br>1:100 (3xTg study) | N/A | Horse | Anti goat |
| Normal human tau | HT7 | Source Bioscience, Nottingham, UK | 1:1000 | N/A | Horse | Anti mouse |
| Tau hyperphosphorylated at S202 (AT8) | AT8 | Thermo Fisher Scientific, Cramlington, UK | 1:150 | N/A | Horse | Anti mouse |

**Table 2.3: Details of antibodies used in immunohistochemistry studies**

Details of the antibodies used for immunohistochemical staining, including supplier, working dilution, antigen retrieval and appropriate secondary antibodies and normal sera.

Sections were then washed in PBS and blocked for 1 hour in protein concentrate solution. After draining off the protein concentrate solution primary antibody, diluted in protein concentrate solution was applied overnight at 4°C. Following washing in PBS, sections were incubated for 1 hour in biotinylated anti-mouse secondary antibody from the kit. From this point on the protocol was carried out as usual. When assessing amyloid precursor protein (APP) and amyloid β staining in white matter this kit was found to decrease staining in white matter close to the injury site so analyses of white matter pathology using these antibodies were carried out in sections stained in the previously described manner by Mr. Tommy Dingwall.

*2.6.2 Quantification of axonal damage*

Axonal pathology was assessed in the cingulum, corpus callosum, cortex, external capsule, internal capsule and in the dorsal thalamus. Axonal damage was identified in APP immunostained sections and defined as the presence of intense APP immunoreactivity in swollen or bulbous axons (McKenzie et al., 1996).

A counting grid of defined area was used to count axonal bulbs per $mm^2$ of each region. Counting was carried out at 600x magnification on an Olympus BX51 (Olympus UK, Southend-on-Sea, UK) microscope in the study of wild-type mice and at 400x magnification on a Leica DMR microscope (Leica microsystems, Milton Keynes, UK) in the 3xTg study. Counts were conducted twice, on separate days and an average taken, these values underwent the transformation $\log_{10}(\text{count} + 1)$ before analysis. The total area sampled in each region in the studies in wild type mice was

as follows; cingulum 0.0028mm$^2$, corpus callosum, external capsule, internal capsule 0.0056mm$^2$; cortex, thalamus 0.0556mm$^2$. The total area sampled in each region in the studies in 3xTg mice was as follows; cingulum 0.0063mm$^2$, corpus callosum, external capsule, internal capsule 0.0125mm$^2$; cortex, thalamus 0.125mm$^2$. To establish the reproducibility of this technique, slides were taken from 3 animals at random for each study. Damaged axons were counted as described above 3 times. If results were within 10% of the median score reproducibility was deemed to be sufficient.

*2.6.3 Quantification of myelin damage*

Myelin integrity was assessed in MBP immunostained sections. Relative optical density (ROD) values were measured using an image analysis system (MCID 7.0, InterFocus Imaging Ltd, Cambridge, UK) and QImaging QICAM Fast 1394 camera (QImaging, Surrey, BC, Canada) connected to a microscope (Leica Microsystems UK, Milton Keynes, UK). Measurements for all cases were taken at the same light intensity at 100x magnification. ROD readings were taken in the cortex, cingulum, corpus callosum, external capsule, internal capsule and in the dorsal thalamus. Eight ROD measurements were taken from each region bilaterally using a sampling box of 0.01mm$^2$ in the cortex and thalamus and of 0.001mm$^2$ in all other regions. ROD values were averaged for each region and ipsilateral measurements expressed as a percentage of the corresponding contralateral measurement to control for possible differences in exposure time during staining. In order to establish the reliability of this technique slides from three animals were chosen at random from each group of

animals to be examined and analysed as described three times. The measure was deemed reproducible when the 3 measurements fell within 10% of the median value.

Due to variations between the regions in the appearance of normal staining, particularly, the low level of staining in the thalamus, image analysis of MAG immunostaining was not possible. Instead myelin integrity as indicated by the presence of myelin debris was graded in MAG immunostained sections based on photographs of the cingulum, corpus callosum, external capsule, internal capsule and thalamus taken at 200x magnification on a Leica DMR microscope (Leica Microsystems UK, Milton Keynes, UK) using a QImaging QICAM Fast 1394 (QImaging, Surrey, BC, Canada). Myelin debris appeared as small, darkly stained points in white matter. The grade assigned to the pathology present in each structure was based on the most severe pathology evident in that structure. In studies in wild-type mice the grades were defined as follows; normal, even staining of white matter (grade 0), minimal myelin debris (grade 1), modest myelin debris (grade 2). Examples of each grade are shown in Figure 2.3. Reproducibility of MAG quantification was established was again established by selecting slides from 3 animals at random and grading carried out three times as described above. Assessment was regarded as reproducible when the grades assigned in each assessment agreed. In 3xTg mice damage was assessed as present or absent as the low levels of damage in this group meant it was not possible to reliably differentiate between different levels of damage.

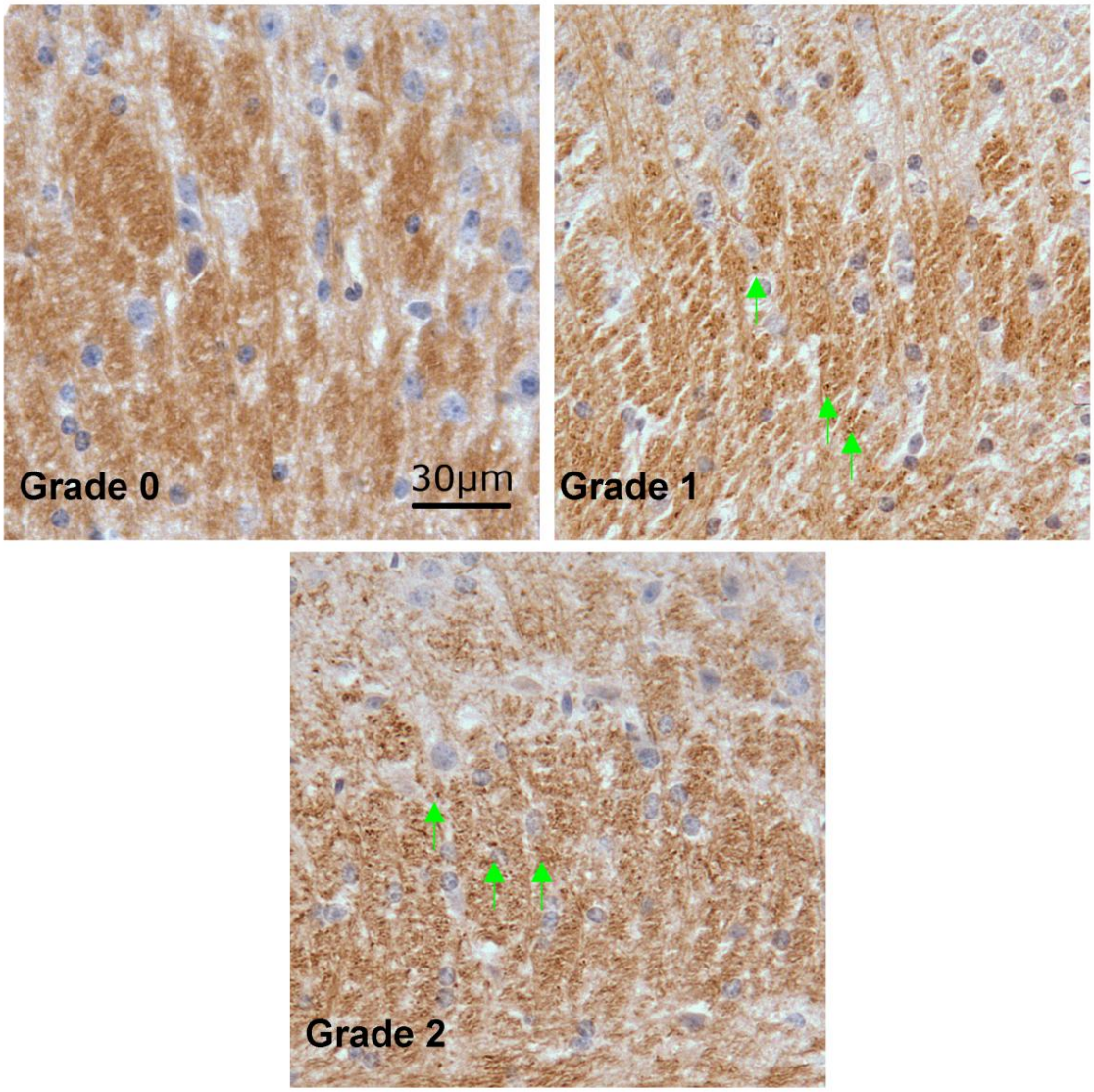


**Figure 2.3: Grading scale of damage visualised using MAG immunostaining in wild–type mice following FPI**
Myelin damage visualised using MAG staining was graded on a scale from 0 to 2 in the cingulum. The grades were defined as follows; normal, even staining of white matter (grade 0), minimal myelin debris (green arrows), vacuolation, and disorganisation of fibres (grade 1), modest myelin debris (green arrows), vacuolation, and disorganisation of fibres (grade 2).

*2.6.4 Quantification of amyloid β pathology*

Immunostaining for amyloid β was assessed in both white matter and in cell bodies. Amyloid β staining in white matter tracts was defined as the presence of darkly stained bulbs. This staining was quantified in the same way as APP staining in studies involving 3xTg mice (above). Reproducibility was also established in the same way as for APP staining.

Intracellular staining was measured in the amygdala, cortex and the CA1, CA2, CA3 and dentate gyrus subfields of the hippocampus. Images of these regions were taken at 100x magnification on an Olympus BX51 microscope (Olympus UK, Southend-on-Sea, UK) using a QImaging MicroPublisher 3.3 camera (QImaging, Surrey, BC, Canada). Images were converted to greyscale and the percentage surface area stained in each region photographed was measured in ImageJ (U. S. National Institutes of Health, Bethesda, USA). Values obtained in this way underwent the transformation $\log_{10}(\text{count} + 1)$ before analysis. The total area sampled in each region was as follows; amygdala, $0.14mm^2$; cortex $0.56mm^2$; CA1 and CA3 $0.08mm^2$; CA2 and dentate gyrus $0.04mm^2$. Reproducibility was established similarly to other techniques, with a random selection of three animals being quantified three times and values within 10% of the median being taken to indicate acceptable reproducibility.

*2.6.5 Quantification of tau pathology*

Normal human tau was quantified and reproducibility established in the same way as intracellular amyloid β staining.

As the amount of staining of abnormally phosphorylated tau visualised was very low, this staining did not lend itself to quantification and the presence or absence of abnormally phosphorylated tau in the cingulum, corpus callosum, cortex, external capsule, internal capsule and in the dorsal thalamus was recorded. In white matter regions positive staining appeared as darkly stained spheroids, while in the grey matter areas immunopositive neurons were recorded.

## 2.7 Tissue preparation

Animals selected for biochemical analysis following FPI were terminated by cervical dislocation. The brains were removed and a 4mm coronal section of tissue around the injury site was dissected out. The hypothalamus was removed and the section divided into hemispheres. Dissections were carried out on ice. The pieces of tissue were placed in labelled eppendorf tubes and snap frozen on liquid nitrogen before storage at -80°C.

*2.7.1 Tissue homogenisation*

Tissue for biochemical analysis was homogenised in buffer containing 250mM sucrose, 20mM Tris Base, 1mM (ethylenediaminetetraacetic acid) EDTA and 1mM (ethylene glycol tetraacetic acid) EGTA in distilled water. Protease and phosphatase inhibitors (Merck, Nottingham, UK) at concentrations of 1:100 and 1:50, respectively were added to the buffer. After homogenisation with a Dounce homogeniser samples were mixed 1:1 with buffer containing 0.4% diethylamine and 0.1M NaCl. Samples were spun for 5 minutes at a rotor speed of 3000 rpm in a Sigma 1-13 benchtop centrifuge (Sci Quip Ltd., Shrewsbury, UK) and the supernatant removed and stored at -80°C before use.

*2.7.2 Determination of protein content of samples*

The amount of protein present in samples was determined using a bicinchoninic acid protein assay kit (Thermo Fisher Scientific, Cramlington, UK). Samples and standards were diluted 1:7 in distilled water and loaded in triplicate on to a 96-well plate. The working reagent (consisting of a solution of sodium carbonate, sodium bicarbonate, bicinchoninic acid and sodium tartrate in 0.1M sodium hydroxide mixed 50:1 with 4% cupric sulphate solution) was added and the plate incubated at 37°C for 30 minutes. The plate was cooled to room temperature before the absorbance was read at 562nm on a Dynex MRX plate reader (Dynex Technologies Ltd., Worthing, UK). Values obtained from protein standards were used to generate a standard curve from which the protein concentration of the samples was calculated.

## 2.8 Western blotting

*2.8.1 Western blotting*

Samples were made up to concentrations of either 1µg/µL or 0.5µg/µL with 0.25µL of 4x Laemelli buffer per µL and the same buffer containing 250mM sucrose, 20mM Tris Base, 1mM EDTA and 1mM EGTA in distilled water that was used in the homogenisation procedure. Control sample, consisting of tissue from two experimentally naïve 10 month-old 3xTg mice was prepared in the same way.
Proteins were denatured by incubation at 70°C for 10 minutes on a water bath and loaded on to precast 4-12% Bis/Tris gels (Invitrogen, Paisley, UK) along with molecular weight marker (Li-Cor, Cambridge, UK). Control samples were loaded twice on each gel. Proteins were separated by sodium dodecyl sulfate polyacrylamide gel electrophoresis (SDS-PAGE) electrophoresis with 2-(N-morpholino)ethanesulfonic acid (MES) running buffer (Invitrogen, Paisley, UK). Samples were run at 80V through the stacking gel (45 minutes) and at 120V to the bottom of the gel (1.5 to 2 hours), except where APP C-terminal fragments were to be detected when samples were run at 80V to the bottom of the gel.

Proteins were transferred to a polyvinylidene fluoride (PVDF) membrane (GE Healthcare, Little Chalfont, UK) at 30V for 2.5 hours in an XCell II™ Blot Module (Invitrogen, Paisley, UK). Transfer success and evenness of loading was estimated by staining gels in Coomasie Blue (Bio-Rad, Hemel Hempstead, UK) for one hour.

Gels that had not transferred well or where loading was uneven across the gel were excluded and repeated. Membranes were rinsed in PBS and placed in light proof boxes and incubated in Odyssey blocking buffer (Li-Cor, Cambridge, UK) made 1:1 with PBS for one hour. Blocking buffer was then drained off and primary antibody made in blocking buffer and also containing anti glyceraldehyde 3-phosphate dehydrogenase (GAPDH) at a concentration of 1:100000 and 0.1% tween-20. The anti-GAPDH antibody that was added to the solution was raised in a different species to the primary antibody of interest. Membranes were incubated in primary antibody overnight at 4°C. Membranes were washed six times for 5 minutes in PBS containing 0.1% tween-20 before incubation for 45 minutes in a solution of the appropriate secondary antibodies tagged with fluorescent infra-red dye (Li-Cor, Cambridge, UK) made at a concentration of 1:3000 in blocking buffer containing 0.1% tween-20 and 0.01% sodium dodecyl sulphate (SDS). The two secondary antibodies used were tagged with dyes that fluoresced at different wavelengths. Membranes were again washed six times for 5 minutes in PBS before finally being washed in PBS before drying and scanning on an Odyssey infrared scanning system (Li-Cor, Cambridge, UK).

Details of the primary antibodies used, including concentrations, appropriate secondary antibodies and the amount of protein required for detection are in Table 2.4.

*2.8.2 Quantification of protein levels*

The scanned images from the blots were analysed using Odyssey application software (version 3.0; Li-Cor, Cambridge, UK) to quantify the intensity of fluorescence of the protein bands of interest. Western blots were run twice for each antibody. The intensity values for the proteins of interest were expressed as a ratio of the intensity of the GAPDH band to control for variation in loading. Bands where there was evidence of bubbles or other noise were excluded from analysis. The values obtained from the two Western blots were averaged for analysis. The intensity of the GAPDH band was also averaged across gels and an independent samples t-test used to compare the values obtained for each group. This was to rule out the presence of a systematic loading bias and was repeated for every set of Western blots conducted. In all cases there was no difference in the intensity of the GAPDH band between the groups ($p > 0.05$ in all cases). Reproducibility of the gel was established by visual comparison of the blots as well as plotting the values obtained in each blot analysed for a given protein on the same axes and visually assessing whether the values obtained showed the same pattern of increases and decreases. A representative example of GAPDH values obtained for each group across a set of Western blots and a reproducibility comparison are shown in Figure 2.4.

| Primary antibody | Clone | Supplier | Dilution | Secondary antibody | Amount of protein loaded |
|---|---|---|---|---|---|
| Amyloid precursor protein (APP) | 22C11 | Millipore, Watford, UK | 1:3000 | Anti mouse | 10µg |
| APP C-terminal fragments | Polyclonal | Merck, Nottingham, UK | 1:1000 | Anti rabbit | 30µg |
| Myelin basic protein (MBP) | 12 | Millipore, Watford, UK | 1:10000 | Anti rat | 5µg |
| Normal human tau | HT7 | Source Bioscience, Nottingham, UK | 1:1000 | Anti mouse | 10µg |
| Tau hyperphosphorylated at S202 (AT8) | AT8 | Thermo Fisher Scientific, Cramlington, UK | 1:500 | Anti mouse | 20µg |
| Glyceraldehyde 3-phosphate dehydrogenase (GAPDH) | GAPDH-71.1 | Sigma-Aldrich, Dorset, UK | 1:100000 | Anti mouse | N/A, dependent on which primary it was combined with |
| Glyceraldehyde 3-phosphate dehydrogenase (GAPDH) | Polyclonal | Sigma-Aldrich, Dorset, UK | 1:100000 | Anti rabbit | |

**Table 2.4: Details of antibodies used in Western blotting studies**

Details the antibodies used for Western blotting, including supplier, working dilution, clone and appropriate secondary antibodies.

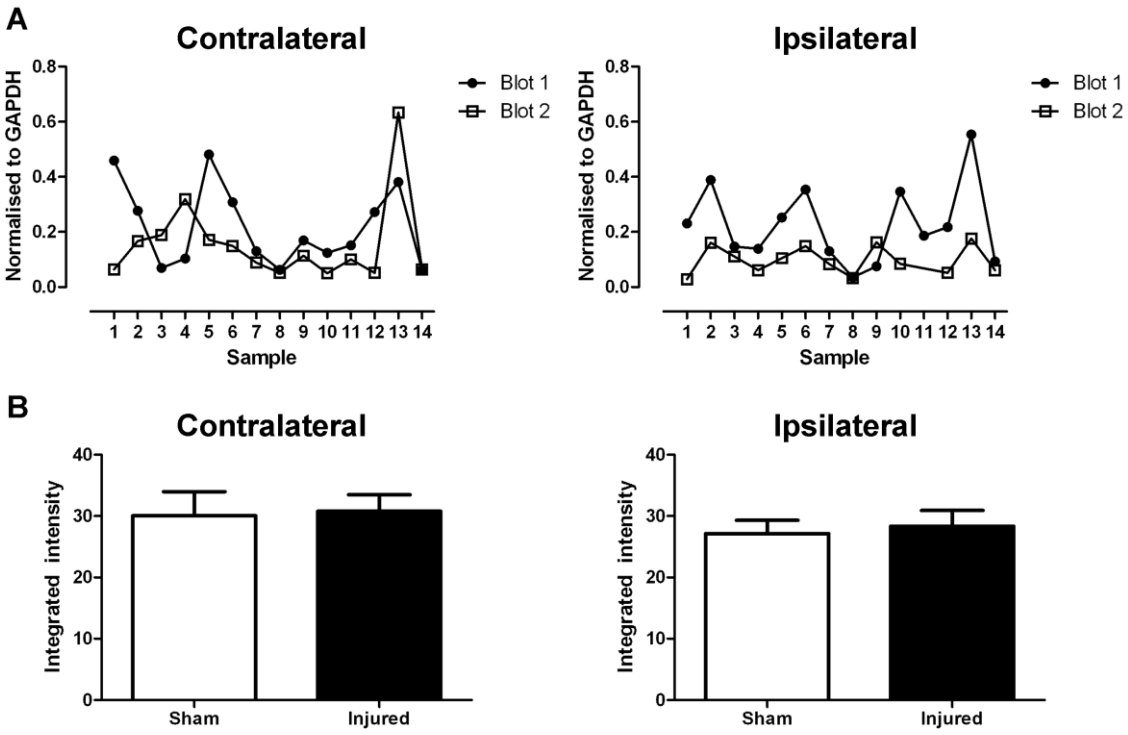


**Figure 2.4: Reproducibility of Western blots and determination of the absence of loading bias**

Reproducibility of Western blots was determined by comparison of the values obtained from each blot to determine whether the pattern of values obtained for the samples was similar. (A) shows reproducible data from AT8 Western blots. (B) Analysis of the intensity of the GAPDH band between groups revealed no significant differences between sham and injured animals. This analysis was conducted for every Western blot carried out. (B) shows representative data from AT8 Western blots.

## 2.9 Dot blot for oligomeric amyloid β

*2.9.1 Dot blot*

Homogenised samples were diluted in PBS so that they contained 2µg of protein per 110µL. Control samples were prepared in the same way from the same tissue used as control sample in Western blotting. An activated nitrocellulose membrane was loaded in to a dot blot apparatus (Bio-Rad, Hemel Hempstead, UK) and samples loaded on to the membrane in duplicate. Samples were drawn through the membrane by means of a vacuum pump and the membrane placed in a light proof box in Odyssey blocking buffer (Li-Cor, Cambridge, UK) made 1:1 with PBS for one hour. The blocking buffer was then drained off and antibody against oligomeric amyloid β (clone A11; Millipore, Watford, UK) made in blocking buffer at a concentration of 1:500 and also containing 0.1% tween-20 was added. The membrane was incubated in primary antibody overnight at 4°C. The membrane was then washed six times for 5 minutes in PBS containing 0.1% tween-20. Following this, the membrane was incubated in a 1:3000 solution of anti mouse secondary antibody tagged with fluorescent infra-red dye (Li-Cor, Cambridge, UK) made with blocking buffer containing 0.1% tween-20 and 0.01% SDS for 45 minutes. The membrane was again washed six times for five minutes in PBS containing 0.1% tween-20 then washed twice for 2 minutes in PBS. The membrane was stored in PBS at 4°C until scanning on an Odyssey infrared scanning system (Li-Cor, Cambridge, UK).

*2.9.2 Quantification of protein levels*

The scanned images were analysed using Odyssey application software (version 3.0; Li-Cor, Cambridge, UK) to quantify the intensity of fluorescence of each of the dots. Dot blots were run twice. The values obtained from each replicate were averaged and expressed as a percentage of the control sample. Dots where there was evidence of noise or that had not been drawn through the membrane properly were excluded from analysis. The values from the two dot blots were averaged for analysis.

# 3 Effect of mild traumatic brain injury on pathology and cognition in wild-type mice

## 3.1 Introduction

White matter is particularly vulnerable to damage in traumatic brain injury (TBI), with damage to white matter being the primary pathology in human patients with mild TBI (Kraus et al., 2007; Sterr et al., 2006). Additionally, mild TBI can result in persistent cognitive deficits (De Beaumont et al., 2009; Lipton et al., 2008; Matser et al., 1999) and predisposes individuals to an increased risk of developing Alzheimer's disease (AD) (Guskiewicz et al., 2005), making this a potentially useful model for investigating the relationship between white matter pathology and AD.

Characterisation of models of mild TBI is lacking in comparison to models of more severe injury levels. Axonal pathology has been demonstrated to be a prominent feature of mild TBI in rodent models, in both the hours (Dikranian et al., 2008; Huh et al., 2008; Li et al., 2006) and weeks after injury (Laurer et al., 2001). This axonal pathology is often observed in conjunction with variable levels of cell death, reflecting the variety of experimental models used to model mild injuries. Use of the controlled cortical impact (e.g. Dikranian et al., 2008; Huh et al., 2008) and weight drop models (Tang et al., 1997a; b) has been shown to produce significant neuronal loss. However, in the study of an injury level where damage occurs primarily to the

white matter, the relevance of models showing widespread neuronal loss is limited. Changes in myelin following mild TBI remain uncharacterised.

Mild TBI-induced axonal damage in the absence of grey matter damage is associated with cognitive deficits measured from hours after injury (Li et al., 2006) to weeks (Long et al., 2009) however, to date no studies have been conducted to examine long-lasting cognitive changes associated with white matter damage, similar to what is observed in human mild TBI.

### *3.1.1 Aims and hypotheses*

The study described in this chapter aimed to examine the effects of mild TBI on white matter and cognition. To investigate this, a detailed examination of axons, myelin and neuronal cell bodies was undertaken at time points ranging from 4 hours to 6 weeks as well as an investigation of learning and memory 3 and 6 weeks after injury.

It was hypothesised that mild TBI would cause selective damage to axons at short and long-term time points after injury as well as inducing a persistent deficit in learning and memory.

## 3.2 Methods

### *3.2.1 Fluid percussion surgery and animals*

Male C57Bl/6J mice (Charles River, UK) weighing 24 – 30g underwent mild lateral FPI (injury severity = 0.9 ± 0.1atm) or sham surgery as described in chapter 2.1. Righting times for injured animals (217 ± 32 seconds) were significantly longer than for control animals (51 ± 9 seconds, $p < 0.001$). Surgical procedures were carried out by Dr. Jill Fowler.

### *3.2.2 Spatial reference memory testing in the Morris water maze*

Water maze testing was carried out according to the protocol detailed in chapter 2.2. Prior to behavioural testing animals were handled for 5 minutes per day for 5 consecutive days to minimise stress resulting from handling. In order to exclude animals showing an abnormal stress response one day of training on the cued version of the water maze task was carried out prior to surgery. No animals were excluded on this basis from this study. Training on the cued version of the water maze task was repeated for four days, beginning 1 week after surgery. Each animal received 4 training trials per day, with a 20 minute interval between trials. Spatial reference memory training began 3 days after the end of training in the cued version of the task. Animals were trained over 5 days with 4 trials per day and a 10 minute

intertrial interval. Probe tests were carried out 10 minutes and 24 hours after the final trial of spatial reference training. Beginning 2 weeks after this the same animals were retested using the same spatial reference memory training protocol in a different water maze with the same dimensions as the first but a different set of cues. The timing of behavioural testing is illustrated in Figure 3.1.

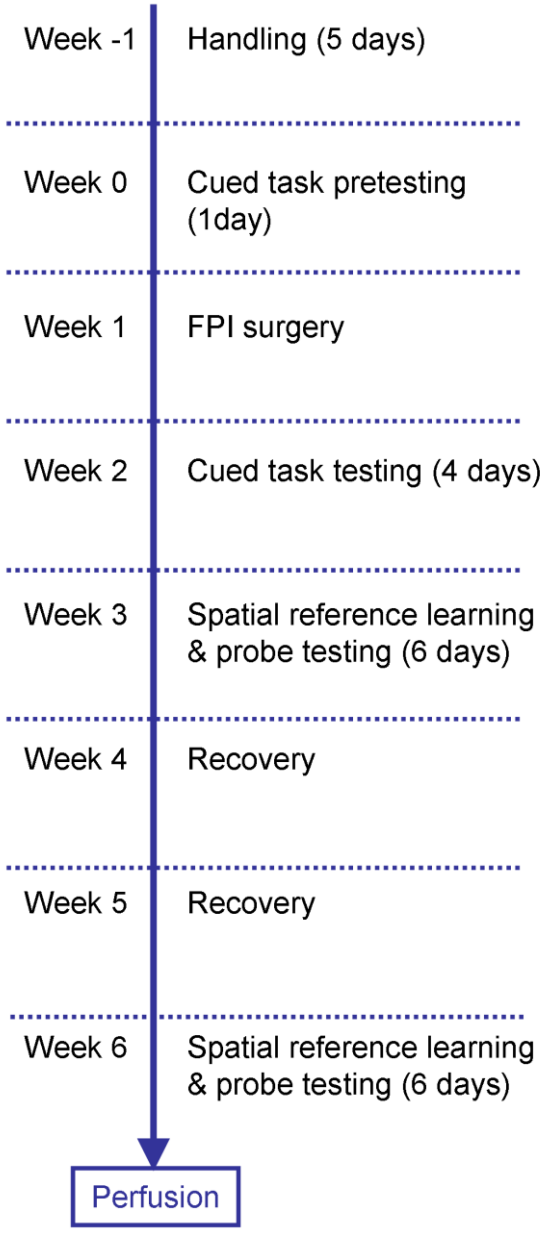


**Figure 3.1: Timeline of behavioural testing**

Animals were handled and pretested in the cued water maze task prior to injury. Further testing on the cued task and in the spatial reference learning task was carried out at two time points following injury

*3.2.3 Histology and immunohistochemistry*

Animals that underwent behavioural testing (n = 7 sham, 10 injured) were sacrificed 6 weeks after injury. Further cohorts of animals were sacrificed at 4 hours (n = 4 sham, 5 injured), 24 hours (n = 4 sham, 5 injured), 72 hours (n = 3 sham, 4 injured) and 4 weeks (n = 5 sham, 5 injured) after surgery for pathological investigation. At termination animals were deeply anaesthetised and transcardially perfused with 20 mL heparinised 0.9% saline in 0.1% phosphate buffer followed by 4% paraformaldehyde in 0.1% phosphate buffer. Brains were postfixed and embedded in paraffin as described in chapter 2.4. 6 µm thick sections were cut and mounted in pairs on poly-L-lysine coated slides. Slides containing sections from the level corresponding to -1.94mm from bregma according to Franklin and Paxinos were selected for staining with haematoxylin and eosin (H&E) and fluoro-jade C (FJC) to determine the presence of neuronal damage. A section from a mouse that had undergone transient focal ischaemia for 1 hour with 23 hours survival at the level corresponding to 0.50mm from bregma served as a positive control for FJC staining. Sections adjacent to those used for histological staining were selected for immunohistochemical staining. Immunohistochemistry for amyloid precursor protein (APP) was performed to detect axonal damage. Myelin damage was investigated using antibodies against myelin associated glycoprotein (MAG) and myelin basic protein (MBP). The histological and immunohistochemical techniques used are described in detail in chapters 2.5 and 2.6. The methods used to quantify neuronal, axonal and myelin damage are detailed in chapter 2.6. Briefly, damage to neuronal perikarya was identified using FJC or H&E stained sections in the cortex,

hippocampus and dorsal thalamus. In H&E stained sections the presence or absence of damaged eosinophilic neurons was recorded. In FJC stained sections the presence or absence of fluorescent, damaged neurons was noted. APP stained sections were used to count axonal bulbs per $mm^2$ in the cingulum, corpus callosum, cortex, external capsule, internal capsule and dorsal thalamus. Counts of axonal bulbs in APP stained sections were log transformed for analysis. MBP stained sections were used to assess myelin integrity in the cortex, cingulum, corpus callosum, external capsule, internal capsule and in the dorsal thalamus. Relative optical density (ROD) measurements were used to quantify myelin integrity in these sections. ROD values were averaged for each region and ipsilateral measurements expressed as a percentage of the corresponding contralateral measurement to control for possible differences in exposure time during staining. MAG staining was graded on a 3 point rating scale from 0 to 2 as illustrated in Figure 2.3.

### *3.2.4 Statistical analysis*

Behavioural data were analysed using two-way ANOVA, using the Greenhouse-Geiser correction where data were significantly not normally distributed (i.e. where Mauchly's test returned a value of $p < 0.05$). *Post hoc* comparisons were made using unpaired t-test. Swim speeds from cued water maze testing were analysed using unpaired t-test. Data from axonal counts and MBP image analysis were analysed using unpaired t-tests. Data from grading of MAG staining were tested for significance using Mann-Whitney U.

## 3.3 Results

### *3.3.1 Spatial reference learning is impaired 3 weeks after mild traumatic brain injury*

Both injured and sham animals decreased their latency to the cued platform over the training period ($F_{(1.871,28.071)}$ = 26.731, $p$ < 0.001; Figure 3.2A). There was no difference in performance between the injured and the sham-operated groups ($F_{(1,15)}$ = 2.698, $p$ = 0.121). Escape latencies averaged less than 10 seconds in both groups by the end of training. Mean swim speed across all trials did not differ significantly between injured and sham-operated animals (20.756 ± 0.768 cm/s vs. 19.456 ± 0.957 cm/s; |t| = 1.067, df = 15, $p$ = 0.303 respectively, mean ± SEM).

Mild TBI impaired the ability of animals to learn the location of a hidden platform (Figure 3.2B). The latency for injured animals to find the platform did not change significantly over the five training days ($F_{(4,36)}$ = 1.401, $p$ = 0.253). The latency for sham animals to find the platform decreased significantly over the same training period ($F_{(1.312,7.870)}$ = 9.993, $p$ = 0.011). The performance of the two groups was significantly different from each other on days 4 (|t| = 2.175, df = 15, $p$ = 0.046) and 5 (|t| = 2.434, df = 15, $p$ = 0.028) of testing. Both groups showed the same degree of preference for the training quadrant when probed both 10 minutes (group x quadrant interaction, $F_{(1.715,25.719)}$ = 2.639, $p$ = 0.098; Figure 3.2C) and 24 hours (group x quadrant interaction, $F_{(3,45)}$ = 0.525, $p$ = 0.667; Figure 3.2D) after the end of training.

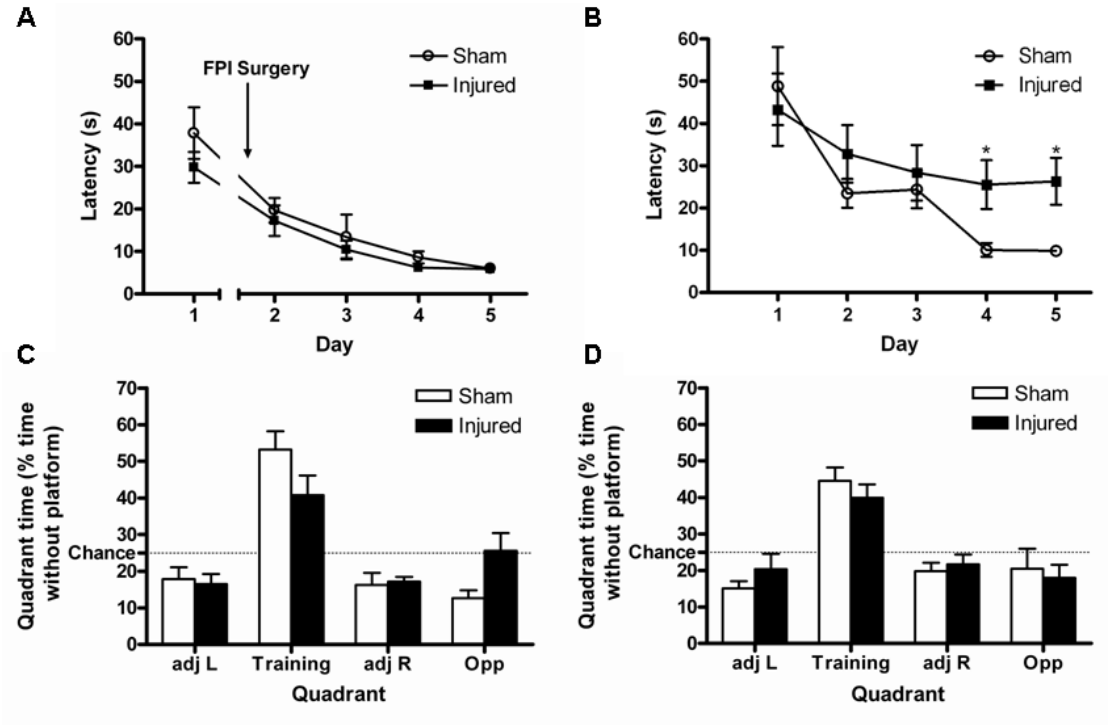


**Figure 3.2: Water maze performance 3 weeks after mild TBI in wild-type mice**

Sham and injured mice both improved their performance in the cued version of the water maze task over the training period (A). Injured mice did not significantly improve their latency to the hidden platform over the training days, while sham animals did (B). Both groups also displayed equivalent retention of the training platform location at both 10 minutes (C) and 24 hours after training (D). Graphs show mean + SEM. * = $p \leq 0.05$ vs. sham. adjL = adjacent left, adjR = adjacent right

### *3.3.2 No impairment of spatial reference learning and memory 6 weeks after mild traumatic brain injury*

At 6 weeks after injury both injured and sham animals decreased their latency to the platform significantly over the training days ($F_{(4,36)}$ = 7.100, $p$ < 0.001 and $F_{(4,24)}$ = 7.037, $p$ = 0.001 respectively; Figure 3.3A). Injured and sham animals showed no difference in their preference for the training quadrant when retention for the platform location was probed at 10 minutes (group x quadrant interaction, $F_{(1.752,26.283)}$ = 0.176, $p$ = 0.912; Figure 3.3B) and 24 hours (group x quadrant interaction, $F_{(1.908,28.619)}$ = 0.549, $p$ = 0.575; Figure 3.3C) after the end of training.

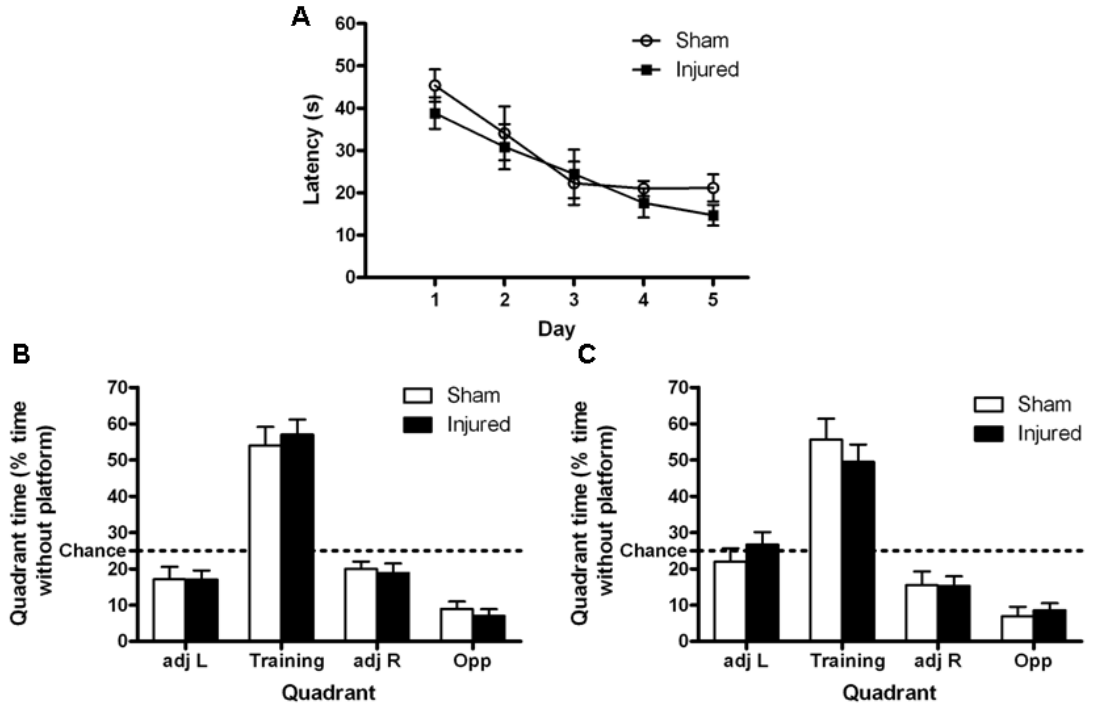


**Figure 3.3: Water maze performance 6 weeks after mild TBI in wild-type mice**

Sham and injured mice both improved their latency to the hidden platform over the training days (A). Both groups also displayed equivalent retention of the training platform location at both 10 minutes (B) and 24 hours after training (C). Graphs show mean + SEM. adjL = adjacent left, adjR = adjacent right

.

*3.3.3 Cell death is not increased following mild traumatic brain injury*

H&E staining identified damaged neurons which were distinguishable from dark cell change by their eosinophilic appearance and pyknotic nuclei (Figure 3.4, arrowheads; Jortner, 2006). In the cortex local to the craniotomy site, nine of fourteen brain-injured animals and six of eleven sham-injured animals had moderate neuronal damage at 4, 24 and 72 hours after injury. In both groups damage was confined to cortical layers I and II. At 4 weeks after injury, only one of five brain-injured animal displayed eosinophilic neurons in the hippocampus. No damage was seen in any animal 6 weeks after injury. Notably, in the hippocampus there was minimal evidence of neuronal damage in either the TBI or sham group and only isolated damaged neurons were observed in the CA1 of the ipsilateral hippocampus at 4, 24 and 72 hours after injury in both sham and injured animals and in 3 brain-injured animals at 6 weeks after injury. No damaged neurons were observed in the thalamus in either hemisphere at any time point (Appendix A.7).

FJC staining identified damaged neuronal cell bodies by the presence of green fluorescently labelled cells against a dark background. The pattern of damage observed in FJC stained sections mirrored that observed using H&E. Damaged cells were seen almost exclusively in the cortex local to the craniotomy site. Five out of nine brain-injured animals and six out of eight sham-injured showed damaged cells in this region at 24 and 72 hours after injury. Four weeks after injury two of five brain-injured animals and one of five sham-injured animals displayed damage in this region and at 6 weeks after injury there was evidence of damage only in one injured

animal. No FJC positive cells were observed in the hippocampus or thalamus in either hemisphere at any time point. FJC positive cells were visible throughout the ipsilateral striatum of the positive control section. These data are summarised in Appendix A.7.

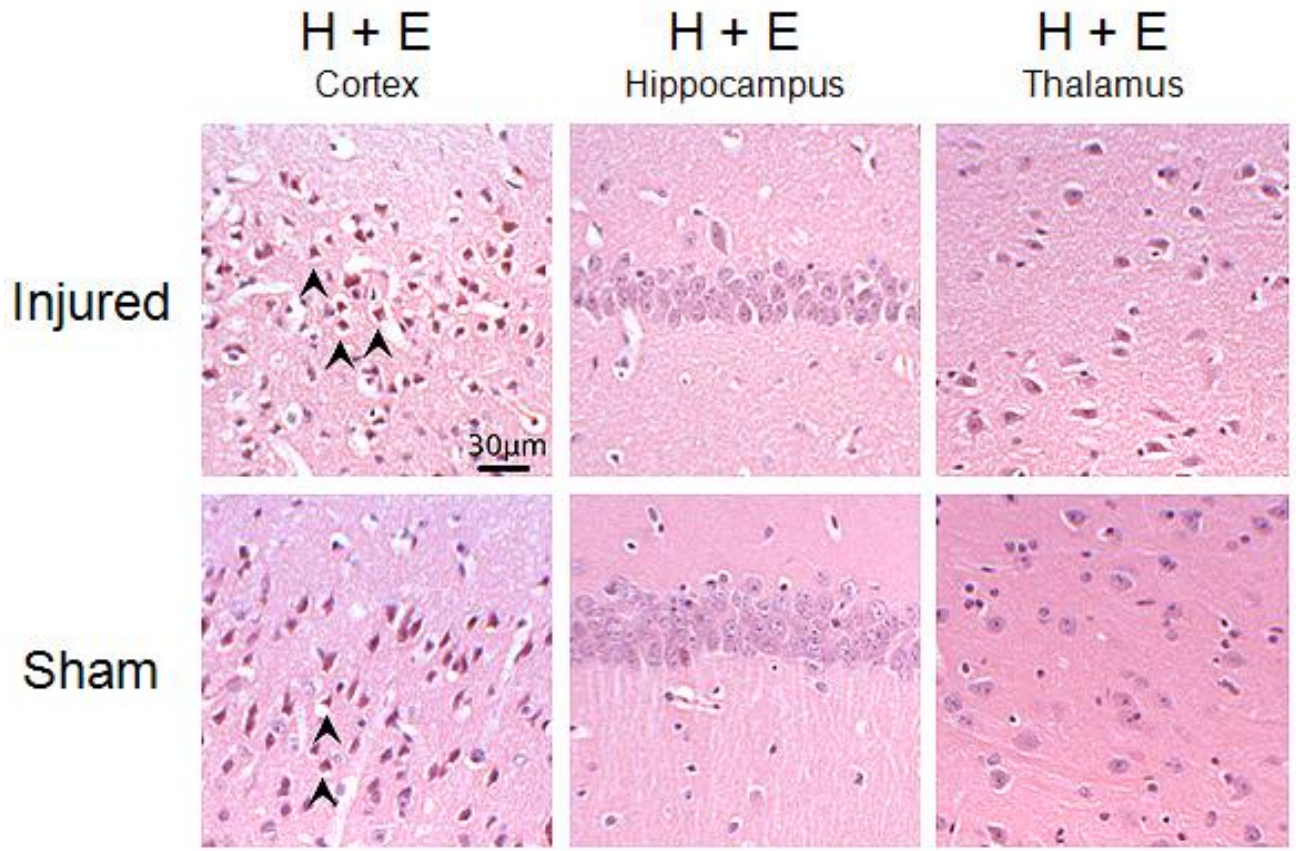


**Figure 3.4: Cellular changes in the ipsilateral hemisphere after mild TBI**

Both injured and sham animals show damaged neurons in the cortex close to the injury site but not in the hippocampus or thalamus as demonstrated by H&E staining. Arrowheads indicate damaged neurons. Neuronal damage is most prominent at 4 to 72 hours after injury and is absent at 8 weeks after injury.

### *3.3.4 Progressive axonal damage following mild traumatic brain injury*

Damaged axons were identified by the presence of intense APP immunoreactivity in swollen or bulbous axons (McKenzie et al., 1996). Brain-injured animals showed extensive and localised axonal damage at all time points as compared to sham. The location of the damage was time dependent. In the short-term response to injury, axonal changes were confined to brain regions adjacent to the site of injury. At 4 hours after injury there was significantly more axonal damage in the ipsilateral cingulum of brain-injured animals than sham injured controls ($|t| = 3.483$, $p = 0.010$; Appendix A.1). There were no significant differences between the groups in other regions at this time point. At 24 and 72 hours after injury there were no significant differences in the levels of axonal damage observed in each of the two groups. 4 weeks after injury brain-injured animals showed significantly higher numbers of axonal bulbs than shams in the external capsule ($|t| = 2.433$, $p = 0.041$). Other regions were unaffected at this time point. A significant difference between the groups was observed in the external capsule and thalamus at 6 weeks after injury ($|t| = 2.377$, $p = 0.041$ and $|t| = 5.418$, $p < 0.001$, Appendix A.4) while no differences were apparent in other regions examined. Representative examples of APP immunostaining in the external capsule and thalamus at each time point are shown in Figures 3.5 and 3.6. The pattern of change in axonal pathology in the ipsilateral hemisphere is shown in Figure 3.7.

### *3.3.5 No damage to myelin following mild traumatic brain injury*

In general, at all time points in all regions studied, there was minimal evidence of myelin pathology as assessed using either MAG or MBP immunostaining. In MAG immunostained sections there was no evidence of small, darkly stained points of myelin debris in white matter at 4 (Appendix A.2) and 72 hours after injury in any region. Two out of five injured animals showed mild to moderate debris accumulations in the ipsilateral cingulum, corpus callosum and external capsule at 24 hours after injury but this was not significantly different from shams (cingulum; 0.0 + 0.9 vs. 0.0 ± 0.0, $p = 0.730$, corpus callosum; 0.0 + 0.5 vs. 0.0 ± 0.0 $p = 0.413$, external capsule; 0.0 + 0.9 vs. 0.0 ± 0.0, $p = 0.413$). At 4 weeks after injury myelin debris was evident in the ipsilateral cingulum of two out of five injured animals this was not significantly different to sham animals (0.0 + 0.9 vs. 0.0 ± 0.0, $p = 0.310$). Two injured animals showed myelin damage in the ipsilateral internal capsule, this was not significantly different to sham animals (0.0 + 0.9 vs. 0.0 ± 0.0, $p = 0.310$). Six weeks after injury four out of 10 injured animals showed mild levels of myelin pathology in the ipsilateral cingulum and external capsule and two animals displayed mild debris accumulation in the internal capsule but this did not differ significantly from shams (cingulum; 0.0 + 0.5 vs. 0.0 + 0.8, $p = 1.000$, external capsule; 0.0 + 0.5 vs. 0.0 ± 0.0 $p = 0.193$, internal capsule; 0.0 + 0.4 vs. 0.0 ± 0.0, $p = 0.536$; Appendix A.5). There were no statistically significant differences in the levels of myelin pathology observed in sham and injured animals at any time point in any region. Representative examples of MAG immunostaining in the external capsule and thalamus are shown in Figure 3.8.

In general, at all time points in all regions studied there was minimal evidence of myelin pathology as assessed using MBP immunostaining. In MBP immunostained sections there were no statistically significant differences in myelin integrity in any region at any time point. Representative MBP staining results from 4 hours and 6 weeks after injury are shown in Appendices A.3 and A.6. Representative examples of MBP immunostaining in the external capsule and thalamus are shown in Figures 3.5 and 3.6.

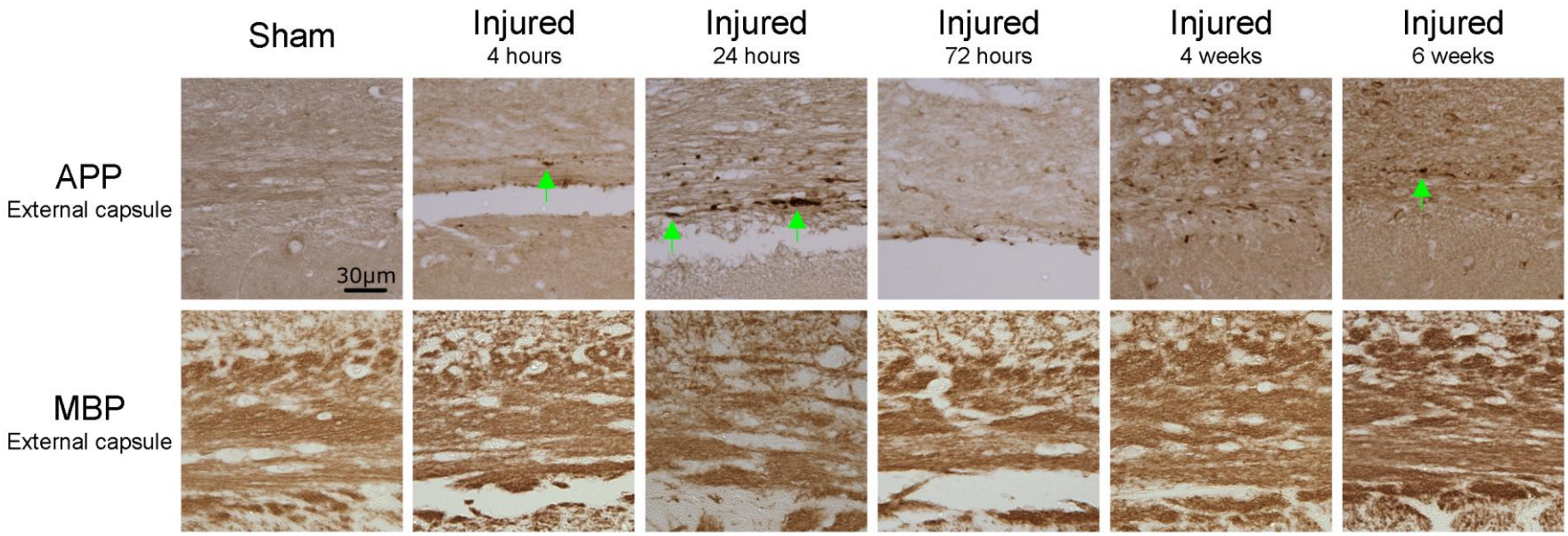


**Figure 3.5: Pattern of axonal and myelin changes in the ipsilateral external capsule from 4 hours to 6 weeks after mild TBI**

APP and MBP staining in the ipsilateral hemisphere over time after injury. Significantly different levels of APP accumulation in the external capsule of injured animals as compared to shams were observed at 4 and 6 weeks after injury. Green arrows indicate damaged axons visualised with APP immunostaining.

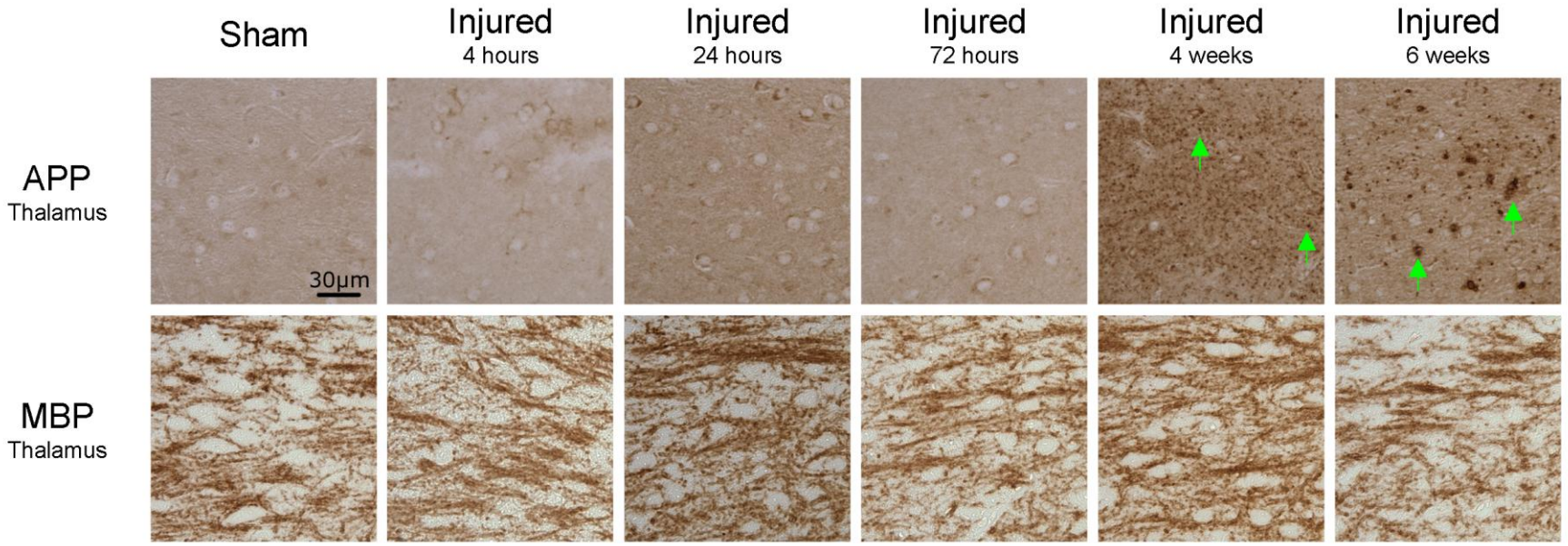


**Figure 3.6: Pattern of axonal and myelin changes in the ipsilateral thalamus from 4 hours to 6 weeks after mild TBI**
APP and MBP staining in the ipsilateral hemisphere over time after injury. Significantly higher levels of APP accumulation in the thalamus of injured animals as compared to shams were observed at 6 weeks after injury. Green arrows indicate damaged axons visualised with APP immunostaining

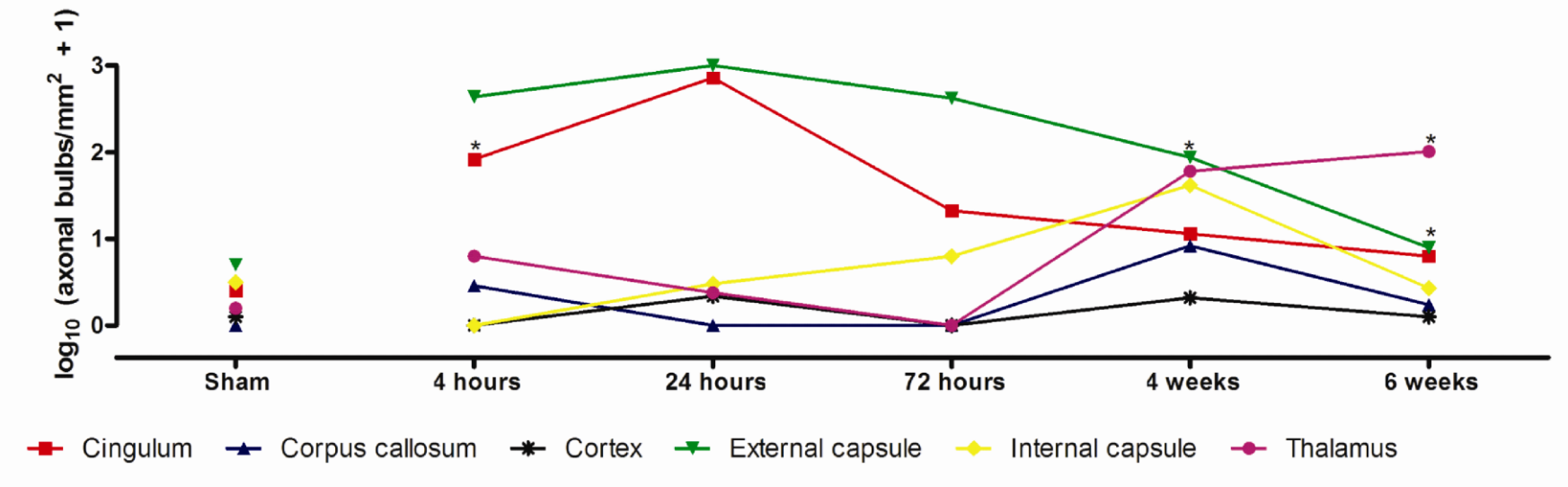


**Figure 3.7: Changing location of damaged axons over time following mild TBI**

Regions where injured animals showed significantly higher numbers of damaged axons to sham controls varied across time after injury. At 4 hours after injury damage was significantly higher in the cingulum of injured animals than in shams. At 6 weeks after injury the areas where injured animals showed increased axonal damage compared to shams were the external capsule and thalamus. Graph shows mean values. * = $p < 0.05$ vs. sham at the same time point.

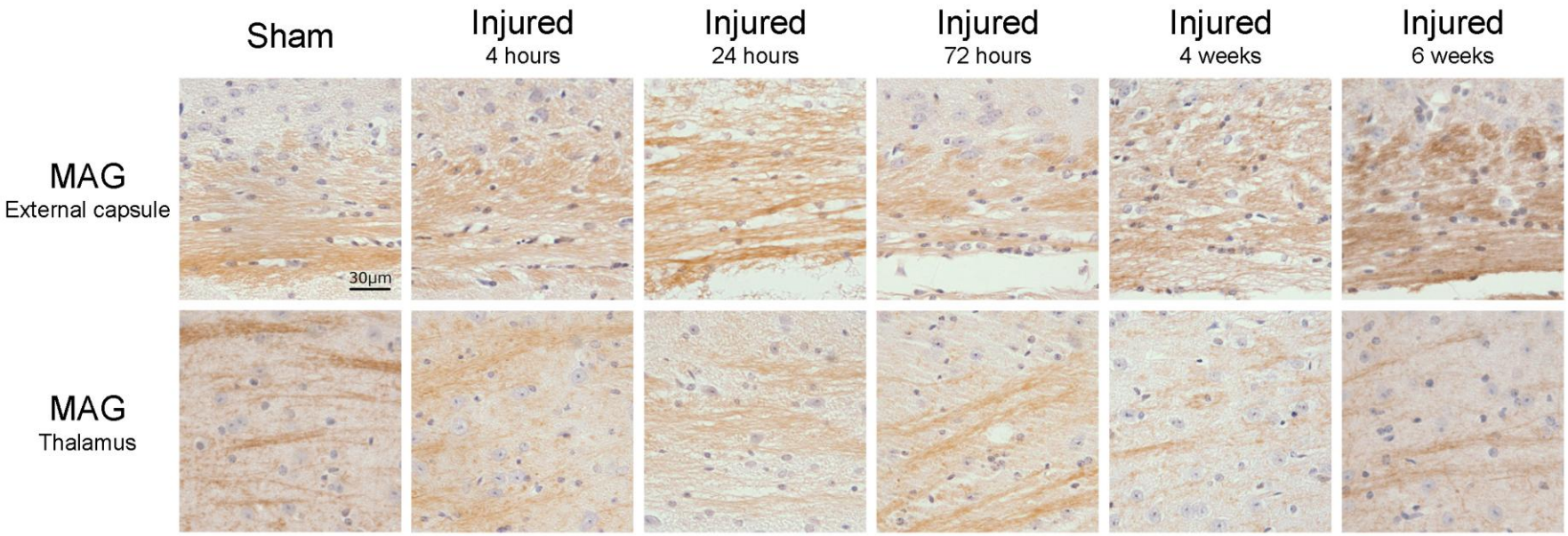


**Figure 3.8: Examples of MAG immunostaining at time points up to 6 weeks after mild TBI**
There were no significant differences in MAG immunostaining between injured and sham animals at any time point in any region examined.

## 3.4 Discussion

Mild TBI is a source of persistent cognitive deficits and damage to white matter as well as a risk factor for AD. Identification of potentially modifiable targets for treatment is necessary to reduce both impairment as a direct result of injury and the risk of developing AD in the future. This requires relevant animal models of mild TBI in order to understand the pathology leading to cognitive impairment and the processes underlying the increased risk of AD after injury. The current study examined pathological and cognitive changes after mild TBI. The hypothesis that mild TBI would cause selective damage to axons was upheld with the observation of selective axonal pathology that showed a spatial progression over time after injury. The hypothesis that mild TBI would produce a persistent deficit in learning and memory was partially upheld with a deficit in spatial reference learning being observed at 3 but not 6 weeks after injury.

Axonal pathology in this model was observed only in specific regions distinct to each time point investigated. APP deposition was first visible in the cingulum close to the injury site. Over the course of 6 weeks damage in the external capsule and dorsal thalamus became evident. The spatial progression of axonal damage indicates a chronic degenerative process following injury and is illustrated in Figure 3.9. Initial axonal damage may be due directly to changes induced by the injury such as dysregulation of ionic homeostasis, compression of the cytoskeleton (Meythaler et al., 2001) or mechanically induced changes in permeability (Pettus and Povlishock,

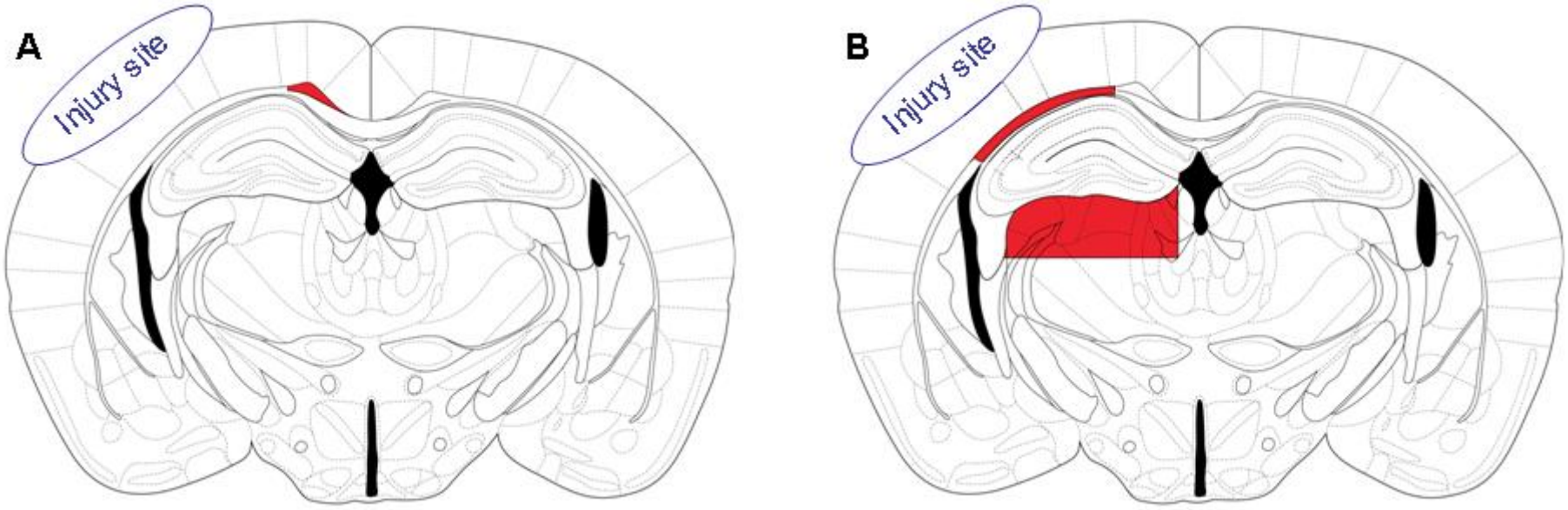


**Figure 3.9: Changing locations of axonal damage up to 6 weeks after mild TBI**
The pattern of axonal damage in the model changes over time. Damage is most evident in the cingulum at 4 hours after injury (A). By 6 weeks after injury damage in these areas is most pronounced in the thalamus and external capsule (B). Damaged areas shown in red.

1996). As degeneration progresses along the affected axons, damage becomes visible in regions sending out or receiving inputs from the damaged tracts. Thalamic damage is predictable in such a model of degeneration, owing to the presence of thalamic projections in the cingulum (Domesick, 1970; Meunier and Destrade, 1988) and also indirect connections between the external capsule and thalamus through the internal capsule (Saper, 1984). The specific projections involved in this study could not be identified from examination of a single coronal level.

The rapid appearance of axonal damage following injury and its decrease from 24 to 72 hours after injury is consistent with previous reports (Dikranian et al., 2008; Huh et al., 2008; Li et al., 2006). A delay in the appearance of thalamic damage has previously been observed (Carbonell and Grady, 1999; Conti et al., 1998; Laurer et al., 2001) but is not a universal finding with some reporting that thalamic damage may be an acute event after injury (Dikranian et al., 2008; Huh et al., 2008). The timing of the appearance of damage in the thalamus does not necessarily seem to be related to injury severity. Instead, it may reflect heterogeneity of different models of mild TBI and the difficulty in comparing the relative severities of various models of TBI.

Modelling axonal injury in mice differs mechanically from human injury owing to the small brain size of mice compared to humans. The small mass of the mouse brain renders it less vulnerable to the shearing and tensile forces responsible for primary diffuse axonal injury in humans and making this type of injury difficult to replicate in mice (Marmarou et al., 1994; Ross et al., 1994). The axonal injury

observed in this model is associated initially with the injury site, indicating that the injury itself, rather than shearing forces within the brain are responsible for the primary injury. Despite the difference in the mechanics of how axons are initially damaged the presence of persistent damage after injury in both this model and humans points to common secondary mechanisms that could be potentially targeted for therapeutic intervention. Currently treatment options for persistent cognitive deficits after mild TBI are limited and focused on alleviating cognitive symptoms without addressing underlying damage to the brain (Willer and Leddy, 2006). The results presented here show that axons are suitable targets for prevention of future cognitive deficits. Factors involved in axonal degeneration that have the potential to be beneficially modified include calpain activation and rises in intracellular calcium in order to maintain the structure of the neuronal cytoskeleton (Coleman, 2005).

Previously, the myelin response to mild TBI has not been characterised and this study demonstrated unaltered myelination using MAG and MBP staining in regions where axonal damage was found. Myelination remained unaltered up to 6 weeks after injury, suggesting that myelination at times between those investigated was also unaltered. It is possible that the axons damaged after injury were unmyelinated. Greater vulnerability of unmyelinated axons to TBI has previously been described (Reeves et al., 2005; 2007) and may be due to greater exposure of the axolemma to post-traumatic processes. In human mild TBI axonal damage has been suggested to be the most persistent pathological feature (Kraus et al., 2007).

The present study did not address the effects of mild TBI on the glial component of white matter. Increased numbers of astrocytes have been observed to persist in white matter for as long as 16 weeks after mild TBI (Uryu et al., 2002) and microglial staining has been observed in the fimbria up to 1 week after mild TBI (Graham et al., 2000). Both these cell types may play a role, as elements of the inflammatory response to injury, in the development of pathology following mild TBI (Morganti-Kossmann et al., 2007). The effect of mild TBI on oligodendrocytes is unknown, although moderate injury in rats has been shown to induce apoptosis of oligodendrocytes which may impact on axonal survival following injury (Conti et al., 1998).

The limited amount of cell death observed and its presence in both sham and injured animals at all time points allows cell death to be excluded as a cause of cognitive changes in this study. In the absence of lesions to grey matter structures, disruption of neural networks necessary for the water maze task may explain the cognitive deficits observed. Damage in the dorsal thalamus is apparent at one week after the time point at which a learning deficit was observed. Lesions of the thalamus have been demonstrated to impair acquisition of the water maze task, probably due to disruption of connections between the thalamus and hippocampus (Cain et al., 2006; Warburton and Aggleton, 1999; Warburton et al., 2001). Damage observed in other regions may also play a role in the deficits observed. The cingulum, in addition to its thalamic connections, contains projections to the hippocampus and has been implicated in spatial memory processes (Meunier and Destrade, 1988) and involvement of the external capsule in memory, due to the projections to the

amygdala that it contains has also been demonstrated (Lin et al., 2003). Although neuronal damage is minimal, there may be other pathologies which have not been examined, contributing to the observed cognitive deficits, such as dendritic atrophy or synaptic loss.

In cued platform testing in the water maze motor and visual impairments were ruled out as confounding variables by the equivalent performance of sham and injured animals. In the hidden platform version of the task at 3 weeks after injury injured animals were unable to improve their performance over five days of training. The performance of sham animals improved over the same period of time, so that they were able to find the platform significantly faster than injured animals on the final two days of training, indicating that injured animals were impaired in their ability to learn the location of the platform. Injured animals were able to successfully recall the location of the platform as well as shams at both 10 minutes and 24 hours after training, showing that their short- and long-term memory was intact. The inability of injured mice to improve their latency to find the platform over the training days, despite having intact memory for its location suggests that they may not have been using an optimal strategy to search for the platform. Thalamic lesions have been demonstrated to produce deficiencies in search strategy learning in rats (Cain et al., 2006; Warburton and Aggleton, 1999). The absence of a learning or memory deficit at 6 weeks after injury does not necessarily indicate that cognitive deficits injured animals had resolved by this time point. Prior testing in the water maze can result in savings in task acquisition that may persist for several months in mice and rats (Dellu et al., 1997; Pitsikas et al., 1991; Vicens et al., 2002). This pretraining effect may

have been sufficient to overcome any cognitive changes persisting to 6 weeks in this model.

The current study described a model of TBI in which specific and localised axonal damage in the absence of alterations in myelin is sufficient to produce an impairment in spatial learning that is detectable at 3 weeks after injury. We have also documented an evolution in axonal pathology over time that occurs in white matter tracts that are implicated in cognition. The association of axonal damage with cognitive deficits in this model suggests that preservation of axons following injury is a suitable therapeutic target for preserving cognition after mild TBI.

# 4 Effect of mild traumatic brain injury on white matter and Alzheimer's disease pathology in an Alzheimer's disease model

## 4.1 Introduction

Traumatic brain injury (TBI) is a major environmental risk factor for Alzheimer's disease (AD) but relatively little is known about the underlying mechanisms. This is in part due to the lack of models applying mild TBI to transgenic models of AD. The previous chapter described the development of a mouse model of mild traumatic brain injury (TBI) which shows selective, progressive axonal damage. This model of mild TBI can now be used to provide mechanistic insight to links between TBI and development of AD.

A number of epidemiological studies have documented an increased risk of AD in individuals with a history of TBI (Guskiewicz et al., 2005; Johnson et al., 2010; Szczygielski et al., 2005). In neuropathological studies, deposition of amyloid β (Aβ) and the occurrence of fibrillary inclusions of hyperphosphorylated tau in brain in injured brains indicate that AD-like pathology may develop in response to TBI. In contrast to human studies of the effects of TBI and the development of AD-like pathology, studies in mouse models have produced equivocal results (Szczygielski et al., 2005), with some studies even reporting a decrease in amyloid pathology

following severe TBI (Nakagawa et al., 2000). Imaging studies have suggested that white matter damage is another source of commonality between TBI and AD as both brain injured (Kraus et al., 2007) and AD (Targosz-Gajniak et al., 2009) patients show white matter damage associated with cognitive impairment.

Transgenic animals are crucial for investigating links between mild TBI and AD as examination of this in humans is difficult due to the low proportion of individuals with mild TBI who present clinically and to the low mortality rates immediately following injury in this group (Bruns and Hauser, 2003). Modelling mild TBI in transgenic models of AD in addition to enabling elucidation of possible mechanisms for the link between TBI and AD may also allow identification of pathological stages suitable for clinical intervention.

### *4.1.1 Aims and hypotheses*

To investigate the effect of mild TBI on amyloid β, tau and white matter pathology in a transgenic mouse model of AD, axons, myelin, amyloid β and tau as well as the levels of axonal and AD-related proteins were examined at 24 hours after mild TBI.

In a transgenic model of AD it was hypothesised that mild TBI would cause axonal damage as well as deposition of Aβ and in white matter in the hours after injury as well as increases in intracellular levels of Aβ and tau. It was also predicted that overall levels of APP, Aβ and normal and hyperphosphorylated tau would be increased.

## 4.2 Methods

### *4.2.1 Fluid percussion surgery and transgenic mice*

Twenty-eight 9 to 10 month old male triple transgenic (3xTg) mice weighing 27 – 30g underwent mild lateral FPI (injury severity = 0.8 ± 0.1atm) or sham surgery as described in chapter 2.1. Righting times for injured animals (167 ± 15 seconds) were significantly longer than for control animals (17 ± 6 seconds, $p < 0.001$). Surgical procedures were carried out by Dr. Jill Fowler. These animals were divided into two cohorts. Cohort 1 was used for histological and immunohistochemical analyses and consisted of 6 sham and 8 injured animals. Cohort 2 was used for biochemical analyses and comprised 7 sham and 7 injured animals.

The 3xTg mice, as described by Oddo et al. (2003a; b), carry $APP_{Swe}$, $PS1_{M146V}$ and $tau_{P301L}$ transgenes. The $APP_{Swe}$ and $PS1_{M146V}$ are mutant human transgenes encoding amyloid precursor protein (APP) and presenilin 1, respectively. Both of these mutations have been identified in familial Alzheimer's disease and are associated with increased Aβ. The $tau_{P301L}$ transgene harbours a mutation that causes neurofibrillary tangle formation in frontotemporal dementia with parkinsonism linked to chromosome 17 (FTDP-17). These mice have been reported to develop age-related Aβ pathology from 3 months of age and tau pathology from 12 months (Oddo et al., 2003).

*4.2.2 Histology and immunohistochemistry*

Cohort 1 animals were sacrificed 24 hours after injury. Animals were deeply anaesthetised and transcardially perfused with 20 ml heparinised 0.9% saline in 0.1% phosphate buffer followed by 4% paraformaldehyde in 0.1% phosphate buffer. Brains were postfixed and embedded in paraffin as described in chapter 2.4. 6 µm thick sections were cut and mounted in pairs on poly-L-lysine coated slides. Slides containing sections from the level corresponding to -1.94mm from bregma according to Franklin and Paxinos were selected for staining with haematoxylin and eosin (H&E) and fluoro-jade C (FJC) to determine the presence of neuronal damage. A section from a mouse that had undergone transient focal ischaemia for 1 hour with 23 hours survival at the level corresponding to 0.50mm from bregma served as a positive control for FJC staining. Sections adjacent to those used for histological staining were selected for immunohistochemical staining. Immunohistochemistry for amyloid precursor protein (APP) was performed to detect axonal damage. Aβ pathology was detected using an antibody recognising an epitope between amino acids 18-22 (clone 4G8). Myelin damage was investigated using antibodies against myelin associated glycoprotein (MAG) and myelin basic protein (MBP). Normal tau was detected using an antibody recognising an epitope between amino acids 159-163 (clone HT7) and abnormally phosphorylated tau was detected with an antibody recognising tau phosphorylated at Ser202 (clone AT8) The histological and immunohistochemical techniques used are described in detail in chapters 2.5 and 2.6. The methods used to quantify neuronal, axonal, myelin, amyloid and tau pathology are detailed in chapter 2.6. Briefly, damage to neuronal perikarya was identified

using FJC or H&E stained sections in the cortex, hippocampus and dorsal thalamus. In H&E stained sections the presence or absence of damaged eosinophilic neurons was recorded. In FJC stained sections the presence or absence of fluorescent, damaged neurons was noted. APP stained sections were used to count axonal bulbs per $mm^2$ in the cingulum, corpus callosum, cortex, external capsule, internal capsule and dorsal thalamus. Counts of axonal bulbs in APP stained sections were log transformed for analysis. In sections stained for Aβ darkly stained immunopositive bulbs were counted and analysed in the same way as in APP stained sections. MBP stained sections were used to assess myelin integrity in the cingulum, corpus callosum, external capsule and internal capsule. Relative optical density (ROD) measurements were used to quantify myelin integrity in these sections. ROD values were averaged for each region and ipsilateral measurements expressed as a percentage of the corresponding contralateral measurement to control for possible differences in exposure time during staining. Myelin debris in MAG stained sections was recorded as present or absent as was the presence of abnormal tau staining detected using AT8 and HT7 in the corpus callosum, cingulum, external capsule and internal capsule. In 4G8 and HT7 stained sections intracellular staining was also assessed in the amygdala, cortex and CA1, CA2, CA3 and dentate gyrus subfields of the hippocampus using image analysis. The regions of interest were photographed and the percentage surface area stained in each region photographed was measured in ImageJ (U. S. National Institutes of Health, Bethesda, USA). The values obtained were log transformed for analysis.

### *4.2.3 Western blotting*

Cohort 2 animals were terminated by cervical dislocation 24 hours after injury. The brains were removed and homogenised in tissue homogenisation buffer and diethylamine buffer as described in chapter 2.7. Western blotting was performed to detect APP, APP C-terminal fragments, normal human tau and abnormally phosphorylated tau. Oligomeric Aβ was detected by dot blot. Both Western blotting and dot blot procedures are detailed in chapter 2.8. The intensity of fluorescence of the bands or dots was detected using Odyssey application software (version 3.0; Li-Cor, Cambridge, UK).

### *4.2.4 Statistical analysis*

Data from axonal counts in APP and 4G8 stained sections as well as and MBP, 4G8 and HT7 image analysis were analysed using unpaired t-tests. Western blot and dot blot data were also analysed using unpaired t-tests.

## 4.3 Results

### *4.3.1 Early accumulation of APP and Aβ in white matter after mild traumatic brain injury*

Injured animals had evidence of axonal damage in white matter tracts close to the injury site. Aβ staining was also present in the same white matter regions in injured animals. There were significantly higher levels of axonal damage in the ipsilateral cingulum and external capsule of injured animals ($|t| = 3.483$, $p = 0.022$ and $|t| = 6.233$, $p < 0.001$, respectively; Figure 4.1B). There were no significant differences between the groups in these regions in the contralateral hemisphere ($|t| = 0.153$, $p = 0.881$, cingulum; $|t| = 1.000$, $p = 0.363$, external capsule; Appendix B.1). There were no differences between sham and injured animals in the corpus callosum ($|t| = 0.857$, $p = 0.408$, ipsilateral; $|t| = 0.204$, $p = 0.841$, contralateral; Appendix B.2), cortex ($|t| = 1.908$, $p = 0.098$, ipsilateral; no damage observed in either group contralaterally; Appendix B.2), internal capsule ($|t| = 1.572$, $p = 0.177$, ipsilateral; $|t| = 0.081$, $p = 0.937$, contralateral; Appendix B.2) and thalamus ($|t| = 0.222$, $p = 0.828$, ipsilateral; $|t| = 886$, $p = 0.393$, contralateral; Appendix B.2).

Injured animals had more Aβ accumulations than shams the same regions that showed axonal damage in APP immunostaining. There was significantly more Aβ accumulation in the ipsilateral cingulum and external capsule of injured animals compared to shams ($|t| = 5.494$, $p < 0.001$ and $|t| = 13.413$, $p < 0.001$, respectively;

Figure 4.1B). No difference was observed between the groups in these regions in the opposite hemisphere (|t| = 0.350, $p$ = 0.732, cingulum; |t| = 0.476, $p$ = 0.643, external capsule; Appendix B.1). Injured animals did not show more evidence of Aβ staining in the corpus callosum (|t| = 0.857, $p$ = 0.408, ipsilateral; no damage observed in either group contralaterally; Appendix B.2), cortex (|t| = 1.480, $p$ = 0.183, ipsilateral; no damage observed in either group contralaterally; Appendix B.2), internal capsule (|t| = 0.152, $p$ = 0.172, ipsilateral; no damage observed in either group contralaterally; Appendix B.2) and thalamus (|t| = 1.474, $p$ = 0.173, ipsilateral; |t| = 857, $p$ = 0408, contralateral; Appendix B.2) than shams.

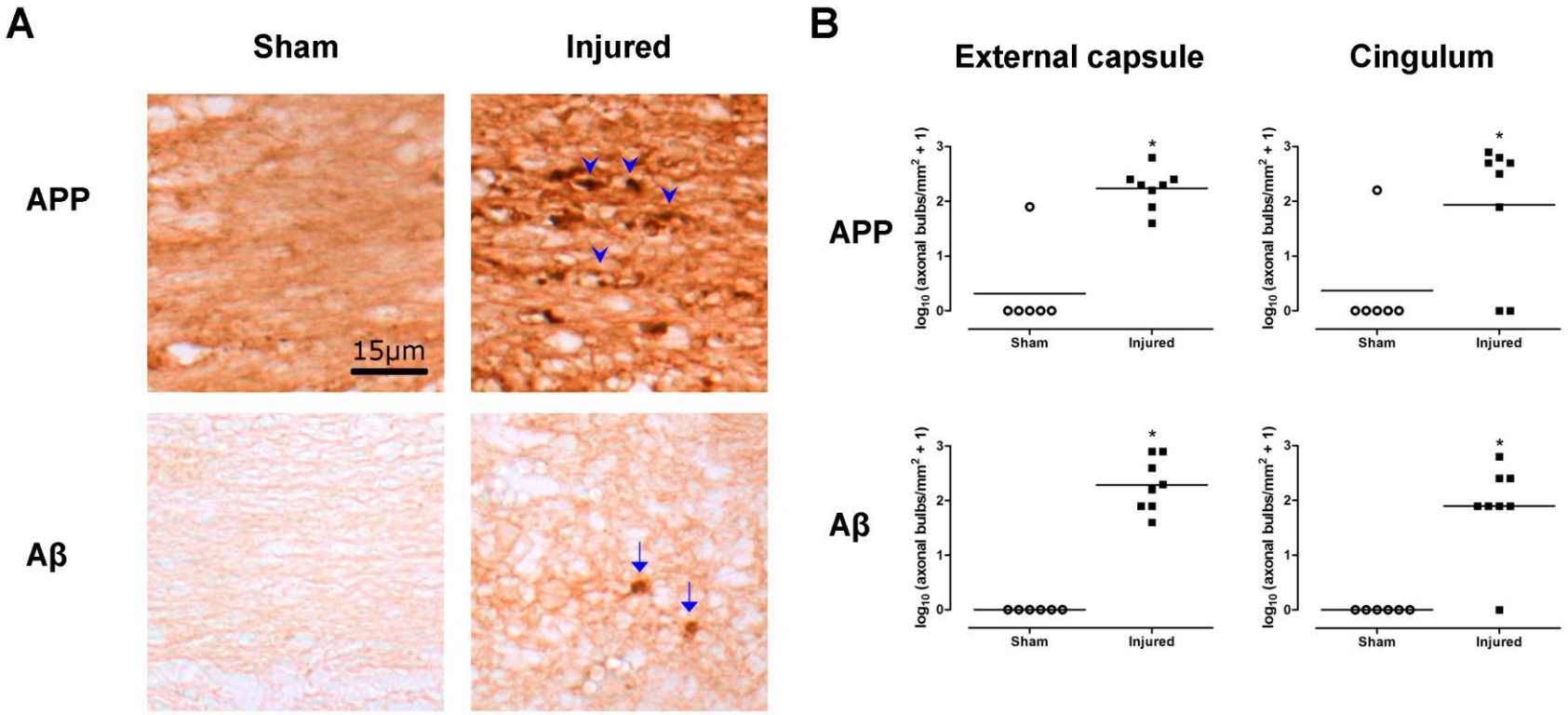


**Figure 4.1: Accumulation of APP and Aβ in white matter in the same regions after mild TBI** Following mild TBI APP and Aβ were found to be accumulated in white matter in the cingulum and external capsule. Representative staining from the external capsule taken at 40x magnification is shown. Blue arrowheads on APP stained sections indicate accumulations of APP and blue arrows on Aβ stained sections indicate accumulations of Aβ (A). The difference between the groups in the number of accumulations counted was significant in the ipsilateral external capsule and cingulum but not in the same regions contralaterally (B; line represents mean).

### *4.3.2 No tau changes in white matter after mild traumatic brain injury*

In sections stained for both total and hyperphosphorylated tau there was no evidence of staining in the corpus callosum, cingulum, external capsule or internal capsule in any animal from any group. No accumulations of normal or hyperphosphorylated tau were observed in any of the regions examined. Figure 4.2 shows representative examples of tau staining in the external capsule.

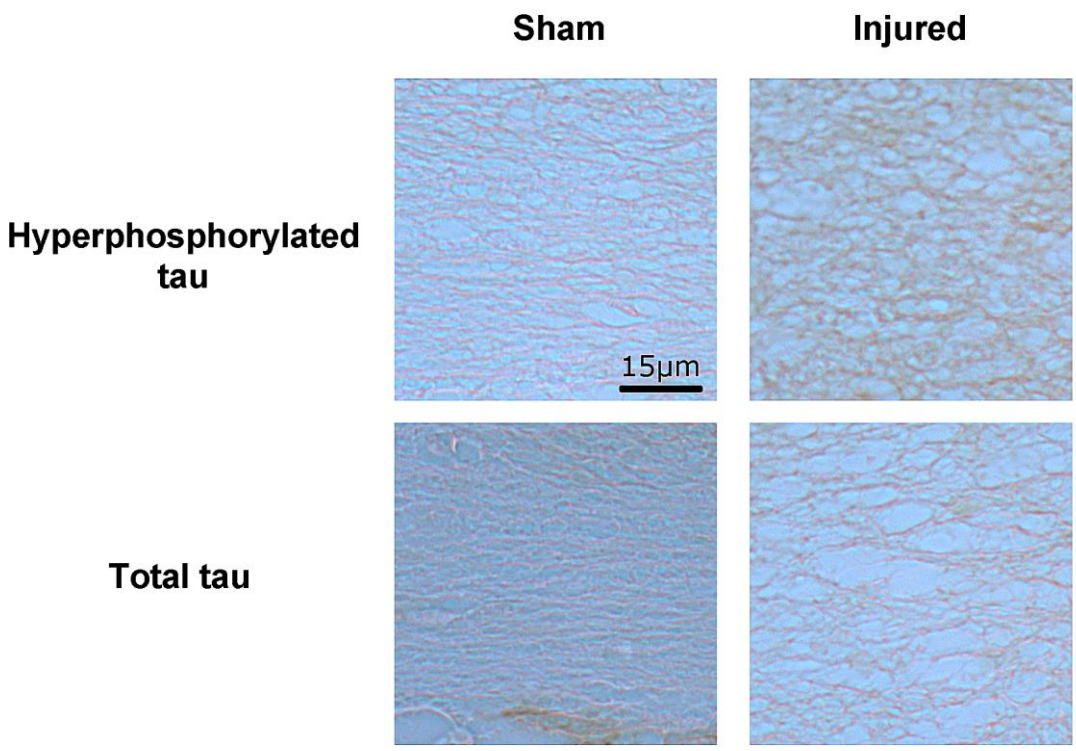


**Figure 4.2: No abnormal tau staining was observed following injury** Examination of white matter regions in sections stained for both hyperphosphorylated and total tau showed no abnormal staining after injury. Representative images from the ipsilateral external capsule at 40x magnification are shown.

*4.3.3 No change in intraneuronal amyloid after mild traumatic brain injury*

There was no significant difference between the groups in the level of intraneuronal Aβ in any region examined. Injured and sham animals showed the same level of Aβ staining in all regions examined ipsilaterally including the amygdala ($|t| = 0.482$, $p = 0.639$; Appendix B.4), cortex ($|t| = 0.220$, $p = 0.829$; Appendix B.4) and hippocampal subfields: CA1 ($|t| = 0.940$, $p = 0.366$; Figure 4.3B), CA2 ($|t| = 0.515$, $p = 0.616$; Appendix B.4), CA3 ($|t| = 0.523$, $p = 0.610$; Appendix B.4) and dentate gyrus ($|t| = 1.047$, $p = 0.316$; Appendix B.4). Staining was also unaltered in injured animals in the contralateral hemisphere ($|t| = 0.345$, $p = 0.736$, amygdala; $|t| = 0.705$, $p = 0.495$, cortex; $|t| = 1.028$, $p = 0.324$, CA1; $|t| = 0.335$, $p = 0.743$, CA2; $|t| = 0.198$, $p = 0.846$, CA3; $|t| = 0.038$, $p = 0.971$, dentate gyrus; Appendix B.4).

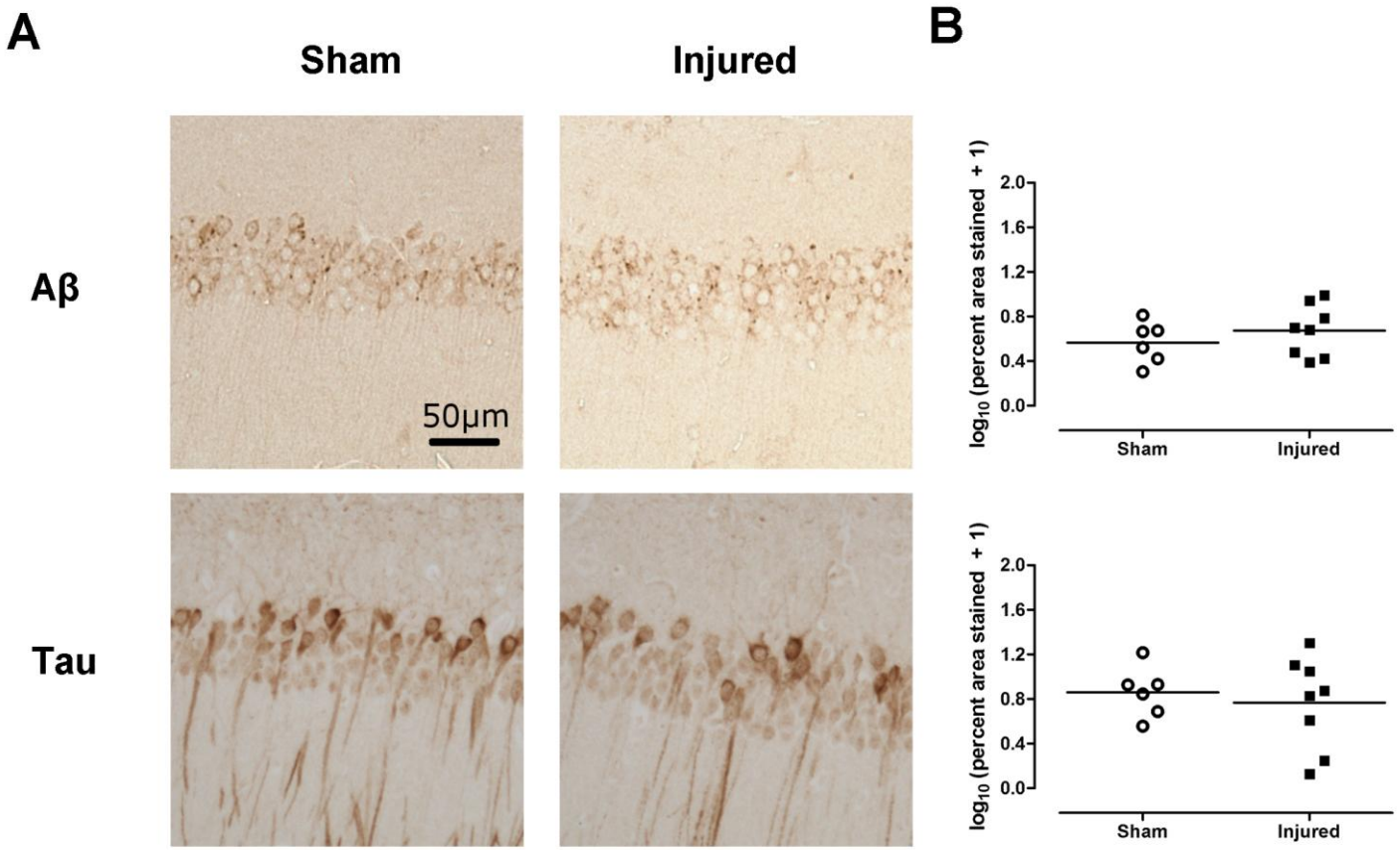


**Figure 4.3: Mild TBI does not produce changes in intracellular Aβ or tau staining** Examination of the percentage area stained revealed no differences in intracellular Aβ or tau following mild FPI. Representative images taken at 10x magnification of staining in the CA1 region of the ipsilateral hippocampus are shown (A). The percentage area stained was not affect by injury (B; line represents mean value).

*4.3.4 No change in intraneuronal tau after mild traumatic brain injury*

There was no significant difference between the groups in the level of tau in any region examined. Staining for normal tau also did not reveal any differences between the groups in the amygdala ($|t| = 0.130$, $p = 0.899$; Appendix B.5), cortex ($|t| = 0.683$, $p = 0.508$; Appendix B.5), CA1 ($|t| = 0.488$, $p = 0.634$; Figure 4.3B), CA2 ($|t| = 1.976$, $p = 0.092$; Appendix B.5), CA3 ($|t| = 0.250$, $p = 0.807$; Appendix B.5) and dentate gyrus ($|t| = 0.482$, $p = 0.639$; Appendix B.5) ipsilaterally. Injured and sham animals also did not differ in the same regions in the contralateral hemisphere ($|t| = 0.319$, $p = 0.755$, amygdala; $|t| = 0.529$, $p = 0.606$, cortex; $|t| = 0.569$, $p = 0.580$, CA1; $|t| = 0.482$, $p = 0.639$, CA2; $|t| = 0.179$, $p = 0.861$, CA3; $|t| = 0.916$, $p = 0.378$, dentate gyrus; Appendix B.5).

*4.3.5 Mild traumatic brain injury does not increase cell death*

Neither H&E nor FJC staining showed evidence of elevated levels of cell death in injured animals. In H&E stained sections cell death was confined to the cortex local to the injury site and isolated damaged neurons in the ipsilateral hippocampus (Figure 4.4). Five injured animals out of 8 showed evidence of cell death in the cortex as did 3 sham animals out of 6. In the ipsilateral hippocampus 3 injured and 1 sham animal had single ischaemic neurons present. One further injured animal had numerous ischaemic cells throughout the hippocampus. There was no evidence of

cell death in the contralateral cortex or hippocampus or bilateral amygdala or thalamus of any animal.

In FJC stained sections a similar pattern of staining was observed with 6 injured and 4 sham animals showing positive cells in the ipsilateral cortex (Figure 4.4). Three injured animals also had single positive cells in the ipsilateral hippocampus and another showed evidence of more extensive hippocampal cell death. No cell death was observed in these regions contralaterally or in the amygdala or thalamus bilaterally.

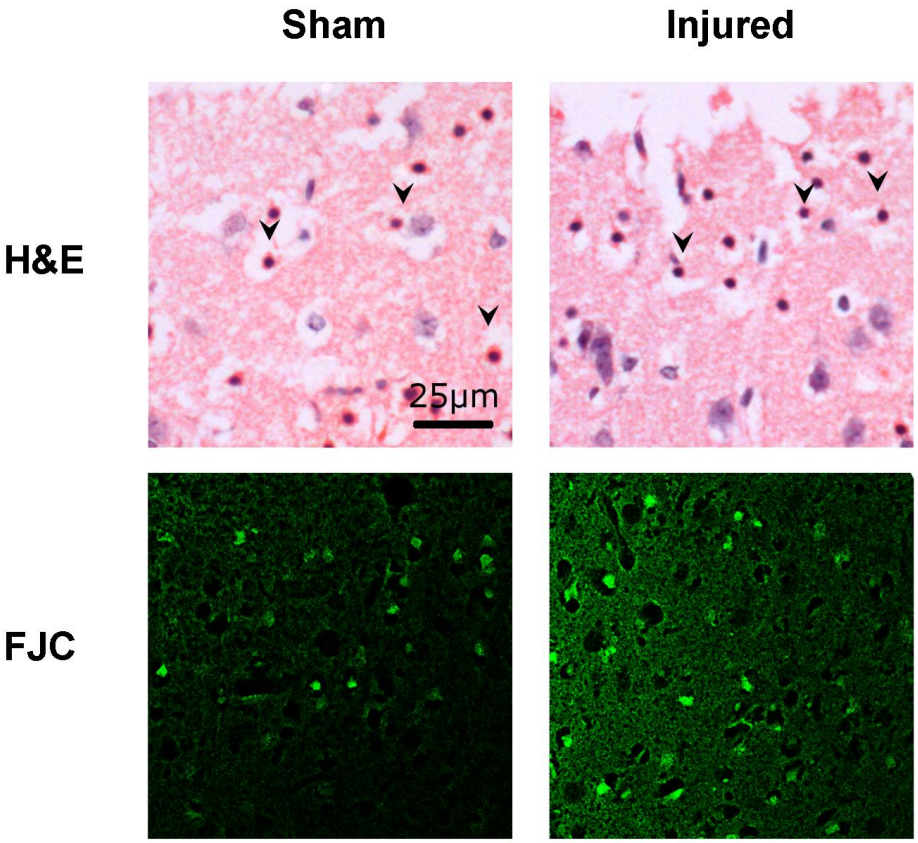


**Figure 4.4: Sham and injured animals show comparable levels of cell death after mild TBI**

Cell death following surgery was evident in both sham and injured animals. Cell death was visible in the cortex close to the injury site and levels were comparable in the two groups. Images are representative of H&E staining and FJC staining in the ipsilateral cortex and taken at 20x magnification. Black arrowheads indicate ischaemic neurons in H&E staining.

### *4.3.6 No evidence of myelin damage following mild traumatic brain injury*

Neither of the two markers used to assess myelin damage showed evidence of alterations after mild TBI. In MBP stained sections, relative optical density of staining in ipsilateral regions expressed as a percentage of control was unaltered: ($|t| = 1.087$, $p = 0.298$, cingulum; $|t| = 0.775$, $p = 0.454$, corpus callosum; $|t| = 1.922$, $p = 0.079$, external capsule; $|t| = 0.389$, $p = 0.704$, internal capsule; Appendix B.3).

In MAG immunostained sections 2 injured and 2 sham animals had evidence of minimal myelin debris in the ipsilateral cingulum. The 2 injured animals with ipsilateral cingulum damage also showed minor amounts of debris in the contralateral cingulum, while one sham animal also had evidence of myelin debris in the contralateral hemisphere. A single injured and 1 sham animal showed small amounts of myelin debris in the ipsilateral internal capsule and low levels of myelin debris were visible in the contralateral internal capsule of 2 injured animals. There was no evidence of myelin debris in any animal in the external capsule or corpus callosum.

### *4.3.7 No change in levels of APP and related proteins after mild traumatic brain injury*

There were no changes detected in the levels of APP related proteins investigated following mild TBI. Levels of APP, C-terminal fragments and oligomeric Aβ were

unaltered in injured animals compared to shams. Western blotting for APP showed a double band at 100kDa. No difference in the amount of APP was detected between injured or sham animals in the ipsilateral ($|t| = 0.273$, $p = 0.790$) or contralateral ($|t| = 1.448$, $p = 0.173$; Figure 4.5A) hemispheres. The C99 C-terminal fragment that is formed by the amyloidogenic processing pathway produced a band at 9kDa, was not altered in the ipsilateral ($|t| = 1.052$, $p = 0.313$) or contralateral ($|t| = 2.147$, $p = 0.064$; Figure 4.6) hemispheres. Dot blots for oligomeric Aβ revealed no differences between sham and injured animals ($|t| = 1.246$, $p = 0.236$, ipsilateral; $|t| = 1.545$, $p = 0.148$, contralateral; Figure 4.5B). The C-terminal fragment, C83, formed by the non-amyloidogenic processing pathway produced a band at 11kDa and was also unchanged in both the ipsilateral ($|t| = 1.309$, $p = 0.215$) and contralateral ($|t| = 1.945$, $p = 0.076$; Figure 4.6). The ratio between the two C-terminal fragments was also unchanged in injured animals ($|t| = 0.544$, $p = 0.597$, ipsilateral; $|t| = 1.011$, $p = 0.332$, contralateral; Figure 4.6).

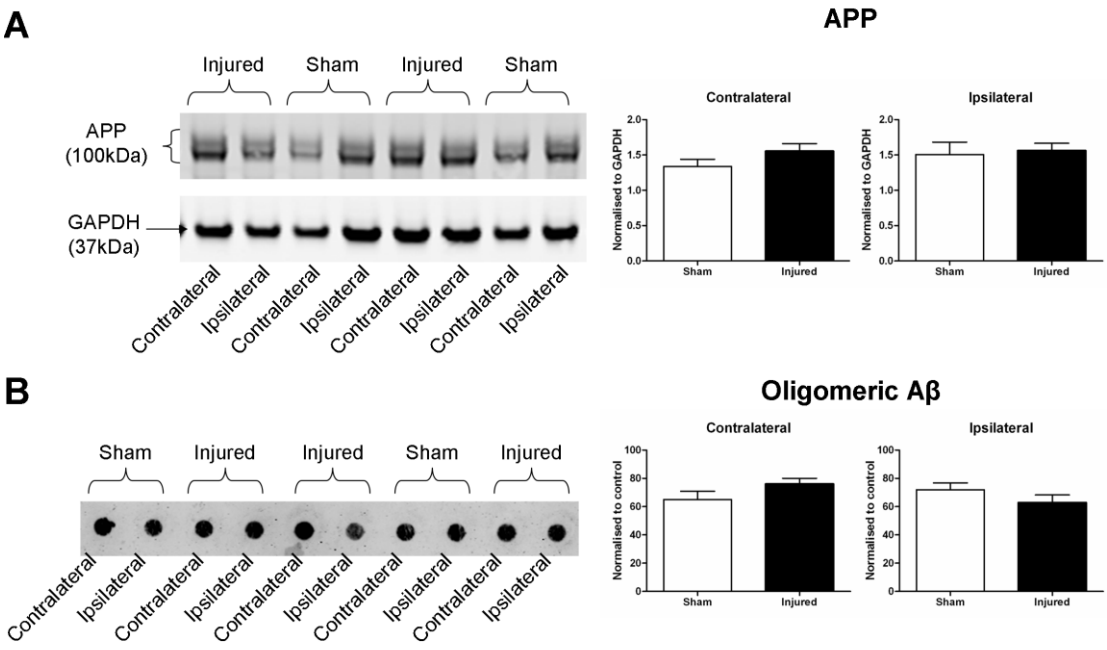


**Figure 4.5: Levels of APP and oligomeric Aβ are unaltered at 24 hours after mild TBI**

Levels of APP and oligomeric Aβ were unaltered 24 hours after mild TBI. Western blotting for APP showed a double band at 100kDa (A). Levels in injured animals were unaltered compared to shams in both hemispheres. Dot blot analysis of oligomeric Aβ levels showed no differences between sham and injured mice in either hemisphere (B). Graphs show mean + SEM.

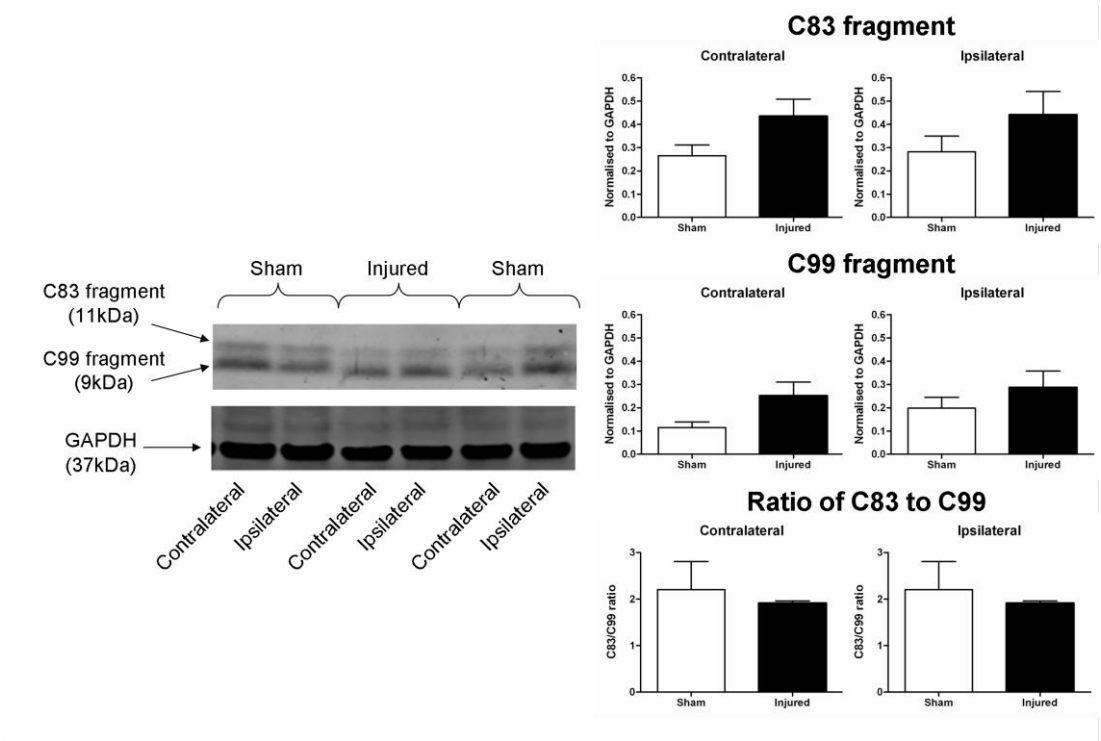


**Figure 4.6: Levels of C-terminal fragments are unaltered at 24 hours after mild TBI**

Levels C-terminal fragments were unaltered 24 hours after mild TBI. In Western blots for C-terminal fragments the C99 fragment generated by amyloidogenic cleavage of APP was visible at 9kDa while the non amyloidogenic fragment was present at 11kDa. Injured animals did not differ from shams in levels of either fragment or in the ratio of the two fragments. Graphs show mean + SEM.

### *4.3.8 No change in levels of tau protein after mild traumatic brain injury*

There were no changes detected in the levels of tau protein after mild TBI. Levels of normal tau detected using the HT7 antibody were unaffected by mild FPI. ($|t| = 0.582$, $p = 0.571$, ipsilateral; $|t| = 0.433$, $p = 0.673$, contralateral; Figure 4.7A) No abnormally phosphorylated tau band was detected using AT8 antibody and analysis of normal tau detected using this antibody showed unchanged levels in injured compared to sham animals ($|t| = 0.209$, $p = 0.838$, ipsilateral; $|t| = 0.484$, $p = 0.643$, contralateral; Figure 4.7B).

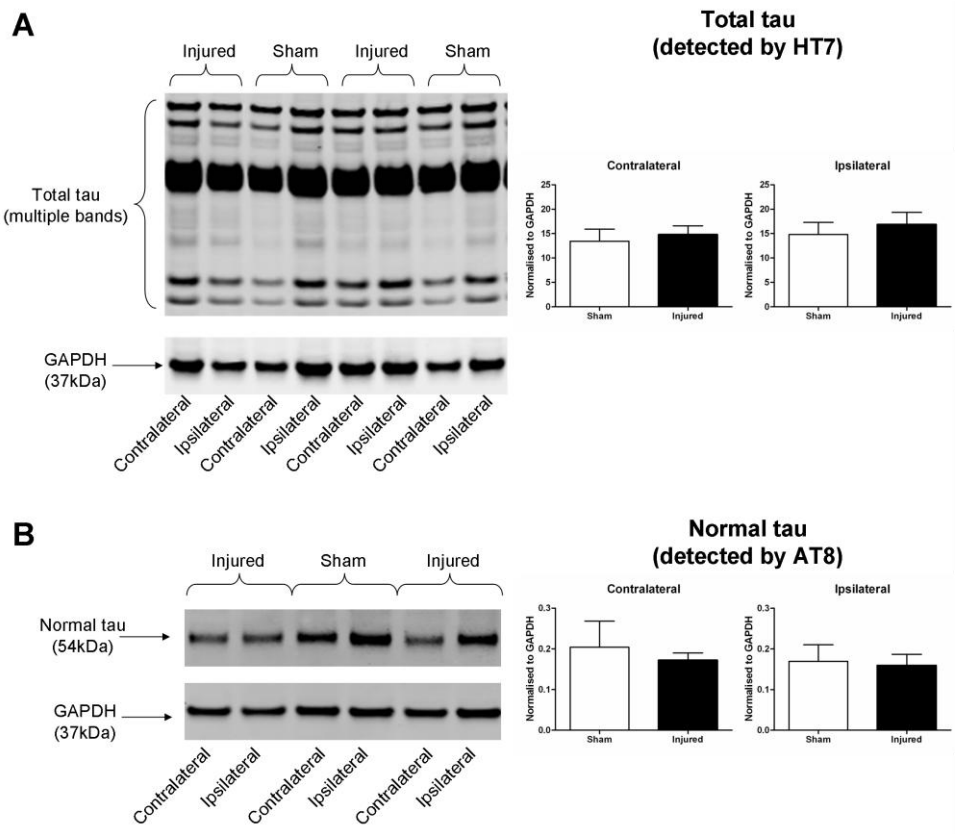


**Figure 4.7: Levels of tau are unaltered at 24 hours after mild TBI** Levels of normal and total tau were unaltered 24 hours after mild TBI. Western blotting for total tau showed no changes in injured animals compared to shams in either hemisphere (A). Use of the AT8 antibody for hyperphosphorylated tau did not show a band of hyperphosphorylated tau but did show a normal tau band at 54kDa (B). Normal tau levels were no different in sham and injured animals in either hemisphere. Graphs show mean + SEM.

## 4.4 Discussion

TBI is the major environmental risk factor for AD. AD-like pathological changes are well documented in humans following moderate and severe TBI but the mechanism of the link between the two is unknown. This study examined the effect of mild TBI on axons, myelin, amyloid β and tau as well as the levels of axonal and AD-related proteins. The hypothesis that mild TBI would cause axonal damage as well as deposition of Aβ in white matter was upheld with the observation of accumulations of Aβ and APP staining in white matter regions. The hypothesised increase in intracellular levels of Aβ and tau was not observed as no difference in intracellular Aβ or tau staining was observed between injured and sham animals. It had also been hypothesised that overall levels of APP, Aβ and normal and hyperphosphorylated tau would be increased, however these levels of these proteins were not found to be altered in injured animals compared to sham controls.

In injured animals, Aβ staining was observed in white matter tracts that also displayed axonal damage, as measured by APP staining, in areas close to the injury site. Co-accumulation of APP, Aβ and other components of the APP cleavage pathway has been found in axons in human brains following TBI (Chen et al., 2009; Uryu et al., 2007) and similar findings have been made in pigs in a TBI model designed to produce axonal pathology (Chen et al., 2004; Smith et al., 1999) and in rats after moderate TBI (Iwata et al., 2002). Accumulated APP in axons after TBI has been proposed as a substrate for increased Aβ production after injury (Johnson et

al., 2010; Szczygielski et al., 2005). The axonal location of APP cleavage to Aβ is unknown. Experiments showing that APP, β-secretase and presenilin are transported along the axon together and that APP may be cleaved to Aβ during transport (Kamal et al., 2001) have been contradicted by later reports (Lazarov et al., 2005). An alternative axonal location for cleavage of APP to Aβ is lipid rafts, assemblies of cholesterol and sphingolipids located in the external layer of the plasma membrane. The axonal membrane is enriched in lipid rafts (Simons and Toomre, 2000) and APP has been shown to be present in lipid rafts (Taylor and Hooper, 2007) which have been suggested as necessary for β-secretase cleavage of APP (Ehehalt et al., 2003). Although the location of APP processing following TBI is unclear it is known that both β- and γ-secretase activity is upregulated by oxidative stress (Tamagno et al., 2005; 2008). Therefore increases in oxidative stress following TBI may be responsible for enhanced production of Aβ from accumulated APP. The present study did not demonstrate co-accumulation of APP and Aβ, however, nor did it confirm that the observed Aβ accumulated in axons. Confirmation of both these points could be achieved in a multi-labelling immunohistochemistry study to investigate whether APP and Aβ staining co-localises and whether Aβ is accumulated in neurofilament positive axons.

Axonal damage has been identified as an early pathological event in a transgenic mouse models of AD as well as in human AD (Stokin et al., 2005). If axonal pathology is a precipitating factor for other aspects of AD pathology under non injury conditions this suggests that damage to axons would accelerate the development of AD pathology. Stokin et al. (2005) and Johnson et al. (2010)

propose that accumulated Aβ in axons may be released by lysis of degenerating injured axons, leading to the extracellular pathology that is considered definitive of AD. This is supported by the observation of Aβ plaques in white matter close to damaged axons in individuals who died days after TBI (Smith et al., 2003b). Aβ accumulations in white matter have been found to persist for up to 6 months following injury in a pig model (Chen et al., 2004), and 1 year in a rat model (Iwata et al., 2002), providing a potential long-term pool of Aβ. In addition to axonal damage caused by TBI, intra- and extracellular Aβ are capable of impairing axonal transport (Muresan and Muresan, 2006; Pigino et al., 2009) and may contribute to further development of axonal pathology after TBI. The appearance of Aβ accumulations 24 hours after injury in this study indicates that early intervention after injury may have a role in preventing long-term accumulation of Aβ. Assessing the efficacy of such an intervention first requires assessment of the development of pathology in this model over the weeks following injury. Examination of longer term survival after injury will indicate whether the regional distribution of Aβ accumulations changes over time after injury, as observed with APP accumulation in the previous chapter.

The use of transgenic models of AD pathology in TBI research has focused on plaque pathology as a clear indicator of pathological similarities to both AD in humans and studies demonstrating extracellular deposition of Aβ after injury (Ikonomovic et al., 2004; Smith et al., 2003c). However, in contrast to studies in humans the effects of TBI on Aβ deposition in transgenic mouse models have given somewhat mixed results. In fact, severe TBI in aged PDAPP mice has been shown to

induce reductions in Aβ deposition at 9 and 16 weeks after injury as well as reducing the amount of Aβ deposited over time following injury in young mice (Nakagawa et al., 1999; 2000). In these studies a severe injury level was used, resulting in massive loss of hippocampal neurons and reducing the potential pool of Aβ producing cells which may explain these anomalous findings. However, mild TBI, without cell loss has been shown to produce an increase in Aβ deposition at the same time points (Uryu et al., 2002). In the current study no plaque pathology was observed, however the time point observed here encompassed only the most acute events after injury, in the interests of observing early changes in AD-type pathology that may be suitable for therapeutic intervention.

No changes were observed in the amount of intracellular Aβ staining observed after injury in this study. Given that this model of TBI did not produce any other cellular changes this is not surprising. Increases in intracellular Aβ have been reported following TBI in rats (Hoshino et al., 1998; Iwata et al., 2002) or in mice with a human familial AD *APP* mutation knocked into murine *APP* (Abrahamson et al., 2006). In all these studies there was also significant neuronal loss following injury, owing to the greater injury magnitudes used.

The absence of abnormalities in tau staining in both grey and white matter are likely a reflection of the temporal order in which AD pathology progresses, with accumulation of Aβ appearing prior to neurofibrillary tau tangles. It may be that mild TBI is not in itself sufficient to induce changes in tau but tau pathology may occur downstream of TBI-induced Aβ pathology. In the mouse model used in the

study described here it has previously been shown that vaccination against Aβ cleared extracellular and intracellular Aβ as well as deposits of tau (Oddo et al., 2004). Tau pathology reemerged only after the reappearance of Aβ deposits, indicating that in this transgenic model the development of tau pathology is dependent on the presence of Aβ pathology. Furthermore, in the case of dementia pugilistica, a dementia whose primary pathology is deposition of neurofibrillary tangles, patients are typically boxers, who suffer repeated injuries over the course of their careers (Marklund et al., 2009; Toth et al., 2005) rather than in individuals who have suffered a single TBI, suggesting that a single incident of mild TBI may not be sufficient to induce neurofibrillary tangles.

Overall, levels of proteins relevant to amyloid pathology in AD; APP, oligomeric Aβ and C-terminal fragments as well as levels of tau protein were unaltered following mild TBI. Hyperphosphorylated tau was not detected by Western blot in any animal. This is not necessarily a finding inconsistent with the results of the pathological investigation. Accumulation of APP and Aβ was confined to a small anatomical region in immunohistochemical analysis and these changes may have been too small to be detectable in tissue samples incorporating a relatively larger amount of tissue from unaffected regions. Examination of protein levels specifically in damaged white matter has demonstrated elevations in APP and the amyloidogenic C99 C-terminal fragment in a model of diffuse axonal injury (Chen et al., 2004). Aβ levels in PDAPP mice are also known to increase sharply after injury, peaking at 2 hours before declining again over the following hours (Smith et al., 1998). Human investigations of Aβ levels in the acute period after injury have relied on

measurements of Aβ in cerebrospinal fluid or dialysate and have returned mixed results in terms of temporal changes in Aβ levels. In general the results suggest that there is a short term increase in Aβ levels followed by a decrease (Brody et al., 2008; Franz et al., 2003; Marklund et al., 2009; Raby et al., 1998). Analysis of dialysate from the brains of patients with diffuse axonal damage showed lower levels of tau than in a group with focal damage (Marklund et al., 2009), although the implications of this in the absence of an appropriate control population are unclear.

This chapter describes the effects of mild TBI in a transgenic model of AD. The model shows accumulation of Aβ associated with axonal damage at 24 hours after injury. We have determined that intracellular Aβ and tau in both grey and white matter are unaffected at this time point. Accumulation of Aβ in white matter regions that also show axonal damage shows a role for axonal damage in mediating the link between TBI and AD. Additionally, the accumulation of Aβ at 24 hours after injury demonstrates that AD-related pathological changes occur soon after injury, implying that early intervention may be necessary to reduce the risk of AD following mild TBI.

# 5 Effect of chronic cerebral hypoperfusion on white matter and cognition in mice

## 5.1 Introduction

Chronic cerebral hypoperfusion has been associated with poor performance in cognitive testing in adults over 55 years old (Appelman et al., 2010; Ruitenberg et al., 2005; Tiehuis et al., 2008). It has been suggested that this effect is mediated by white matter damage (Pantoni and Garcia, 1997) and white matter changes have been correlated with deficits in executive function, processing speed and episodic memory in aging populations (Bucur et al., 2008; Deary et al., 2003; Delano-Wood et al., 2009; Kennedy and Raz, 2009; Vernooij et al., 2009). Additionally, changes in white matter in aging populations have been associated with changes in cerebral blood flow (CBF) in cross-sectional (Bisschops et al., 2004; Vernooij et al., 2008) and post-mortem studies (Fernando et al., 2006).

The difficulty in establishing a causal relationship in studies with a correlational design and in populations where pathologies other than hypoperfusion may confound the results has necessitated the development of animal models of chronic cerebral hypoperfusion. In rats this is achieved by permanent occlusion of both common carotid arteries and produces a model with a combination of neuronal cell body damage and white matter damage (Farkas et al., 2007 for review). Although deficits

in performance have been observed in both the water maze (Farkas et al., 2004b; Pappas et al., 1996) and radial arm maze (Murakami et al., 2000; Pappas et al., 1996) up to 5 months after in induction of hypoperfusion; the presence of variable levels of neuronal damage in this model makes interpretation of these findings with regard to white matter changes difficult

More recently, a mouse model of chronic cerebral hypoperfusion was developed involving permanent narrowing of the common carotid arteries by application of microcoils (Shibata et al., 2004). This resulted in diffuse, selective damage to white matter, visible after 14 days of hypoperfusion. Behavioural analysis conducted in a separate cohort of animals found a deficit in working memory after 2 months of hypoperfusion without deficits in spatial reference memory or contextual and cued fear conditioning (Shibata et al., 2007). The absence of parallel behavioural and pathological analysis in the same animals and additionally the relative novelty of the model means that there is room for investigation of the robustness of these findings and examination of further aspects of cognitive function relevant to human cognitive decline linked to white matter damage and cerebral hypoperfusion.

### *5.1.1 Aims and hypotheses*

To investigate the effects of chronic cerebral hypoperfusion on cognition and white matter pathology in wild-type mice, axonal and myelin damage as well as a number of cognitive domains were investigated after one or two months of hypoperfusion.

Chronic cerebral hypoperfusion was hypothesised to cause damage to elements of white matter as well as a deficit in spatial learning, memory, serial spatial learning or working memory.

## 5.2 Methods

### *5.2.1 Induction of chronic cerebral hypoperfusion and animals*

3-4 month old male C57Bl6/J mice (Charles River, UK) weighing 25 – 30g underwent bilateral common carotid artery stenosis or sham surgery as described in chapter 2.1. Surgical procedures were carried out by Dr. Karen Horsburgh. Prior to behavioural testing animals were handled for 5 minutes per day for 5 consecutive days to minimise stress resulting from handling. Separate cohorts of animals were used for each behavioural test.

### *5.2.2 Testing of spatial reference learning and memory*

Water maze testing was carried out according to the protocol detailed in chapter 2.2. A day of pretraining on the cued version of the water maze task was carried out before surgery to exclude animals showing an abnormal stress response. No animals were excluded on this basis from this study. Five days of training on the cued version of the water maze task were carried out, beginning 2 weeks after surgery. Each animal received 4 training trials per day, with a 20 minute interval between trials. Spatial reference memory training began 3 days after the end of training in the cued version of the task and continued for 5 days with 4 trials per day and a 10

minute intertrial interval. Probe tests were carried out 10 minutes and 24 hours after the final trial of spatial reference training.

### *5.2.3 Testing of episodic memory*

Animals were trained for one day before surgery on the cued version of the water maze task to exclude animals showing an abnormal stress response. No animals were excluded on this basis from this study. Four days of training on the cued version of the water maze task were carried out, beginning 2 weeks after surgery. Episodic memory was tested using a trials to criterion protocol as described by Chen et al. (2000). The protocol used is described in detail in chapter 2.2. Briefly, testing was as per the spatial reference memory procedure described above, with the following modifications: training on a task was stopped when the animal reached a criterion of an average of less than 20 seconds to the platform on 3 consecutive trials, the maximum number of trials permitted per day was 8 and once the performance criterion was reached or the animal reached 32 trials (except on task 1 where the maximum number of trials permitted was 40), training was stopped and training on a new platform location begun on the following day. This was carried out for a minimum of 10 training days or until 5 platform locations had been learned. Retention was probed as described above at 10 minutes and again at 3 hours after reaching criterion on the first 5 tasks.

*5.2.4 Testing of working memory*

Working memory was tested in an 8-arm radial maze (Olton and Samuelson, 1976) using a protocol adapted from Shibata et al. (2007). Animals were food deprived to between 85 and 90% of initial body weight beginning 4 weeks after surgery. Pre-training to acclimatise animals to the maze environment and to allow them to learn to retrieve food pellets from the food wells began 3 weeks after surgery. After 2 days of pre-training training on the working memory task began. All 8 arms of the maze were baited with food pellets during training trials. At the start of a trial the animal was placed in the centre of the maze and allowed to choose an arm. When the animal returned to the centre of the maze they were confined there for 5 seconds before being allowed to make another arm choice. A re-entry into a previously visited arm counted as an error. Each trial lasted until the animal had retrieved all 8 food pellets or 25 minutes had elapsed. Each animal completed one trial per day of training. After 16 days an extra 2 minute confinement in the centre of the maze was introduced after the animal had made 4 arm choices. Further details of this protocol can be found in chapter 2.2.

Two cohorts of animals were tested in this task, owing to the high proportion of hypoperfused mice showing ischaemic neuronal damage in the first cohort. This left group numbers too low for reliable statistical analysis. The second cohort of animals was tested in the radial arm maze 11 months after the first by Ms. Jess Smith, Dr. Gillian Scullion and Ms. Yanina Tsenkina.

*5.2.5 Pathological assessment*

The histological and immunohistochemical staining described in this chapter was carried out by Mrs. Fiona Scott and Mr. Tommy Dingwall while all analysis with the exception of degraded myelin was carried out by Mr. Robin Coltman. Sections stained for degraded myelin were assessed by Dr. Horsburgh. Perfusions were carried out by Mr. Coltman, Ms. Smith and Ms. Tsenkina. Mice that underwent spatial reference training were perfused at one month after surgery. Mice that had undergone episodic memory and working memory testing were perfused at two months after surgery.

For assessment of ischaemic damage to neuronal cell bodies sections were stained using haematoxylin and eosin (H&E) as described in chapter 2.5. Sections were immunostained as described in Chapter 2.6 with antibodies against myelin associated glycoprotein (MAG; 1:500 dilution, Santa Cruz), amyloid precursor protein (APP; 1:1000 dilution, Millipore), degraded myelin basic protein (dMBP; 1:300 dilution, Millipore) and anti-ionised calcium-binding adaptor molecule, a marker of activated microglia (Iba-1; 1:750 dilution; Biocare Medical).

Ischaemic damage to neuronal cell bodies was assessed as being present or absent throughout the brain. Immunohistochemical staining was analysed in the corpus callosum, external capsule, internal capsule, fimbria, optic tract and fibre bundles of the caudate (Figure 5.4K). Immunostaining against MAG showed myelin damage, defined as disorganisation and vacuolation of white matter fibres and the presence of

debris. This was graded on a 4 point scale from normal (grade 0), through minimal (grade 1), modest (grade 2) and extensive (grade 3). dMBP immunostaining revealed degraded myelin which was also graded on a 4 point scale; beginning with normal staining (grade 0), minimal areas of degraded myelin (grade 1), moderate areas of degraded myelin (grade 2) and extensive areas of degraded myelin (grade 3). Axonal damage was identified by APP staining of swollen or bulbous axons and graded as normal (grade 0), minimal (grade 1); moderate (grade 2) and extensive (grade 3). Grades for each region were assigned to both hemisphere Activated microglia were counted in a grid of defined size in random fields within each region examined and the number of Iba-1 positive cells per square millimetre calculated. Cell counts were averaged across hemispheres.

### *5.2.5 Statistical analysis*

Data from the water maze and radial arm maze studies were analysed using two-way ANOVA, using the Greenhouse-Geiser correction where data were significantly non-normal (i.e. where Mauchly's test returned a value of $p < 0.05$). Radial arm maze data were analysed across blocks of two averaged training days. *Post hoc* comparisons were made using unpaired t-test. Swim speeds from cued water maze testing and the number of tasks learned in the episodic memory task were analysed using unpaired t-test. Graded scores obtained from pathological analysis were summed and analysed using Fisher's exact test. The numbers of activated microglia were analysed using unpaired t-test.

## 5.3 Results

### *5.3.1 Diffuse white matter damage after chronic cerebral hypoperfusion*

A minority of hypoperfused animals showed evidence of ischaemic neuronal damage. These animals were excluded from all pathological and behavioural analyses. The numbers of animals excluded from each cohort are detailed below. Analysis of MAG staining showed widespread myelin damage in hypoperfused animals after both 1 and 2 months of hypoperfusion (Figure 5.1C, D; Figure 5.2). Levels of degraded myelin as identified using dMBP staining were increased in hypoperfused animals at both one and two months after induction of hypoperfusion (Figure 5.1E, F; Figure 5.2). Axonal damage was observed in some hypoperfused animals at both time points but not in shams (Figure 5.1G, H; Figure 5.2). Hypoperfused animals also displayed elevated microglial activation compared to shams (Figure 5.1I, J; Figure 5.2).

| Behavioural cohort | Number of mice excluded | Reason | Final numbers |
|---|---|---|---|
| *Spatial reference learning and memory* | 2 hypoperfused | Ischaemic neuronal damage | 9 sham, 9 hypoperfused |
| | 3 sham, 1 hypoperfused | Persistent floating behaviour | |
| *Episodic memory* | 4 hypoperfused | Ischaemic neuronal damage | 11 sham, 10 hypoperfused |
| | 1 sham, 1 hypoperfused | Persistent floating behaviour | |
| *Radial arm maze (cohort 1)* | 7 hypoperfused | Ischaemic neuronal damage | 10 sham, 3 hypoperfused |
| *Radial arm maze (cohort 2)* | 17 hypoperfused | Ischaemic neuronal damage | 17 sham, 7 hypoperfused |

**Table 5.1: Numbers of animals excluded from behavioural analyses** Summary of the numbers of animals excluded from each behavioural analysis and the reason for exclusion.

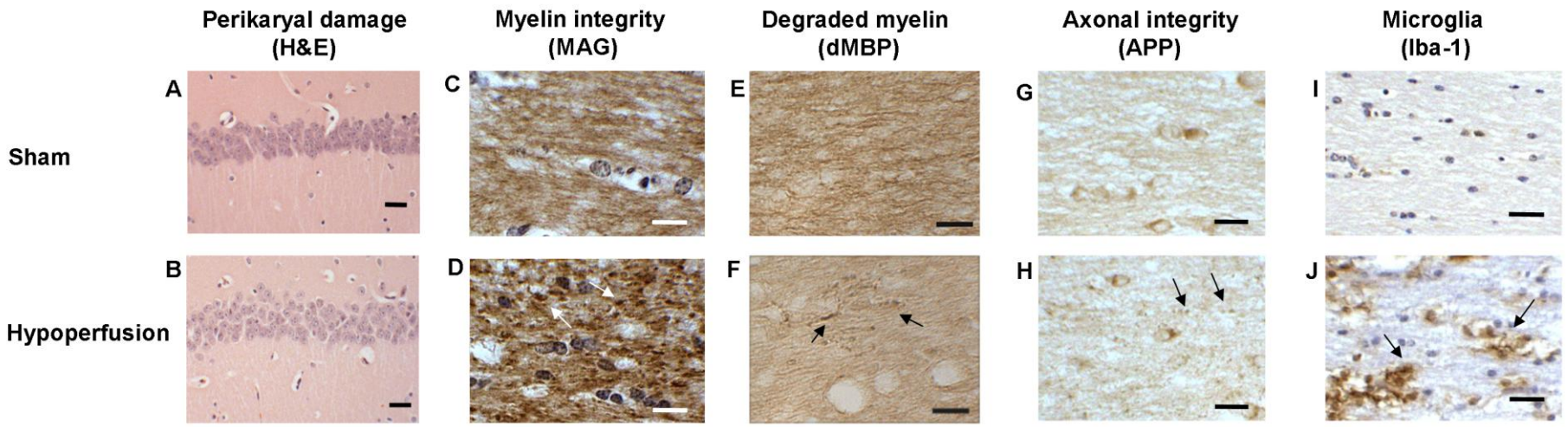


**Figure 5.1: Representative images of pathology after one month of hypoperfusion in mice**

Images show pathology in sham and hypoperfused animals 1 month after the induction of hypoperfusion. Neuronal cell bodies in the hippocampal CA1 were intact (A, B). Hypoperfused animals showed a loss of myelin integrity in the optic tract (C, D). Hypoperfused animals also displayed myelin debris in the optic tract (E, F). Damaged axons were visible in the optic tract of some hypoperfused animals (G, H). Microglial activation was also evident in the optic tract of hypoperfused animals (I, J). Scale bar represents 15 µm (A - B) and 30µm (C - J). Adapted from Coltman et al. (In press).

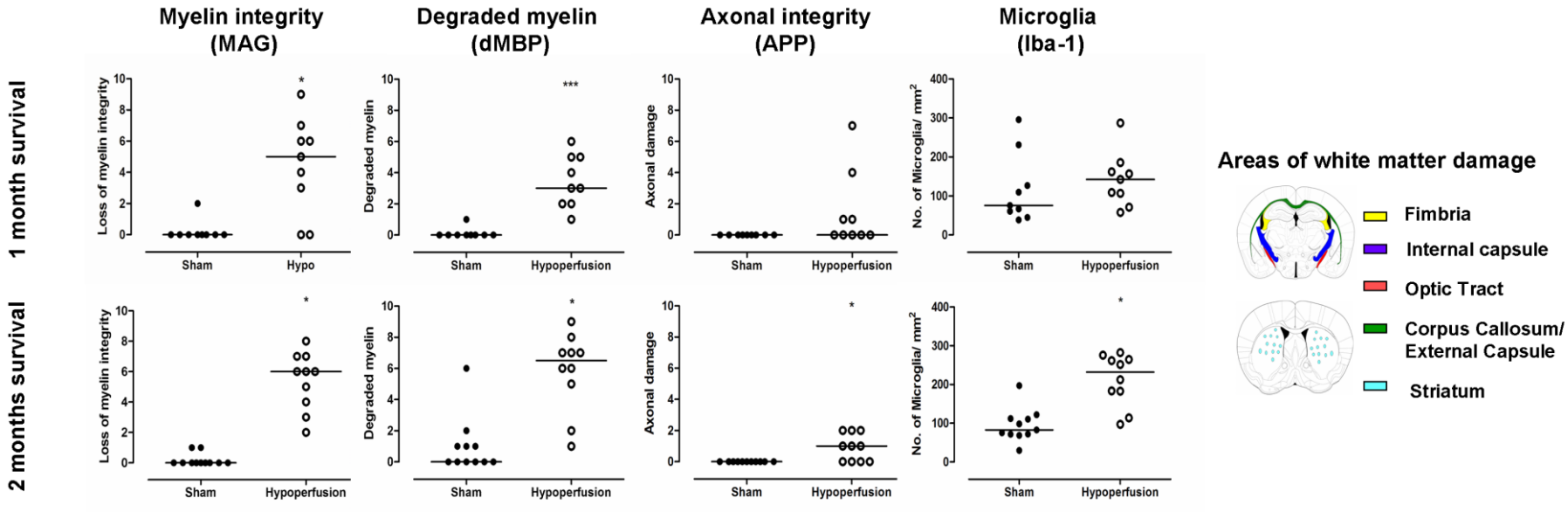


**Figure 5.2: Analysis of pathology after one and two months of hypoperfusion in mice**

Scores for pathology in each region examined were summed to give total scores for analysis. There was a significant loss of myelin integrity, identified using MAG immunostaining in hypoperfused animals at both 1 and 2 months of hypoperfusion. The amount of degraded myelin, identified using dMBP immunostaining was significantly increased in hypoperfused animals at both 1 and 2 months after the induction of hypoperfusion. There was evidence of axonal damage in hypoperfused animals and this was significantly different from shams after 2 months of hypoperfusion. Hypoperfused animals also showed elevated microglial activation, which was significantly different to shams after 2 months of hypoperfusion. Line in microglial activation graph represents the mean value; in all other graphs line represents the median value. Representative graphs of pathological data for 2 months of hypoperfusion show data from animals that underwent episodic memory testing. * = $p \leq 0.05$ vs. sham. Modified from Coltman et al. (In press).

*5.3.2 No impairment of spatial reference learning or memory following chronic cerebral hypoperfusion*

Animals showing persistent floating behaviour throughout the testing were excluded from the final analysis (n = 3 sham, 1 hypoperfused). Animals which showed evidence of ischaemic neuronal damage were also excluded from the behavioural analysis (n = 2 hypoperfused). This meant that the final numbers for analysis were n = 9 sham and n = 9 hypoperfused.

Both injured and sham animals decreased their latency to the cued platform over the training period ($F_{(1.317,21.072)}$ = 21.961, $p$ < 0.001; Figure 5.3A). There was no difference in performance between the injured and the sham-operated groups ($F_{(1,16)}$ = 0.002, $p$ = 0.969). Escape latencies averaged less than 10 seconds in both groups by the end of training. Mean swim speed across all trials did not differ significantly between injured and sham-operated animals (26.408 ± 0.974 cm/s vs. 26.440 ± 0.933 cm/s; |t| = 0.024, df = 16, $p$ = 0.981 respectively, mean ± SEM).

In the spatial reference learning version of the water maze task both groups were able to learn the location of a hidden platform over the 5 training days ($F_{(4,64)}$ = 10.327, $p$ < 0.001; Figure 5.3B). There was no significant difference between the groups in their ability to learn the platform location ($F_{(1,16)}$ = 0.206, $p$ = 0.656). Both groups showed the same degree of preference for the training quadrant when probed both 10 minutes (group x quadrant interaction, $F_{(3,48)}$ = 0.088, $p$ = 0.966; Figure 5.3C) and 24

hours (group x quadrant interaction, $F_{(2.099,33.591)} = 0.664$, $p = 0.578$; Figure 5.3D) after the end of training.

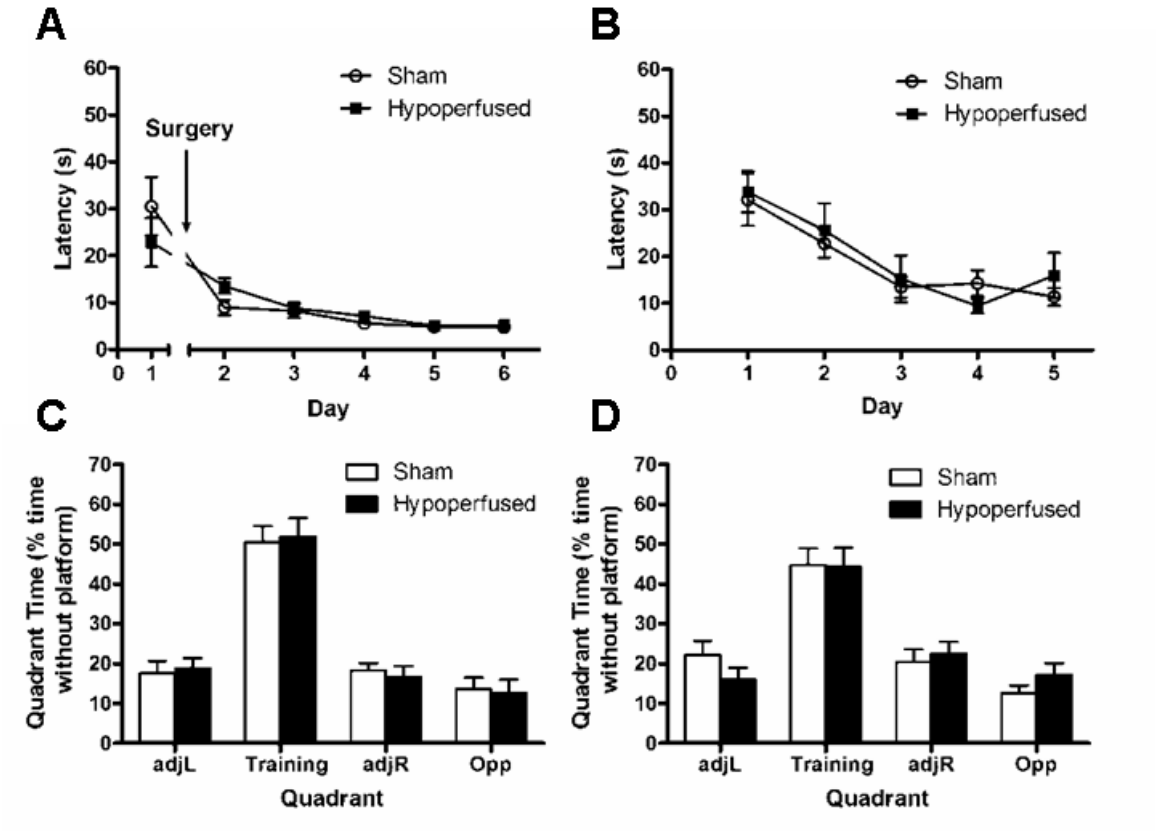


**Figure 5.3: Results of testing in the spatial reference memory task in the Morris water maze**

No difference between the groups was seen in any aspect of spatial reference memory testing (A – D). Animals performed equally well in the cued version of the task (A), in the hidden platform version of the task (B) and in the probes at 10 minutes (C) and 24 hours (D). Graphs show mean + SEM. adjL = adjacent left, adjR = adjacent right

*5.3.3 No impairment of episodic memory following chronic cerebral hypoperfusion*

Animals showing persistent floating behaviour throughout the testing were excluded from the final analysis (n = 1 sham, 1 hypoperfused). Animals which showed evidence of ischaemic neuronal damage were also excluded from the behavioural analysis (n = 4 hypoperfused). This meant that the final group numbers for analysis were n = 11 sham and n = 10 hypoperfused.

In pre-training on the cued version of the water maze task there was no difference in average swim speed between the two groups (25.254 ± 1.042 cm/s vs. 26.440 ± 0.763 cm/s; |t| = 0.902, df = 19, $p$ = 0.379 sham vs. hypoperfused, mean ± SEM). Both sham and hypoperfused animals successfully learned to swim to the visible platform over the 5 training days ($F_{(1.768,33.600)}$ = 34.538, $p < 0.001$; Figure 5.4A). The groups did not differ in their ability to learn this task ($F_{(1,19)}$ = 0.054, $p$ = 0.818).

The number of tasks animals required to learn the platform location to criterion did not change over the first 5 platform locations ($F_{(4,76)}$ = 1.566, $p$ = 0.192; Figure 5.4B). Hypoperfusion did not affect the number of tasks required to learn the first 5 platform locations to criterion ($F_{(1,19)}$ = 0.035, $p$ = 0.853). Analysis of the time spent in the training quadrant during probe testing across the first 5 platform locations revealed no difference between sham and hypoperfused animals in either the 10 minute ($F_{(1,18)}$ = 0.018, $p$ = 0.894; Figure 5.4C) or 3 hour probes ($F_{(1,19)}$ = 0.151, $p$ = 0.702; Figure 5.4D. Hypoperfused mice did not differ from sham controls in the

number of tasks learned in the first 10 training days ($|t| = 0.756$, $df = 18$, $p = 0.459$; Figure 5.4E).

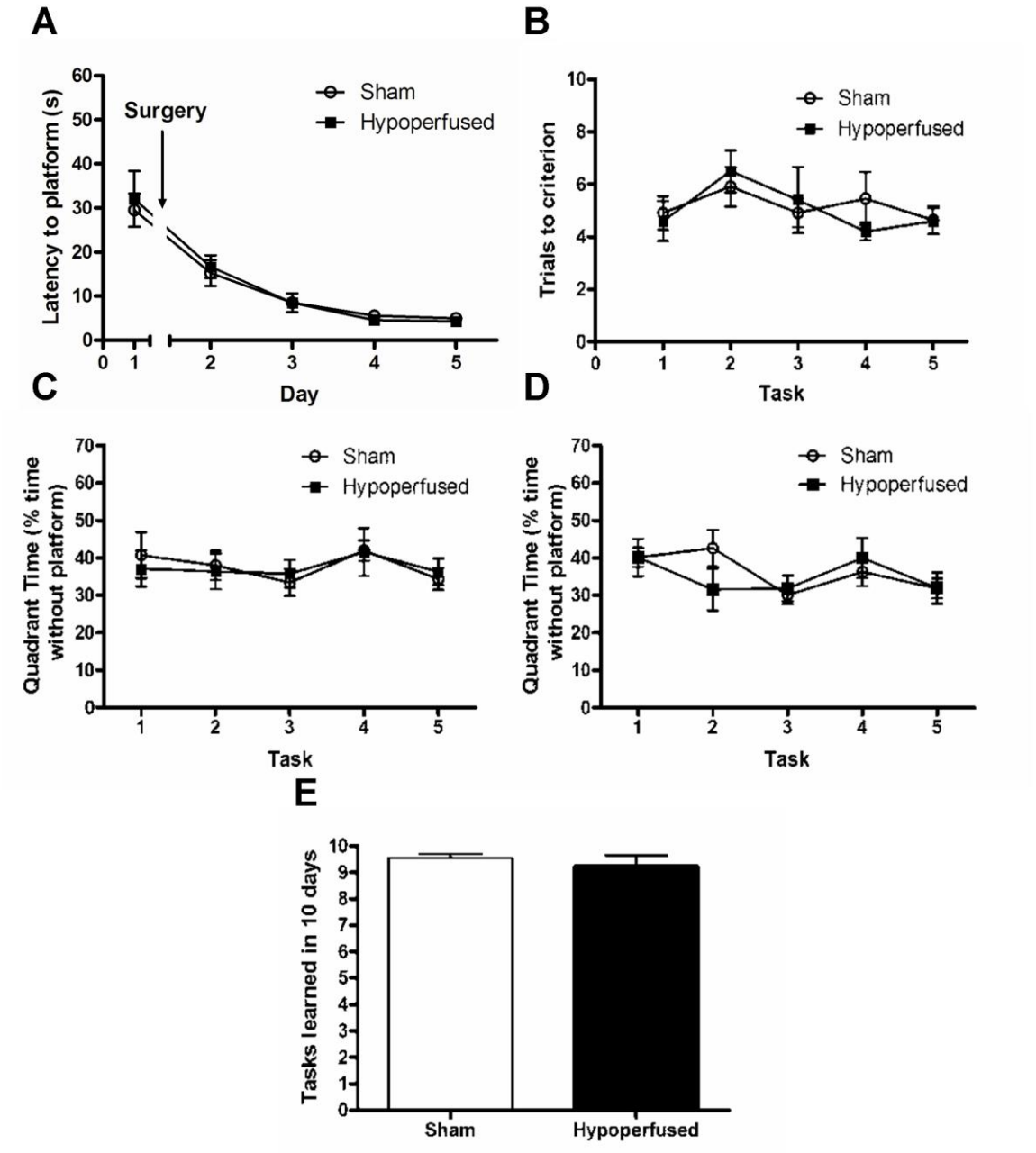


**Figure 5.4: Results of testing in the episodic memory task in the Morris water maze**

No difference was observed between sham and hypoperfused animals in the episodic memory task (A – E). Hypoperfused animals performed as well as shams in the cued task (A) and in the number of trials taken to learn a platform location (B) and showed no impairment in probe tests (C, D) or learning capacity (E). Graphs show mean + SEM.

*5.3.4 Impaired working memory following chronic cerebral hypoperfusion*

In the first cohort tested on this task 7 hypoperfused animals were excluded from the analysis due to evidence of ischaemic neuronal damage, giving final group numbers for analysis of 10 sham and 3 hypoperfused animals.

In the radial arm maze task hypoperfused mice showed a significantly higher rate of errors than sham operated controls ($F_{(1,11)} = 7.926$; $p = 0.017$; Figure 5.5A). There were significant differences between the groups in the number of errors made in training blocks 5 and 7 ($p < 0.05$ in each case). Overall, both groups reduced the number of errors committed in each trial across the training period ($F_{(7,77)} = 8.935$; $p < 0.001$). There was no significant difference between the groups in the number of novel arm entries made within the first eight arm entries ($F_{(1,11)} = 0.930$; $p = 0.356$; Figure 5.5B). Both groups improved the number of novel entries made in the initial eight arm entries over the training period ($F_{(7,77)} = 3.240$; $p = 0.005$). In the final training trials with a two minute delay after the fourth arm entry there was no difference between the groups in the number of errors committed ($F_{(1,11)} = 1.495$; $p = 0.247$). Hypoperfused and sham animals also showed no difference in the number of novel arm entries made in the initial eight entries ($F_{(1,11)} = 1.088$; $p = 0.319$).

In the second cohort of animals tested on this task 17 hypoperfused animals were excluded due to the presence of ischaemic neuronal damage. This meant that the final group numbers for analysis were 17 sham and 7 hypoperfused.

Hypoperfused mice in this cohort committed significantly more errors in the working memory task than shams ($F_{(1,22)} = 6.981$; $p = 0.015$; Figure 5.5C). *Post hoc* tests did not show differences between the groups on individual blocks. There was a significant reduction in the number of errors committed across the training days by both groups ($F_{(7,154)} = 10.687$; $p < 0.001$). Hypoperfused mice also made significantly fewer novel arm entries in their first eight arm entries than shams ($F_{(1,22)} = 5.619$; $p = 0.027$; Figure 5.5D). A significant difference between the groups was observed in training block 7 ($p < 0.05$). Both groups significantly increased the number of novel entries made in the first eight entries across the training days ($F_{(7,154)} = 9.223$; $p < 0.001$). In trials with an extra two minute delay there was no significant difference between hypoperfused and sham animals in the number of errors made ($F_{(1,22)} = 3.110$; $p = 0.092$) or in the number of novel entries made in the first eight entries ($F_{(1,22)} = 2.529$; $p = 0.126$).

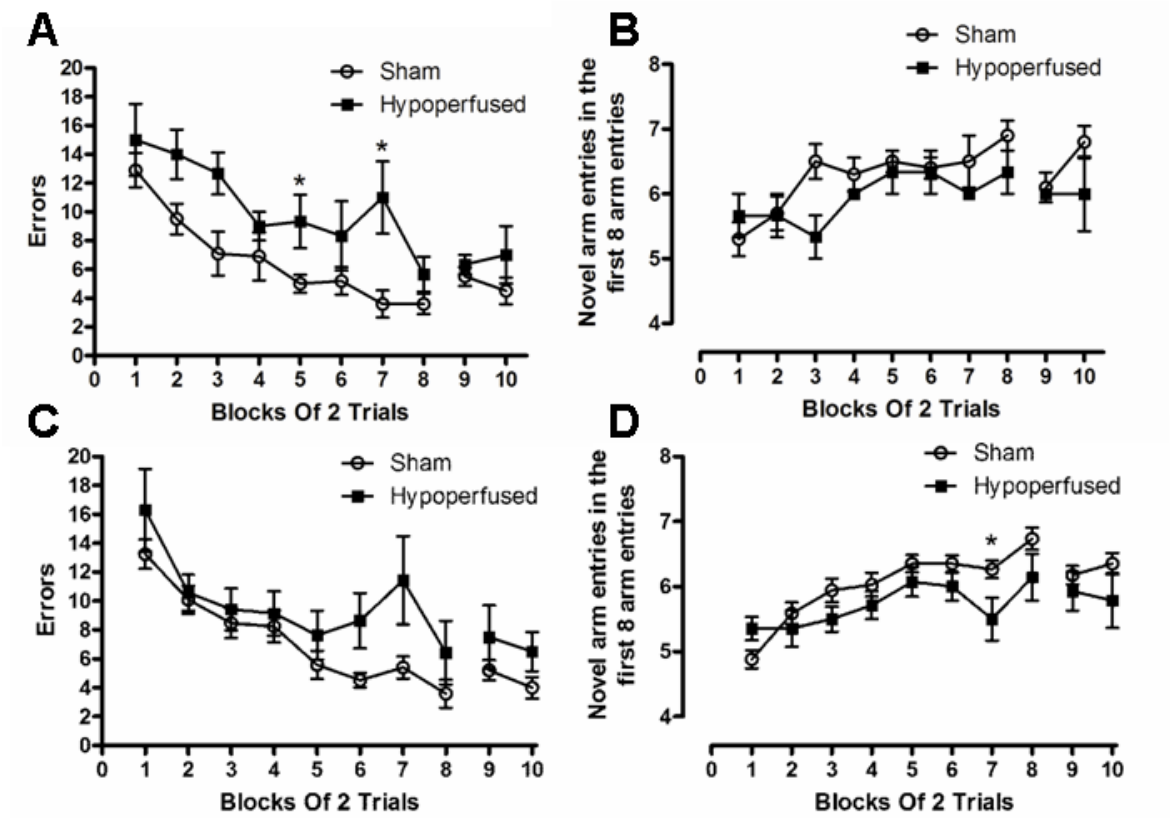


**Figure 5.5: Working memory deficit in hypoperfused mice in the 8-arm radial maze task**

In the first cohort tested (A, B) hypoperfused mice made more working memory errors than sham operated controls in both the initial testing phase and that with a 2 minute delay (A). There was no difference between the groups in the number of novel arm entries made in the first 8 arm entries until the extra delay was introduced (B). In the second cohort tested hypoperfused mice made significantly more errors (C) and visited significantly fewer novel arms in the first 8 arm entries (D). There was no difference between the groups on either measure when the extra delay was introduced. * = $p \leq 0.05$ vs. sham. Graphs show mean + SEM.

## 5.4 Discussion

Evidence from studies of aging populations suggests a link between chronic cerebral hypoperfusion, white matter and cognition. In humans a number of pathological states, such as atherosclerosis and diabetes are associated with hypoperfusion, making isolation of the effects of hypoperfusion alone on white matter and cognition difficult without the use of animal models. The present study investigated the effects of chronic cerebral hypoperfusion on cognition and white matter pathology in wild-type mice after one or two months of hypoperfusion. The hypothesis that chronic cerebral hypoperfusion would cause damage to elements of white matter was upheld by the observation of diffuse changes to myelin, microglia and axons. The hypothesised deficit in working memory in hypoperfused animals was observed while predicted deficits in spatial learning, memory and serial spatial learning were not.

Diffuse loss of myelin integrity was observed at both one and two months after onset of chronic cerebral hypoperfusion and was accompanied by microglial activation and minimal damage to axons. The observation of diffuse white matter damage and microglial activation in this study agrees with the findings of Shibata (2004). These authors did not examine the cellular components of white matter and a novel finding of the study described here is the observation of axonal damage and alterations in specific myelin markers. The behavioural results described in this study also agree with previous descriptions of behaviour in this model (Shibata et al., 2007), that is,

spatial working memory is impaired while spatial reference memory is intact. The present study has the advantage that behavioural testing and pathological assessment were undertaken in the same animals, allowing direct extrapolation from the pathological to behavioural findings. Additionally this study examined episodic memory, which has not previously been examined in this model and found that chronic hypoperfusion does not impact on this aspect of cognition.

Cerebral hypoperfusion is associated with white matter damage and cognitive deficits in studies of aging humans (Breteler, 2000; Vernooij et al., 2008) as well as in rat models of reduced CBF (Farkas et al., 2007). The underlying molecular mechanism resulting in damage to white matter following a period of cerebral hypoperfusion is unclear but the presence of white matter damage in the absence of a focal ischaemic lesion indicates that sustained sub-ischaemic levels of CBF reduction are capable of a pathological effect on the brain. Shibata et al. (2004) report modest decreases in CBF of no more than 30% in the model used in this study and this should not be sufficient to cause tissue damage. Clear disruption of cellular elements of white matter was observed in this study, with particular effects on myelin. Degradation of the myelin sheath can affect axon survival due to impairment of trophic support (Nave, 2010). MAG was specifically shown to be affected by hypoperfusion in this study and is implicated in axo-glial interactions (Quarles, 2009). Disruption of MAG may affect axonal survival due to the role of MAG in expression and phosphorylation of elements of the axonal cytoskeleton (Dashiell et al., 2002). Following myelin damage, microglial activation may further exacerbate disruptions in myelination through secretion of inflammatory cytokines (Schmitz and

Chew, 2008). The present study does not explain how damage to white matter arises as a result of chronic cerebral hypoperfusion but it does demonstrate a clear relationship between chronic cerebral hypoperfusion, white matter damage and cognitive deficits.

Spatial reference learning and memory were assessed in the Morris water maze after one month of hypoperfusion and hypoperfused animals showed no deficit in this task, consistent with the findings of Shibata et al. (2007). Miki et al. (2008) reported a deficit in this task in their modified version of this model, however these authors also report hippocampal cell loss, which, given the importance of the hippocampus in learning this task (D'Hooge and De Deyn, 2001) is the most likely explanation of the deficits in this instance. Similarly Nishio et al. (2010) found hippocampal atrophy in this model after 5 to 6 months of hypoperfusion which was associated with a spatial reference memory deficit. Deficits in the spatial reference learning task can also be produced by lesions of connections to both the hippocampus (Nilsson et al., 1987) and other brain regions such as the thalamus (Savage et al., 1997), however the degree of damage observed in this model is not equivalent in severity to the type of lesion described in these studies and therefore may not be sufficient to produce a deficit by itself.

The trials to criterion protocol has previously been used to examine "episodic-like memory" in transgenic models of Alzheimer's disease (Chen et al., 2000; Daumas et al., 2008; Morris, 2001). The number of trials taken for an animal's performance to reach criterion on a given platform location is indicative of its ability to selectively

retrieve the information most relevant for swimming to this platform location and to ignore the information related to other platform locations and this acts as a measure of "episodic-like memory" (Chen et al., 2000). Episodic memory deficits are relevant to the cognitive changes associated with white matter damage in humans (Bucur et al., 2008; Deary et al., 2003; Gold et al., 2010) but were not detectable in this model of hypoperfusion after two months of hypoperfusion. The hippocampus is involved in episodic memory in rodents (Smith et al., 2006; Wood et al., 1999) but white matter involvement in episodic memory in rodents is not well investigated. In humans, loss of white matter integrity in the medial temporal lobe is associated with deficits in episodic memory (Carmichael et al., In press; Charlton et al., 2010; Goldstein et al., 2009). In this study it may have been the case that the training criterion used was not sufficiently stringent to expose subtle alterations in episodic memory function (Daumas et al., 2008).

The presence of working memory deficits is another persistent theme in studies of white matter damage and cognitive deficits in humans (Appelman et al., 2010; Kennedy and Raz, 2009; O'Sullivan et al., 2001) and the radial arm maze task is a well established measure of working memory ability in rodents (Cole and Chappell-Stephenson, 2003; Hyde et al., 1998; Olton and Samuelson, 1976). This task has previously been used to demonstrate a deficit in working memory in this model of chronic cerebral hypoperfusion (Shibata et al., 2007), a finding which has been successfully replicated here. This demonstrates that chronic cerebral hypoperfusion can, in isolation, produce sufficient damage to white matter to produce a cognitive impairment. The specific attribution of cognitive deficits to chronic cerebral

hypoperfusion, regardless of its cause, has implications for how best to improve cognitive function and to measure improvements in individuals with chronic cerebral hypoperfusion, where there may be a range of coexisting pathologies. In individuals with diabetes, for instance, there may be impairment in multiple cognitive domains (Kodl and Seaquist, 2008) but in addition to changes in white matter these individuals also show grey matter atrophy (Lobnig et al., 2006) which may affect different aspects of cognition to white matter damage. This makes selection of the cognitive domain in which to assess the efficacy of interventions targeting white matter and chronic cerebral hypoperfusion related cognitive impairment important in order to avoid erroneously disregarding potentially useful interventions.

Myelin pathology in this model was widespread in nature, with damage having been observed in the fimbria, internal capsule, optic tract, corpus callosum/external capsule and striatum. This was true at both one and two months after the onset of hypoperfusion and no difference between the two time points in the level of damage present was observed (Coltman et al., In press). This diffuse damage does not allow attribution of the cognitive deficit seen here to damage in a specific region, unlike some human investigations of cognitive impairments and white matter damage (Delano-Wood et al., 2009; Kennedy and Raz, 2009). The hippocampus, parahippocampal region and prefrontal cortex are implicated in working memory in rodents (Hodges, 1996; Shaw et al., 1993). In the case of the hippocampus, transection of its connections has been demonstrated to produce working memory deficits while leaving the grey matter structures intact (Aggleton et al., 1992; Wiig et al., 1995). Given the number of brain regions involved in working memory tasks it

may be the case, in this model that disruption, rather than severance, of signalling between multiple brain regions is sufficient to produce a deficit in working memory. Other models of myelin loss have previously shown deficits in working memory in the Y maze (Xu et al., 2009) and T maze (Tanaka et al., 2009) and this has been linked with decreased conduction velocities and decreased axon diameters in the demyelinated fibres (Tanaka et al., 2009).

Here, a model of chronic cerebral hypoperfusion, which produces selective damage to white matter, has been shown to display a deficit in working memory but not spatial reference memory, episodic like memory or memory flexibility. This study has also been able to directly attribute the observed behavioural changes to white matter damage arising from chronic cerebral hypoperfusion and to identify the effects of chronic hypoperfusion on different components of white matter. The working memory deficit demonstrated here may be attributable to a disruption of signalling between the numerous regions involved in working memory and is relevant to human investigations of cognitive impairment associated with white matter damage.

# 6 Discussion

## 6.1 Summary

In general these studies indicated the vulnerability of white matter to brain injury and the importance of white matter injury in cognitive impairment which could also act as a link to Alzheimer's disease (AD). Initially, axonal pathology and an associated cognitive deficit were characterised in a model of mild traumatic brain injury (TBI). The effects of axonal damage on AD-related pathology were then examined by combining this TBI model with a transgenic model of AD. Finally, selective myelin damage was found to be associated with an impairment in the specific cognitive domain of working memory in a model of chronic cerebral hypoperfusion.

## 6.2 White matter pathology and cognitive outcomes in traumatic brain injury and hypoperfusion

Both the mild TBI and hypoperfusion models used in this thesis demonstrate that selective damage to a specific element of white matter is sufficient to produce cognitive deficits. The models are characterised by deficits in different cognitive domains and damage to different white matter components; impaired spatial reference learning was associated with axonal pathology in response to mild TBI and a spatial working memory deficit was linked to white matter damage, mainly of

myelin, in response to chronic cerebral hypoperfusion. It is significant in both these models that the level of damage, whether to axons or myelin, is not equivalent in severity to the lesions of white matter tracts used in investigations of deficits produced by disconnection of different brain regions (e.g. Aggleton et al., 1992; Shaw et al., 1993; Wiig et al., 1995). The anatomical patterns of damage observed in each model are very different, a potential basis for the differing cognitive deficits observed. The mild TBI model demonstrates axonal pathology confined to specific, though changing regions over time; while the white matter pathology observed with chronic cerebral hypoperfusion is distributed diffusely. This reflects the difference between the focal insult resulting from mild TBI and the global changes produced by chronic cerebral hypoperfusion. In mild TBI disruption of projections from the thalamus, external capsule or cingulum could affect the coordination of input to the hippocampus or other regions required for spatial learning. In chronic cerebral hypoperfusion diffuse loss of myelin integrity could affect conduction velocities in a number of tracts, also affecting harmonisation of inputs to regions needed for successful performance in a working memory task. Although the specific mechanisms of cognitive dysfunction observed in the two models may differ, in both cases the observed damage may exert its behavioural effects by disrupting synchronous input to different regions necessary for cognitive function (Bartzokis, 2004; Fields, 2008). The presence of a loss of signal strength or decrease in conduction velocity could be determined by via electrophysiological measurement of extracellular field potentials and intracellular recordings of axonal conduction velocity (e.g. Ai et al., 2007; Teigler et al., 2009; Yamazaki et al., 2007).

One of the advantages of the present studies has been the ability to define which of the cellular components of white matter are affected by injury. In human studies of cognitive changes and white matter damage resulting from TBI or cerebral hypoperfusion, identification of which elements of white matter are damaged is difficult using conventional imaging techniques. Studies using diffusion tensor imaging (DTI) have the potential to address this issue by allowing separation of measures of myelin and axonal integrity by comparison of alterations in the diffusion pattern of water molecules. An increase in diffusion of water molecules perpendicular to the white matter tract of interest is proposed to reflect reduced myelin integrity; while a decrease in diffusion parallel to the tract has been suggested to indicate compromised axonal integrity (Song et al., 2003). The low spatial resolution of DTI compared to pathological investigation may result in ambiguity in the interpretation of imaging results but recent work from this group has demonstrated that DTI measurements correlate well with pathological assessment of myelin damage in the model of chronic cerebral hypoperfusion used in these studies (Holland et al., In press).

The two models used in this thesis demonstrate that damage to either myelin or axons can have significant cognitive consequences and that the component injured, as well as the anatomical distribution of damage, may influence the type of deficit observed. Typically, studies of patients who have suffered a mild TBI or those with white matter damage associated with cognitive deficits show impairments in a number of cognitive domains and the studies described here may indicate that multiple deficits reflect multiple pathologies in an individual. Also assessment of

cerebral perfusion by single photon emission computed tomography (SPECT) imaging indicates that chronic regional hypoperfusion may exist in mild TBI patients who present with persistent cognitive impairment (Bonne, 2003), suggesting that there may be a role for both pathologies investigated here in persistent impairment after mild TBI. It is not possible to rule out that mild TBI results in local hypoperfusion and subsequent damage to white matter in the model used in this thesis. However, this may be unlikely given that hypoperfusion was shown to cause damage primarily to myelin, which was not damaged after mild TBI. Establishment of regional perfusion levels in this model would determine its suitability for investigation of the respective contributions of brain trauma and subsequent hypoperfusion in mild TBI.

As well as demonstrating different roles for different components of white matter in cognition the behavioural results presented in this thesis also have implications for cognition in disorders other than TBI and chronic hypoperfusion. The white matter damage observed in AD (e.g. Brun and Englund, 1986; Englund et al., 1988) could contribute to the cognitive impairments characteristic of the disease. Cognitive impairments also affects at least 40% of people with multiple sclerosis (Amato et al., 2006), a primarily demyelinating disorder that also involves axonal damage. Current treatment for AD focuses on cholinesterase inhibitors and blockade of NMDA receptors (Roberson and Mucke, 2006). Cholinesterase inhibitors have also been adopted as treatments for cognitive impairment in multiple sclerosis (Porcel and Montalban, 2006) as well as mild TBI (Willer and Leddy, 2006) but their efficacy is limited and endures only as long as treatment is continued. Addressing the white

matter pathology underlying the impairment in these disorders may offer a more permanent solution to cognitive impairment. Axon degeneration may be targeted by calpain inhibitors, in an attempt to prevent breakdown of the neuronal cytoskeleton or blockade of the sodium–calcium exchanger in order to prevent a rise in intraaxonal calcium (Stys, 1998; Wang et al., 2004). Reversal or prevention of myelin damage may rely on inhibition of inflammatory events or stimulation of remyelination by oligodendrocytes (Peru et al., 2008; Schmitz and Chew, 2008).

## 6.3 White matter pathology and the development of Alzheimer's disease

The studies presented in this thesis demonstrate that cognitive dysfunction occurs in parallel with selective white matter damage. Additionally the presence of axonal pathology following mild TBI may have implications for the development of another pathological condition, Alzheimer's disease. The presence of amyloid β (Aβ) accumulations at only 24 hours after injury demonstrates that early intervention may be important in ameliorating the effects of TBI on subsequent development of AD. Taken in conjunction with the progression of APP accumulations marking damaged axons observed following mild TBI the data suggests a mechanism by which Aβ accumulation may be distributed throughout the brain after injury. The changing location of APP accumulations over time following injury may provide a spatially distributed pool of substrate for cleavage by β- and γ-secretases. The temporal

progression of axonal damage, if mirrored by the progression of Aβ accumulation may also explain delayed onset of AD following TBI.

Johnson et al. (2010) and Stokin et al. (2005) propose that accumulations of Aβ in axon bulbs result from cleavage of APP co-accumulated in axonal bulbs with β- and γ - secretase due to failure of axonal transport or to injury. The axonal bulbs containing Aβ then lyse and expel Aβ into the parenchyma were it aggregates. This does not provide an explanation for changes in Aβ levels in neuronal cell bodies in AD. The continual development of axonal pathology after TBI in wild type mice implies a chronic pathological process such as Wallerian degeneration or retraction of the damaged axon rather than static levels of damage to axons. Retraction of the damaged axon, along with proteins accumulated there towards the cell body (Saxena and Caroni, 2007) might elevate Aβ levels within the cell body but it is not possible to determine from the present studies whether this is the mechanism involved in axonal degeneration in this model. Axonal retraction can be distinguished from Wallerian degeneration by the preservation of axonal material within the retracting axonal process rather than the axonal segmentation and subsequent phagocytosis characteristic of Wallerian degeneration (Saxena and Caroni, 2007). Microtubule associated proteins might serve as useful markers to distinguish between these processes, with microtubule filaments remaining intact during axonal retraction and being disassembled in Wallerian degeneration. The development of grey matter AD pathology may, alternatively, proceed independently of that in white matter. Intracellular increases in both Aβ and APP have been observed following TBI (Gentleman et al., 1993; Iwata et al., 2002), suggesting another pool of Aβ

production in grey matter. In the AD model used here the presence of intracellular Aβ, even in the absence of injury, may make it difficult to detect subtle increases in background Aβ levels changes induced by TBI.

Alterations in amyloidogenic processing of APP may also have implications for TBI, independent of their effects on AD risk. Loane et al. (2009) have demonstrated preservation of cognitive function and attenuation of cell loss after TBI in β - secretase knockout mice and also with chronic partial inhibition of γ-secretase in wild-type mice. These changes were observed in conjunction with either a reduction in or elimination of murine Aβ. A therapeutically relevant study involving acute, short-term inhibition of β- or γ - secretase could indicate a potentially useful preventative measure for long-term axonal damage following TBI or development of AD. Both intracellular and extracellular Aβ can disrupt axonal transport (Decker et al., 2010; Muresan and Muresan, 2009), potentially exacerbating axonal pathology observed after TBI and contributing to its persistence.

Although not addressed here, modelling chronic cerebral hypoperfusion may also be useful in investigating AD. Disease states that can result in hypoperfusion are risk factors for AD (Dickstein et al., 2010) and hypoperfusion is also a feature of AD (Johnson et al., 2005). In a rat model of chronic cerebral hypoperfusion Aβ and β-secretase levels have been shown to be elevated (Zhiyou et al., 2009). Similarly, increases in Aβ have been observed in a transgenic mouse model of AD after chronic hypoperfusion, including in white matter (Kitaguchi et al., 2009). Conversely, the deposition of Aβ in blood vessels, as observed in the brains of AD patients can cause

reduced perfusion by occlusion of capillaries (Thal et al., 2008). Use of this technique for modelling hypoperfusion in transgenic mice would allow investigation of the role of hypoperfusion in AD development.

## 6.4 Future studies

The findings described in this thesis could be extended by further investigation of the mechanisms involved in the pathological and cognitive alterations observed. Identification of the effect of mild TBI or chronic cerebral hypoperfusion on firing synchronicity in neural networks necessary for cognition via electrophysiological techniques (e.g. Ai et al., 2007; Teigler et al., 2009; Yamazaki et al., 2007) would allow comparisons to be made between the effects of damage to particular components of white matter and lesions of entire white matter tracts. This approach would also allow comparisons of the effects of myelin disruption and axonal damage on conduction velocity and signal strength.

Determination of the secondary mechanisms causing progressive axonal pathology and the fate of damaged axons following mild TBI is also crucial for determining targets for modification of pathology following mild TBI. Electron microscopy would allow observation of the effects of injury on the axonal cytoskeleton, allowing a distinction to be made between axonal degeneration and retraction following injury (Coleman, 2005). In the chronic cerebral hypoperfusion model electron microscopy

could elucidate the effects of the observed disruption of specific myelin proteins on the integrity of the myelin sheath (e.g. Edgar et al., 2009).

To further determine the relevance of mild TBI to the future development of AD, extension of studies of mild TBI in a transgenic model of AD is necessary. This would demonstrate whether the pathology observed acutely after injury is associated with an accelerated progression of AD-related pathology in the model as well as allowing scope for investigation of the potential additive effects of mild TBI and AD on cognition.

## 6.5 Conclusion

The results described in this thesis demonstrate that relatively modest pathological alterations in white matter can have an extended impact on cognitive function as well as on development of another disease state. The impact observed on cognition suggests that coordinated communication between different grey matter regions is as necessary for normal function as the integrity of the grey matter regions themselves. As well as being itself associated with persistent cognitive deficits, axonal pathology after mild TBI can also have features relevant in the context of AD soon after injury. This presents alleviation of axonal damage following TBI as a potential target for reducing subsequent risk of AD and repair or prevention of white matter damage as strategies for rescuing cognitive function in individuals who have experienced mild TBI, chronic cerebral hypoperfusion, or other disorders affecting white matter.

# References

af Geijerstam, J.L., Britton, M. (2003) Mild head injury - mortality and complication rate: meta-analysis of findings in a systematic literature review. *Acta Neurochir.* 145, 843.

Aggleton, J.P., Keith, A.B., Rawlins, J.N., Hunt, P.R., Sahgal, A., Aggleton, J.P. (1992) Removal of the hippocampus and transection of the fornix produce comparable deficits on delayed non-matching to position by rats. *Behav. Brain Res.* 52, 61.

Ai, J., Liu, E., Wang, J., Chen, Y., Yu, J., Baker, A.J. (2007) Calpain inhibitor MDL-28170 reduces the functional and structural deterioration of corpus callosum following fluid percussion injury. *J. Neurotrauma* 24, 960.

Alonso, A.C., Grundke-Iqbal, I., Iqbal, K. (1996) Alzheimer's disease hyperphosphorylated tau sequesters normal tau into tangles of filaments and disassembles microtubules. *Nat. Med.* 2, 783.

Amato, M.P., Zipoli, V., Portaccio, E. (2006) Multiple sclerosis-related cognitive changes: a review of cross-sectional and longitudinal studies. *J. Neurol. Sci.* 245, 41.

Appelman, A.P.A., van der Graaf, Y., Vincken, K.L., Mali, W.P.T.M., Geerlings, M.I. (2010) Combined effect of cerebral hypoperfusion and white matter lesions on executive functioning - The SMART-MR study. *Dement. Geriatr. Cog. Disord.* 29, 240.

Arciniegas, D.B., Anderson, C.A., Topkoff, J., McAllister, T.W. (2005) Mild traumatic brain injury: a neuropsychiatric approach to diagnosis, evaluation, and treatment. *Neuropsychiatr. Dis. Treat.* 1, 311.

Bartzokis, G. (2004) Age-related myelin breakdown: a developmental model of cognitive decline and Alzheimer's disease. *Neurobiol. Aging* 25, 5.

Basser, P. (1994) MR diffusion tensor spectroscopy and imaging. *Biophys. J.* 66, 259.

Baumann, N., Pham-Dinh, D. (2001) Biology of oligodendrocyte and myelin in the mammalian central nervous system. *Physiol. Rev.* 81, 871.

Benes, F.M., Turtle, M., Khan, Y., Farol, P. (1994) Myelination of a key relay zone in the hippocampal formation occurs in the human brain during childhood, adolescence, and adulthood. *Arch. Gen. Psychiat.* 51, 477.

Bisschops, R.H., van der Graaf, Y., Mali, W.P., van der Grond, J. (2004) High total cerebral blood flow is associated with a decrease of white matter lesions. *J. Neurol.* 251, 1481.

Blurton-Jones, M., LaFerla, F.M. (2006) Pathways by which Aβ facilitates tau pathology. *Curr. Alz. Res.* 3, 437.

Bonne, O. (2003) Cerebral blood flow in chronic symptomatic mild traumatic brain injury. *Psychia. Res.* 124, 141.

Bramlett, H.M., Dietrich, W.D. (2004) Pathophysiology of cerebral ischemia and brain trauma: similarities and differences. *J. Cereb. Blood Flow Metab.* 24, 133.

Breteler, M.M.B. (2000) Vascular risk factors for Alzheimer's disease: An epidemiologic perspective. *Neurobiol. Aging* 21, 153.

Brun, A., Englund, E. (1986) A white matter disorder in dementia of the Alzheimer type: a pathoanatomical study. *Ann. Neurol.* 19, 253.

Bruns, J., Jr., Hauser, W.A. (2003) The epidemiology of traumatic brain injury: a review. *Epilepsia* 44 Suppl 10, 2.

Bucur, B., Madden, D.J., Spaniol, J., Provenzale, J.M., Cabeza, R., White, L.E. Huettel, S.A. (2008) Age-related slowing of memory retrieval: Contributions of perceptual speed and cerebral white matter integrity. *Neurobiol. Aging 29, 1070*

Bunge, M.B., Bunge, R.P., Ris, H. (1961) Ultrastructural study of remyelination in an experimental lesion in adult cat spinal cord. *J. Biophys. Biochem. Cytol.* 10, 67.

Cain, D.P., Boon, F., Corcoran, M.E. (2006) Thalamic and hippocampal mechanisms in spatial navigation: a dissociation between brain mechanisms for learning how versus learning where to navigate. *Behav. Brain Res.* 170, 241.

Carbonell, W.S., Grady, M.S. (1999) Regional and temporal characterization of neuronal, glial, and axonal response after traumatic brain injury in the mouse. *Acta Neuropathol.* 98, 396.

Carmichael, O., Mungas, D., Beckett, L., Harvey, D., Tomaszewski Farias, S., Reed, B., Olichney, J., Miller, J., Decarli, C. (In press) MRI predictors of cognitive change in a diverse and carefully characterized elderly population. *Neurobiol. Aging*

Cernak, I. (2005) Animal models of head trauma. *NeuroRx* 2, 410.

Charlton, R.A., Barrick, T.R., Markus, H.S., Morris, R.G. (2010) The relationship between episodic long-term memory and white matter integrity in normal aging. *Neuropsychologia* 48, 114.

Chen, G., Chen, K.S., Knox, J., Inglis, J., Bernard, A., Martin, S.J., Justice, A., McConlogue, L., Games, D., Freedman, S.B., Morris, R.G. (2000) A learning deficit related to age and beta-amyloid plaques in a mouse model of Alzheimer's disease. *Nature* 408, 975.

Chen, X.-H., Siman, R., Iwata, A., Meaney, D.F., Trojanowski, J.Q., Smith, D.H. (2004) Long-term accumulation of amyloid-β, β-secretase, presenilin-1, and caspase-3 in damaged axons following brain trauma. *Am. J. Pathol.* 165, 357.

Chen, X.-H., Johnson, V.E., Uryu, K., Trojanowski, J.Q., Smith, D.H. (2009) A lack of amyloid β plaques despite persistent accumulation of amyloid β; in axons of long-term survivors of traumatic brain injury. *Brain Pathol.* 19, 214.

Cole, M.R., Chappell-Stephenson, R. (2003) Exploring the limits of spatial memory in rats, using very large mazes. *Learn. Behav.* 31, 349.

Coleman, M. (2005) Axon degeneration mechanisms: commonality amid diversity. *Nat. Rev. Neurosci.* 6, 889.

Coltman, R., Spain, A., Tsenkina, Y., Fowler, J.H., Smith, J., Scullion, G., Allerhand, M., Scott, F., Kalaria, R.N., Ihara, M., Daumas, S., Deary, I.J., Wood, E., McCulloch, J., Horsburgh, K. (In press) Selective white matter pathology induces a specific impairment in spatial working memory. *Neurobiol. Aging.*

Conti, A.C., Raghupathi, R., Trojanowski, J.Q., McIntosh, T.K. (1998) Experimental brain injury induces regionally distinct apoptosis during the acute and delayed post-traumatic period. *J. Neurosci.*18, 5663.

Corder, E.H., Saunders, A.M., Strittmatter, W.J., Schmechel, D.E., Gaskell, P.C., Small, G.W., Roses, A.D., Haines, J.L., Pericak-Vance, M.A. (1993) Gene dose of apolipoprotein E type 4 allele and the risk of Alzheimer's disease in late onset families. *Science* 261, 921.

D'Hooge, R., De Deyn, P.P. (2001) Applications of the Morris water maze in the study of learning and memory. *Brain Res. Rev.* 36, 60.

Dashiell, S.M., Tanner, S.L., Pant, H.C., Quarles, R.H. (2002) Myelin-associated glycoprotein modulates expression and phosphorylation of neuronal cytoskeletal elements and their associated kinases. *J. Neurochem.* 81, 1263.

Daumas, S., Sandin, J., Chen, K.S., Kobayashi, D., Tulloch, J., Martin, S.J., Games, D., Morris, R.G. (2008) Faster forgetting contributes to impaired spatial memory in the PDAPP mouse: deficit in memory retrieval associated with increased sensitivity to interference? *Learn. Mem.* 15, 625.

Davatzikos, C., Bhatt, P., Shaw, L.M., Batmanghelich, K.N., Trojanowski, J.Q. (In press) Prediction of MCI to AD conversion, via MRI, CSF biomarkers, and pattern classification. *Neurobiol. Aging.*

De Beaumont, L., Theoret, H., Mongeon, D., Messier, J., Leclerc, S., Tremblay, S., Ellemberg, D., Lassonde, M. (2009) Brain function decline in healthy retired athletes who sustained their last sports concussion in early adulthood. *Brain* 132, 695.

de Bortoli, V.C., Zangrossi Júnior, H., de Aguiar Corrêa, F.M., Almeida, S.d.S., de Oliveira, A.M. (2005) Inhibitory avoidance memory retention in the elevated T-maze is impaired after perivascular manipulation of the common carotid arteries. *Life Sci.* 76, 2103.

de Leeuw, F.E., de Groot, J.C., Achten, E., Oudkerk, M., Ramos, L.M., Heijboer, R., Hofman, A., Jolles, J., van Gijn, J., Breteler, M.M. (2001) Prevalence of cerebral white matter lesions in elderly people: a population based magnetic resonance imaging study. The Rotterdam Scan Study. *J. Neurol. Neurosurg. Psychiat.* 70, 9.

Deary, I.J., Leaper, S.A., Murray, A.D., Staff, R.T., Whalley, L.J. (2003) Cerebral white matter abnormalities and lifetime cognitive change: a 67-year follow-up of the Scottish Mental Survey of 1932. *Psychol. Aging* 18, 140.

DeCarli, C., Miller, B.L., Swan, G.E., Reed, T., Wolf, P.A., Carmelli, D., DeCarli, C. (2001) Cerebrovascular and brain morphologic correlates of mild cognitive impairment in the National Heart, Lung, and Blood Institute Twin Study. *Arch. Neurol.* 58, 643.

Decker, H., Lo, K.Y., Unger, S.M., Ferreira, S.T., Silverman, M.A. (2010) Amyloid-β peptide oligomers disrupt axonal transport through an NMDA receptor-dependent mechanism that is mediated by glycogen synthase kinase 3β in primary cultured hippocampal neurons. *J. Neurosci.* 30, 9166.

Delano-Wood, L., Bondi, M.W., Sacco, J., Abeles, N., Jak, A.J., Libon, D.J., Bozoki, A. (2009) Heterogeneity in mild cognitive impairment: differences in neuropsychological profile and associated white matter lesion pathology. *J. Int. Neuropsychol. Soc.* 15, 906

Dellu, F., Mayo, W., Vallee, M., Moal, M.L., Simon, H. (1997) Facilitation of cognitive performance in aged rats by past experience depends on the type of information processing involved: a combined cross-sectional and longitudinal study. *Neurobiol. Learn. Mem.* 67, 121.

Desai, M.K., Sudol, K.L., Janelsins, M.C., Mastrangelo, M.A., Frazer, M.E., Bowers, W.J. (2009) Triple-transgenic Alzheimer's disease mice exhibit region-specific abnormalities in brain myelination patterns prior to appearance of amyloid and tau pathology. *Glia* 57, 54.

Dickstein, D., L., Walsh, J., Brautigam, H., Stockton, J., Steven D., Gandy, S., Hof, P.R. (2010) Role of vascular risk factors and vascular dysfunction in Alzheimer's disease. *Mt. Sinai J. Med.* 77, 82.

Dikranian, K., Cohen, R., Mac Donald, C., Pan, Y., Brakefield, D., Bayly, P., Parsadanian, A. (2008) Mild traumatic brain injury to the infant mouse causes robust white matter axonal degeneration which precedes apoptotic death of cortical and thalamic neurons. *Exp. Neurol.* 211, 551.

Dixon, C.E., Clifton, G.L., Lighthall, J.W., Yaghmai, A.A., Hayes, R.L., Dixon, C.E. (1991) A controlled cortical impact model of traumatic brain injury in the rat. *J. Neurosci. Methods* 39, 253.

Domesick, V.B. (1970) The fasciculus cinguli in the rat. *Brain Res.* 20, 19.

Duff, K., Eckman, C., Zehr, C., Yu, X., Prada, C.M., Perez-tur, J., Hutton, M., Buee, L., Harigaya, Y., Yager, D., Morgan, D., Gordon, M.N., Holcomb, L., Refolo, L., Zenk, B., Hardy, J., Younkin, S. (1996) Increased amyloid-β42(43) in brains of mice expressing mutant presenilin 1. *Nature* 383, 710.

Edgar, J.M., McLaughlin, M., Werner, H.B., McCulloch, M.C., Barrie, J.A., Brown, A., Faichney, A.B., Snaidero, N., Nave, K.-A., Griffiths, I.R. (2009) Early ultrastructural defects of axons and axon-glia junctions in mice lacking expression of Cnp1. *Glia* 57, 1815

Ehehalt, R., Keller, P., Haass, C., Thiele, C., Simons, K. (2003) Amyloidogenic processing of the Alzheimer beta-amyloid precursor protein depends on lipid rafts. *J. Cell Biol.* 160, 113.

Englund, E., Brun, A., Alling, C. (1988) White matter changes in dementia of Alzheimer's type. Biochemical and neuropathological correlates. *Brain* 111, 1425.

Erb, D.E., Povlishock, J.T. (1988) Axonal damage in severe traumatic brain injury: an experimental study in cat. *Acta Neuropathol.* 76,347

Farkas, E., Luiten, P.G. (2001) Cerebral microvascular pathology in aging and Alzheimer's disease. *Prog. Neurobiol.* 64, 575.

Farkas, E., Donka, G., de Vos, R.A.I., Mihály, A., Bari, F., Luiten, P.G.M. (2004a) Experimental cerebral hypoperfusion induces white matter injury and microglial activation in the rat brain. *Acta Neuropathol.* 108, 57.

Farkas, E., Institóris, A., Domoki, F., Mihály, A., Luiten, P.G., Bari, F. (2004b) Diazoxide and dimethyl sulphoxide prevent cerebral hypoperfusion-related learning dysfunction and brain damage after carotid artery occlusion. *Brain Res.* 1008, 252.

Farkas, E., Luiten, P.G.M., Bari, F. (2007) Permanent, bilateral common carotid artery occlusion in the rat: A model for chronic cerebral hypoperfusion-related neurodegenerative diseases. *Brain Res. Rev* 54, 162.

Feeney, D.M., Boyeson, M.G., Linn, R.T., Murray, H.M., Dail, W.G., Feeney, D.M. (1981) Responses to cortical injury: I. Methodology and local effects of contusions in the rat. *Brain Res. Bull.* 211, 67.

Fell, J., Klaver, P., Lehnertz, K., Grunwald, T., Schaller, C., Elger, C.E., Fernández, G. (2001) Human memory formation is accompanied by rhinal-hippocampal coupling and decoupling. *Nat. Neurosci.* 4, 1259.

Fernando, M.S., Simpson, J.E., Matthews, F., Brayne, C., Lewis, C.E., Barber, R., Kalaria, R.N., Forster, G., Esteves, F., Wharton, S. B., Shaw, P.J., O'Brien, J.T., Ince, P.G. (2006) White matter lesions in an unselected cohort of the elderly. *Stroke* 37, 1391.

Fields, R.D. (2008) White matter in learning, cognition and psychiatric disorders. *Trend. Neurosci.* 31, 361.

Findeis, M.A. (2007) The role of amyloid β peptide 42 in Alzheimer's disease. *Pharmacol. Ther.* 116, 266.

Finder, V.H., Glockshuber, R. (2007) Amyloid-beta aggregation. *Neurodeg. Dis.* 4, 13.

Franklin, R.J.M., ffrench-Constant, C. (2008) Remyelination in the CNS: From biology to therapy. *Nat. Rev. Neurosci.* 9, 839.

Franklin, W., Paxinos, G. (1997) The mouse brain in stereotaxic coordinates. New York, Academic Press.

Games, D., Adams, D., Alessandrini, R., Barbour, R., Berthelette, P., Blackwell, C., Carr, T., Clemens, J., Donaldson, T., Gillespie, F., Games, D. (1995) Alzheimer-type neuropathology in transgenic mice overexpressing V717F beta-amyloid precursor protein. *Nature* 373, 523.

Genis, L., Chen, Y., Shohami, E., Michaelson, D.M. (2000) Tau hyperphosphorylation in apolipoprotein E-deficient and control mice after closed head injury. *J. Neurosci. Res.* 60, 559.

Gennarelli, T.A, Thibault, L.E., Adams, J.H., Graham, D.I., Thompson, C.J., Marcincin, R.P. (1982) Diffuse axonal injury and traumatic coma in the primate. *Ann. Neurol. 12, 564.*

Gennarelli, T.A. (1997) The pathobiology of traumatic brain injury. *The Neuroscientist* 3, 73.

Gentleman, S.M., Nash, M.J., Sweeting, C.J., Graham, D.I., Roberts, G.W. (1993) β-amyloid precursor protein (βAPP) as a marker for axonal injury after head injury. *Neurosci. Lett.* 160, 139.

Goedert, M., Spillantini, M.G. (2006) A century of Alzheimer's disease. *Science* 314, 777.

Gold, B.T., Powell, D.K., Xuan, L., Jicha, G.A., Smith, C.D. (2010) Age-related slowing of task switching is associated with decreased integrity of frontoparietal white matter. *Neurobiol. Aging* 31, 512.

Goldstein, F.C., Mao, H., Wang, L., Ni, C., Lah, J.J., Levey, A I. (2009) White matter integrity and episodic memory performance in mild cognitive impairment: A diffusion tensor imaging study. *Brain Imaging Behav.* 3, 132.

Gootjes, L., Teipel, S.J., Zebuhr, Y., Schwarz, R., Leinsinger, G., Scheltens, P., Möller, H.J., Hampel, H. (2004) Regional distribution of white matter hyperintensities in vascular dementia, Alzheimer's disease and healthy aging. *Dement. Geriatr. Cogn. Disord.* 18, 180.

Graham, D.I., Gentleman, S.M., Lynch, A., Roberts, G.W. (1995) Distribution of beta-amyloid protein in the brain following severe head injury. *Neuropathol. Appl. Neurobiol.* 21, 27.

Graham, D.I., Raghupathi, R., Saatman, K.E., Meaney, D., McIntosh, T.K. (2000) Tissue tears in the white matter after lateral fluid percussion brain injury in the rat: relevance to human brain injury. *Acta Neuropathol.* 99, 117.

Gunn-Moore, D.A., McVee, J., Bradshaw, J.M., Pearson, G.R., Head, E, Gunn-Moore, F.J. (2006) Ageing changes in cat brains demonstrated by beta-amyloid and AT8-immunoreactive phosphorylated tau deposits. *J. Feline Med. Surg.* 8, 234.

Gunn-Moore, D., Moffat, K., Christie, L.A., Head, E. (2007) Cognitive dysfunction and the neurobiology of ageing in cats. *J. Small Anim. Pract*. 48, 546.

Guskiewicz, K.M., Marshall, S.W., Bailes, J., McCrea, M., Cantu, R.C., Randolph, C., Jordan, B.D. (2005) Association between recurrent concussion and late-life cognitive impairment in retired professional football players. *Neurosurgery* 57, 719.

Hardy, J. (2009) The amyloid hypothesis for Alzheimer's disease: a critical reappraisal. *J. Neurochem.* 110, 1129.

Hardy, J.A., Higgins, G.A. (1992) Alzheimer's disease: the amyloid cascade hypothesis. *Science* 256, 184.

Hayward, N.M.E.A., Immonen, R., Tuunanen, P., Ndode-Ekane, X.E., Grohn, O.H.J., Pitkanen, A. (In press) Association of chronic vascular changes with functional outcome after TBI in rats. *J. Neurotrauma*.

Head, E., Callahan, H., Muggenburg, B.A., Cotman, C.W., Milgram, N.W. (1998) Visual-discrimination learning ability and beta-amyloid accumulation in the dog. *Neurobiol. Aging* 19, 415.

Head, E., McCleary, R., Hahn, F.F., Milgram, N.W., Cotman, C.W. (2000) Region-specific age at onset of beta-amyloid in dogs. *Neurobiol. Aging* 21, 89.

Headway (2010) Headway Annual Review Nottingham, Headway.

Heyman, A., Wilkinson, W.E., Stafford, J.A., Helms, M.J., Sigmon, A.H., Weinberg, T. (1984) Alzheimer's disease: a study of epidemiological aspects. *Ann. Neurol.* 15, 335.

Hicks, R.R., Smith, D.H., Lowenstein, D.H., Saint Marie, R., McIntosh, T.K. (1993) Mild experimental brain injury in the rat induces cognitive deficits associated with regional neuronal loss in the hippocampus. *J. Neurotrauma* 10, 405.

Higuchi, M., Zhang, B., Forman, M.S., Yoshiyama, Y., Trojanowski, J.Q., Lee, V.M., Higuchi, M. (2005) Axonal degeneration induced by targeted expression of mutant human tau in oligodendrocytes of transgenic mice that model glial tauopathies. *J. Neurosci.* 25, 9434.

Hodges, H. (1996) Maze procedures: the radial-arm and water maze compared. *Cog. Brain Res.* 3, 167.

Holland, P.R., Bastin, M.E., Jansen, M.A., Merrifield, G.D., Coltman, R.B., Scott, F., Nowers, H., Khallout, K., Marshall, I., Wardlaw, J.M., Deary, I.J., McCulloch;, J., Horsburgh, K. (In press) MRI is a sensitive marker of subtle white matter pathology in hypoperfused mice. *Neurobiol. Aging*.

Horsburgh, K., Cole, G.M., Yang, F., Savage, M.J, Greenberg, B.D., Gentleman, S.M., Graham, D.I., Nicoll, J.A. (2000) β-amyloid (Aβ) 42(43), Aβ42, Aβ40 and apoE immunostaining of plaques in fatal head injury. *Neuropathol. Appl. Neurobiol.* 26, 124.

Hoshino, S., Tamaoka, A., Takahashi, M., Kobayashi, S., Furukawa, T., Oaki, Y., Mori, O., Matsuno, S., Shoji, S., Inomata, M., Teramoto, A. (1998) Emergence of immunoreactivities for phosphorylated tau and amyloid-beta protein in chronic stage of fluid percussion injury in rat brain. *Neuroreport* 9, 1879.

Huh, J.W., Widing, A.G., Raghupathi, R. (2008) Midline brain injury in the immature rat induces sustained cognitive deficits, bihemispheric axonal injury and neurodegeneration. *Exp. Neurol.* 213, 84.

Hyde, L.A., Hoplight, B.J., Denenberg, V.H. (1998) Water version of the radial-arm maze: learning in three inbred strains of mice. *Brain Res.* 785, 236.

Ichinohe, N., Hayashi, M., Wakabayashi, K., Rockland, K.S. (2009) Distribution and progression of amyloid-beta deposits in the amygdala of the aged macaque monkey, and parallels with zinc distribution. *Neuroscience* 159, 1374.

Ikonomovic, M.D., Uryu, K., Abrahamson, E.E., Ciallella, J.R., Trojanowski, J.Q., Lee, V.M.Y., Clark, R.S., Marion, D.W., Wisniewski, S.R., DeKosky, S.T. (2004) Alzheimer's pathology in human temporal cortex surgically excised after severe brain injury. *Exp. Neurol.* 190, 192.

Inglese, M., Makani, S., Johnson, G., Cohen, B.A., Silver, J.A., Gonen, O., Grossman, R.I. (2005) Diffuse axonal injury in mild traumatic brain injury: a diffusion tensor imaging study. *J. Neurosurg.* 103, 298.

Iwata, A., Chen, X.-H., McIntosh, T.K., Browne, K.D., Smith, D.H. (2002) Long-term accumulation of amyloid-beta in axons following brain trauma without persistent upregulation of amyloid precursor protein genes. *J. Neuropathol. Exp. Neurol.* 61, 1056.

Johnson, N.A., Jahng, G.-H., Weiner, M.W., Miller, B.L., Chui, H.C., Jagust, W.J., Gorno-Tempini, M.L., Schuff, N. (2005) Pattern of cerebral hypoperfusion in Alzheimer disease and mild cognitive impairment measured with arterial spin-labeling MR imaging: initial experience. *Radiology* 234, 851.

Johnson, V.E., Stewart, W., Smith, D.H. (2010) Traumatic brain injury and amyloid-beta pathology: a link to Alzheimer's disease? *Nat. Rev. Neurosci.* 11, 361.

Jortner, B.S. (2006) The return of the dark neuron. A histological artifact complicating contemporary neurotoxicologic evaluation. *Neurotoxicology* 27, 628.

Kamal, A., Almenar-Queralt, A., LeBlanc, J.F., Roberts, E.A., Goldstein, L.S. (2001) Kinesin-mediated axonal transport of a membrane compartment containing beta-secretase and presenilin-1 requires APP. *Nature* 414, 643.

Kennedy, K.M., Raz, N. (2009) Aging white matter and cognition: Differential effects of regional variations in diffusion properties on memory, executive functions, and speed. *Neuropsychologia* 47, 916.

Kitaguchi, H., Tomimoto, H., Ihara, M., Shibata, M., Uemura, K., Kalaria, R.N., Kihara, T., Asada-Utsugi, M., Kinoshita, A., Takahashi, R. (2009) Chronic cerebral hypoperfusion accelerates amyloid beta deposition in APPSwInd transgenic mice. *Brain Res.* 1294, 202.

Kodl, C.T., Seaquist, E.R. (2008) Cognitive dysfunction and diabetes mellitus. *Endocr. Rev.* 29, 494.

Kraus, M.F., Susmaras, T., Caughlin, B.P., Walker, C.J., Sweeney, J.A., Little, D.M. (2007) White matter integrity and cognition in chronic traumatic brain injury: a diffusion tensor imaging study. *Brain* 130, 2508.

Kurumatani, T., Kudo, T., Ikura, Y., Takeda, M. (1998) White matter changes in the gerbil brain under chronic cerebral hypoperfusion. *Stroke* 29, 1058.

LaFerla, F.M., Green, K.N., Oddo, S. (2007) Intracellular amyloid-β in Alzheimer's disease. *Nat. Rev. Neurosci.* 8, 499.

Laurer, H.L., Bareyre, F.M., Lee, V.M.Y.C., Trojanowski, J.Q., Longhi, L., Hoover, R., Saatman, K.E., Raghupathi, R., Hoshino, S., Grady, M.S., McIntosh, T.K. (2001) Mild head injury increasing the brain's vulnerability to a second concussive impact. *J. Neurosurg.* 95, 859.

Lewen, A., Li, G.L., Nilsson, P., Olsson, Y., Hillered, L. (1995) Traumatic brain injury in rat produces changes of beta-amyloid precursor protein immunoreactivity. *Neuroreport* 6, 357.

Li, S., Kuroiwa, T., Ishibashi, S., Sun, L., Endo, S., Ohno, K. (2006) Transient cognitive deficits are associated with the reversible accumulation of amyloid precursor protein after mild traumatic brain injury. *Neurosci. Lett.* 409, 182.

Li, Y., Liu, L., Barger, S.W., Griffin, W.S.T. (2003) Interleukin-1 mediates pathological effects of microglia on tau phosphorylation and on synaptophysin synthesis in cortical neurons through a p38-MAPK pathway. *J. Neurosci.* 23, 1605.

Lifshitz, J. (2008) Fluid percussion injury. In: Animal Models of Acute Neurological Injuries (Chen J, Xu X-M, Xu ZC, Zhang JH, eds), pp 369. Totowa, NJ: Humana Press.

Lin, C.-H., Lee, C.-C., Gean, P.-W. (2003) Involvement of a calcineurin cascade in amygdala depotentiation and quenching of fear memory. *Mol. Pharmacol.* 63, 44.

Lipton, M.L., Gellella, E., Lo, C., Gold, T., Ardekani, B.A., Shifteh, K., Bello, J.A., Branch, C.A. (2008) Multifocal white matter ultrastructural abnormalities in mild traumatic brain injury with cognitive disability: a voxel-wise analysis of diffusion tensor imaging. *J. Neurotrauma* 25, 1335.

Loane, D.J., Pocivavsek, A., Moussa, C.E.H., Thompson, R., Matsuoka, Y., Faden, A.I., Rebeck, G.W., Burns, M.P. (2009) Amyloid precursor protein secretases as therapeutic targets for traumatic brain injury. *Nat. Med. 15, 377.*

Lobnig, B.M., Krömeke, O., Optenhostert-Porst, C., Wolf, O.T. (2006) Hippocampal volume and cognitive performance in long-standing Type 1 diabetic patients without macrovascular complications. *Diabet. Med.* 23, 32.

Long, J.B., Bentley, T.L., Wessner, K.A., Cerone, C., Sweeney, S., Bauman, R.A. (2009) Blast overpressure in rats: recreating a battlefield injury in the laboratory. *J. Neurotrauma* 26, 827.

Lyeth, B.G., Gong, Q.Z., Shields, S., Muizelaar, J.P., Berman, R.F. (2001) Group I metabotropic glutamate antagonist reduces acute neuronal degeneration and behavioral deficits after traumatic brain injury in rats. *Exp. Neurol.* 169, 191.

Maas, A.I.R., Stocchetti, N., Bullock, R. (2008) Moderate and severe traumatic brain injury in adults. *Lancet Neurol.* 7, 728.

Marklund, N., Blennow, K., Zetterberg, H., Ronne-Engstrom, E., Enblad, P., Hillered, L. (2009) Monitoring of brain interstitial total tau and beta amyloid proteins by microdialysis in patients with traumatic brain injury. *J. Neurosurg*. 110, 1227

Marmarou, A., Foda, M.A., van Den Brink, W., Campbell, J., Kita, H., Demetriadou, K. (1994) A new model of diffuse brain injury in rats. Part I: Pathophysiology and biomechanics. *J. Neurosurg.*80, 291.

Martin, N.A., Patwardhan, R.V., Alexander, M.J., Africk, C.Z., Lee, J.H., Shalmon, E., Hovda, D.A., Becker, D.P. (1997) Characterization of cerebral hemodynamic phases following severe head trauma: hypoperfusion, hyperemia, and vasospasm. *J. Neurosurg.* 87, 9.

Martinez-Coria, H., Green, K.N., Billings, L.M., Kitazawa, M., Albrecht, M., Rammes, G., Parsons, C.G., Gupta, S., Banerjee, P., LaFerla, F.M. Memantine improves cognition and reduces Alzheimer's-like neuropathology in transgenic mice. *Am. J. Pathol.* 176, 870.

Masel, B.S., Dewitt, D. (2010) Traumatic brain injury: A disease process, not an event. *J. Neurotrauma* 27, 1529.

Matser, E.J., Kessels, A.G., Lezak, M.D., Jordan, B.D., Troost, J. (1999) Neuropsychological impairment in amateur soccer players. *JAMA* 282, 971.

Mayevsky, A., Breuer, Z. (1992) Brain vasculature and mitochondrial responses to ischemia in gerbils. I. Basic anatomical patterns and biochemical correlates. *Brain Res.* 598, 242.

McGowan, E., Eriksen, J., Hutton, M. (2006) A decade of modelling Alzheimer's disease in transgenic mice. *Trend. Genet.* 22, 281.

McIntosh, T.K., Vink, R., Noble, L., Yamakami, I., Fernyak, S., Soares, H., Faden, A.L. (1989) Traumatic brain injury in the rat - characterization of a lateral fluid-percussion model. *Neuroscience* 28, 233.

McKenzie, K.J., McLellan, D.R., Gentleman, S.M., Maxwell, W.L., Gennarelli, T.A., Graham, D.I. (1996) Is β-APP a marker of axonal damage in short-surviving head injury? *Acta Neuropathol.* 92, 608.

Messé, A., Caplain, S., Paradot, G., Garrigue, D., Mineo, J.F., Soto Ares, G., Ducreux, D., Vignaud, F., Rozec, G., Desal, H., Pélégrini-Issac, M., Montreuil, M., Benali, H., Lehéricy, S. (In press) Diffusion tensor imaging and white matter lesions at the subacute stage in mild traumatic brain injury with persistent neurobehavioral impairment. *Hum. Brain Mapp.*

Meunier, M., Destrade, C. (1988) Electrolytic but not ibotenic acid lesions of the posterior cingulate cortex produce transitory facilitation of learning in mice. *Behav. Brain Res.* 27, 161.

Meythaler, J.M., Peduzzi, J.D., Eleftheriou, E., Novack, T.A. (2001) Current concepts: diffuse axonal injury-associated traumatic brain injury. *Arch. Phys. Med. Rehab.* 82, 1461.

Miki, K., Ishibashi, S., Sun, L., Xu, H., Ohashi, W., Kuroiwa, T., Mizusawa, H. (2008) Intensity of chronic cerebral hypoperfusion determines white/gray matter injury and cognitive/motor dysfunction in mice. *J. Neurosci. Res.* 87, 1270.

Morales, D.M., Marklund, N., Lebold, D., Thompson, H.J., Pitkanen, A., Maxwell, W.L., Longhi, L., Laurer, H., Maegele, M., Neugebauer, E., Graham, D.I., Stocchetti, N., McIntosh, T.K. (2005) Experimental models of traumatic brain injury: Do we really need to build a better mousetrap? *Neuroscience* 136, 971.

Morganti-Kossmann, M.C., Satgunaseelan, L., Bye, N., Kossmann, T. (2007) Modulation of immune response by head injury. *Injury* 38, 1392.

Morris, R.G. (2001) Episodic-like memory in animals: psychological criteria, neural mechanisms and the value of episodic-like tasks to investigate animal models of neurodegenerative disease. *Philos. Trans. R. Soc. Lond. B Biol. Sci.* 356, 1453.

Murakami, Y., Ikenoya, M., Matsumoto, K., Li, H., Watanabe, H. (2000) Ameliorative effect of tacrine on spatial memory deficit in chronic two-vessel occluded rats is reversible and mediated by muscarinic M1 receptor stimulation. *Behav. Brain Res.* 109, 83.

Muresan, V., Muresan, Z. (2009) Is abnormal axonal transport a cause, a contributing factor or a consequence of the neuronal pathology in Alzheimer's disease? *Fut. Neurol.* 4, 761.

Nakagawa, Y., Reed, L., Nakamura, M., McIntosh, T.K., Smith, D.H., Saatman, K.E., Raghupathi, R., Clemens, J., Saido, T.C., Lee, V.M.Y., Trojanowski, J.Q. (2000) Brain trauma in aged transgenic mice induces regression of established Aβ deposits. *Exp. Neurol.* 163, 244.

Nakamura, S., Tamaoka, A., Sawamura, N., Kiatipattanasakul, W., Nakayama, H., Shoji, S., Yoshikawa, Y., Doi, K. (1997) Deposition of amyloid β protein (Aβ) subtypes [Aβ40 and Aβ42(43)] in canine senile plaques and cerebral amyloid angiopathy. *Acta Neuopathol*. 94, 323.

Nave, K.-A. (2010) Myelination and the trophic support of long axons. *Nat. Rev. Neurosci.* 11, 275.

Nelson, T.J., Alkon, D.L. (2007) Protection against β-amyloid-induced apoptosis by peptides interacting with β-amyloid. *J. Biol. Chem.* 282, 31238.

Nilsson, O.G., Shapiro, M.L., Gage, F.H., Olton, D.S., Björklund, A., Nilsson, O.G. (1987) Spatial learning and memory following fimbria-fornix transection and grafting of fetal septal neurons to the hippocampus. *Exp. Brain Res.* 67, 195.

Niogi, S.N., Mukherjee, P., Ghajar, J., Johnson, C., Kolster, R.A., Sarkar, R., Lee, H., Meeker, M., Zimmerman, R.D., Manley, G.T., McCandliss, B.D. (2008) Extent of microstructural white matter injury in postconcussive syndrome correlates with impaired cognitive reaction time: A 3T diffusion tensor imaging study of mild traumatic brain injury. *Am. J. Neuroradiol.* 29, 967.

Nishio, K., Ihara, M., Yamasaki, N., Kalaria, R.N., Maki, T., Fujita, Y., Ito, H., Oishi, N., Fukuyama, H., Miyakawa, T., Takahashi, R., Tomimoto, H. (2010) A mouse model characterizing features of vascular dementia with hippocampal atrophy. *Stroke* 41, 1278.

Niwa, K., Kazama, K., Younkin, S.G., Carlson, G.A., Iadecola, C. (2002) Alterations in cerebral blood flow and glucose utilization in mice overexpressing the amyloid precursor protein. *Neurobiol. Dis.* 9, 61.

O'Sullivan, M., Jones, D.K., Summers, P.E., Morris, R.G., Williams, S.C.R., Markus, H.S. (2001) Evidence for cortical "disconnection" as a mechanism of age-related cognitive decline. *Neurology* 57, 632.

Oddo, S., Caccamo, A., Kitazawa, M., Tseng, B.P., LaFerla, F.M. (2003) Amyloid deposition precedes tangle formation in a triple transgenic model of Alzheimer's disease. *Neurobiol. Aging* 24, 1063.

Ohtaki, H., Fujimoto, T., Sato, T., Kishimoto, K., Fujimoto, M., Moriya, M., Shioda, S. (2006) Progressive expression of vascular endothelial growth factor (VEGF) and angiogenesis after chronic ischemic hypoperfusion in rat. *Acta Neurochir. Suppl.* 96, 283.

Olton, D.S., Samuelson, R.J. (1976) Remembrance of places passed: Spatial memory in rats. *J. Exp. Psychol. Anim. Behav. Process* 2, 97.

Overgaard, J., Tweed, W.A. (1983) Cerebral circulation after head injury. Part 4: Functional anatomy and boundary-zone flow deprivation in the first week of traumatic coma. *J. Neurosurg.* 59, 439.

Pantoni, L., Garcia, J.H. (1997) Pathogenesis of leukoaraiosis: a review. *Stroke* 28, 652.

Pappas, B.A., de la Torre, J.C., Davidson, C.M., Keyes, M.T., Fortin, T. (1996) Chronic reduction of cerebral blood flow in the adult rat: late-emerging CA1 cell loss and memory dysfunction. *Brain Res.* 708, 50.

Paspalas, C.D., Papadopoulos, G.C. (1998) Ultrastructural evidence for combined action of noradrenaline and vasoactive intestinal polypeptide upon neurons, astrocytes, and blood vessels of the rat cerebral cortex. *Brain Res. Bull.* 45, 247.

Peru, R.L., Mandrycky, N., Nait-Oumesmar, B., Lu, Q.R. (2008) Paving the axonal highway: from stem cells to myelin repair. *Stem Cell Rev.* 4, 304.

Pettus, E.H., Povlishock, J.T. (1996) Characterization of a distinct set of intra-axonal ultrastructural changes associated with traumatically induced alteration in axolemmal permeability. *Brain Res.* 722, 1.

Pierce, J.E., Smith, D.H., Trojanowski, J.Q., McIntosh, T.K. (1998) Enduring cognitive, neurobehavioral and histopathological changes persist for up to one year following severe experimental brain injury in rats. *Neuroscience* 87, 359.

Pigino, G., Morfini, G., Atagi, Y., Deshpande, A., Yu, C., Jungbauer, L., LaDu, M., Busciglio, J., Brady, S. (2009) Disruption of fast axonal transport is a pathogenic mechanism for intraneuronal amyloid beta. *Proc. Nat. Acad. Sci.* 106, 5907.

Pitsikas, N., Biagini, L., Algeri, S. (1991) Previous experience facilitates preservation of spatial memory in the senescent rat. *Physiol. Behav.* 49, 823.

Plassman, B.L., Havlik, R.J., Steffens, D.C., Helms, M.J., Newman, T.N., Drosdick, D., Phillips, C., Gau, B.A., Welsh-Bohmer, K.A., Burke, J.R., Guralnik, J.M., Breitner, J.C. (2000) Documented head injury in early adulthood and risk of Alzheimer's disease and other dementias. *Neurology* 55, 1158.

Porcel, J., Montalban, X. (2006) Anticholinesterasics in the treatment of cognitive impairment in multiple sclerosis. *J. Neurol. Sci.* 245, 177.

Pugliese, M., Mascort, J., Mahy N., Ferrer, I. (2006) Diffuse beta-amyloid plaques and hyperphosphorylated tau are unrelated processes in aged dogs with behavioral deficits. *Acta Neuropathol.* 112, 175

Quarles, R.H. (2009) A hypothesis about the relationship of myelin-associated glycoprotein's function in myelinated axons to its capacity to inhibit neurite outgrowth. *Neurochem. Res.* 34, 79.

Reeves, T.M., Phillips, L.L., Povlishock, J.T. (2005) Myelinated and unmyelinated axons of the corpus callosum differ in vulnerability and functional recovery following traumatic brain injury. *Exp. Neurol.* 196, 126.

Reeves, T.M., Phillips, L.L., Lee, N.N., Povlishock, J.T. (2007) Preferential neuroprotective effect of tacrolimus (FK506) on unmyelinated axons following traumatic brain injury. *Brain Res.* 1154, 225.

Rhein, V., Song, X., Wiesner, A., Ittner, L.M., Baysang, G., Meier, F., Ozmen, L., Bluethmann, H., Dröse, S., Brandt, U., Savaskan, E., Czech, C., Götz, J., Eckert, A.

(2009) Amyloid-β and tau synergistically impair the oxidative phosphorylation system in triple transgenic Alzheimer's disease mice. *Proc. Nat. Acad. Sci.* 106, 20057.

Roberson, E.D., Mucke, L. (2006) 100 years and counting: prospects for defeating Alzheimer's disease. *Science* 314, 781.

Roberts, G. W., Gentleman, S.M., Lynch, A., Murray, L., Landon, M., Graham, D.I. (1994) Beta amyloid protein deposition in the brain after severe head injury: implications for the pathogenesis of Alzheimer's disease. *J. Neurol. Neurosurg. Psychiat.* 57, 419.

Ross, D.T., Meaney, D.F., Sabol, M.K., Smith, D.H., Gennarelli, T.A. (1994) Distribution of forebrain diffuse axonal injury following inertial closed head injury in miniature swine. *Exp. Neurol.* 126, 291.

Ruitenberg, A., den Heijer, T., Bakker, S.L., van Swieten, J.C., Koudstaal, P.J., Hofman, A., Breteler, M.M. (2005) Cerebral hypoperfusion and clinical onset of dementia: The Rotterdam Study. *Ann. Neurol.* 57, 789.

Salat, D.H., Tuch, D.S., van der Kouwe, A.J., Greve, D.N., Pappu, V., Lee, S.Y., Hevelone, N.D., Zaleta, A.K., Growdon, J.H., Corkin, S., Fischl, B., Rosas, H.D. (2010) White matter pathology isolates the hippocampal formation in Alzheimer's disease. *Neurobiol. Aging* 31, 244.

Sani. S., Traul, D., Klink, A., Niaraki, N., Gonzalo-Ruiz, A., Wu, C.K., Geula, C. (2003) Distribution, progression and chemical composition of cortical amyloid-beta deposits in aged rhesus monkeys: similarities to the human. *Acta Neuropathol.* 105, 145.

Saper, C., B. (1984) Organization of cerebral cortical afferent systems in the rat. II. Magnocellular basal nucleus. *J. Comp. Neurol.* 222, 313.

Savage, L.M., Sweet, A.J., Castillo, R., Langlais, P.J., Savage, L.M. (1997) The effects of lesions to thalamic lateral internal medullary lamina and posterior nuclei on learning, memory and habituation in the rat. *Behav. Brain Res.* 82, 133.

Saxena, S., Caroni, P. (2007) Mechanisms of axon degeneration: from development to disease. *Prog. Neurobiol.* 83, 174.

Schmidt, M.L., Zhukareva, V., Newell, K.L., Lee, V.M., Trojanowski, J.Q. (2001) Tau isoform profile and phosphorylation state in dementia pugilistica recapitulate Alzheimer's disease. *Acta Neuropathol.* 101, 518.

Schmithorst, V.J., Wilke, M., Dardzinski, B.J., Holland, S.K., Schmithorst, V.J. (2005) Cognitive functions correlate with white matter architecture in a normal pediatric population: a diffusion tensor MRI study. *Hum. Brain Mapp.* 26, 139.

Schmitz, T., Chew, L.J. (2008) Cytokines and myelination in the central nervous system. *ScientificWorldJournal* 8, 1119.

Schmued, L.C., Stowers, C.C., Scallet, A.C., Xu, L. (2005) Fluoro-Jade C results in ultra high resolution and contrast labeling of degenerating neurons. *Brain Res.* 1035, 24.

Selkoe, D.J. (1991) The molecular pathology of Alzheimer's disease. *Neuron* 6, 487.

Shah, P., Lal, N., Leung, E., Traul, D.E., Gonzalo-Ruiz, A., Geula, C. (2010) Neuronal and axonal loss are selectively linked to fibrillar amyloid-b within plaques of the aged primate cerebral cortex. *Am. J. Pathol.* 177, 325.

Shaw, C., Aggleton, J.P., Shaw, C. (1993) The effects of fornix and medial prefrontal lesions on delayed non-matching-to-sample by rats. *Behav. Brain Res.* 54, 91.

Shibata, M., Ohtani, R., Ihara, M., Tomimoto, H. (2004) White matter lesions and glial activation in a novel mouse model of chronic cerebral hypoperfusion. *Stroke* 35, 2598.

Shibata, M., Yamasaki, N., Miyakawa, T., Kalaria, R.N., Fujita, Y., Ohtani, R., Ihara, M., Takahashi, R., Tomimoto, H. (2007) Selective impairment of working memory in a mouse model of chronic cerebral hypoperfusion. *Stroke* 38, 2826.

Simons, K., Toomre, D. (2000) Lipid rafts and signal transduction. *Nat. Rev. Mol. Cell Biol.* 1, 31.

Smith, C., Graham, D.I., Murray, L.S., Nicoll, J.A.R. (2003a) Tau immunohistochemistry in acute brain injury. *Neuropathol. Appl. Neurobiol.* 29, 496.

Smith, D.H., Chen, X.-H., Xu, B.N., McIntosh, T.K., Gennarelli, T.A., Meaney, D.F. (1997) Characterization of diffuse axonal pathology and selective hippocampal damage following inertial brain trauma in the pig. *J. Neuropathol. Exp. Neurol.* 56, 822.

Smith, D.H., Soares, H.D., Pierce, J.S., Perlman, K.G., Saatman, K.E., Meaney, D.F., Dixon, C.E., McIntosh, T.K. (1995) A model of parasagittal controlled cortical impact in the mouse: cognitive and histopathologic effects. *J. Neurotrauma* 12, 169.

Smith, D.H., Nakamura, M., McIntosh, T.K., Wang, J., Rodriguez, A., Chen, X.-H., Raghupathi, R., Saatman, K.E., Clemens, J., Schmidt, M.L., Lee, V.M.Y., Trojanowski, J.Q. (1998) Brain trauma induces massive hippocampal neuron death linked to a surge in β-amyloid levels in mice overexpressing mutant amyloid precursor protein. *Am. J. Pathol.* 153, 1005.

Smith, D.H., Chen, X.-H., Iwata, A., Graham, D.I. (2003b) Amyloid beta accumulation in axons after traumatic brain injury in humans. *J. Neurosurg.* 98, 1072.

Smith, D.M., Mizumori, S.J. (2006) Hippocampal place cells, context, and episodic memory. *Hippocampus* 16, 716.

Song, S.-K., Sun, S.-W., Ju, W.-K., Lin, S.-J., Cross, A.H., Neufeld, A.H. (2003) Diffusion tensor imaging detects and differentiates axon and myelin degeneration in mouse optic nerve after retinal ischemia. *NeuroImage* 20, 1714.

Sterr, A., Herron, K.A., Hayward, C., Montaldi, D. (2006) Are mild head injuries as mild as we think? Neurobehavioral concomitants of chronic post-concussion syndrome. *BMC Neurol.* 6, 7.

Stokin, G.B., Lillo, C., Falzone, T.L., Brusch, R.G., Rockenstein, E., Mount, S.L., Raman, R., Davies, P., Masliah, E., Williams, D.S., Goldstein, L.S. (2005) Axonopathy and transport deficits early in the pathogenesis of Alzheimer's disease. *Science* 307, 1282.

Stoquart-ElSankari, S., Balédent, O., Gondry-Jouet, C., Makki, M., Godefroy, O., Meyer, M.-E. (2007) Aging effects on cerebral blood and cerebrospinal fluid flows. *J. Cereb. Blood Flow Metab.* 27, 1563.

Stys, P.K. (1998) Anoxic and ischemic injury of myelinated axons in CNS white matter: from mechanistic concepts to therapeutics. *J. Cereb. Blood Flow Metab.* 18, 2.

Sullivan, H.G., Martinez, J., Becker, D.P., Miller, J.D., Griffith, R., Wist, A.O. (1976) Fluid-percussion model of mechanical brain injury in the cat. *J. Neurosurg.* 45, 521.

Szczygielski, J., Mautes, A., Steudel, W.I., Falkai, P., Bayer, T.A., Wirths, O. (2005) Traumatic brain injury: cause or risk of Alzheimer's disease? A review of experimental studies. *J. Neural Transm.* 112, 1547.

Tanaka, H., Ma, J., Tanaka, K.F., Takao, K., Komada, M., Tanda, K., Suzuki, A., Ishibashi, T., Baba, H., Isa, T., Shigemoto, R., Ono, K., Miyakawa, T., Ikenaka, K. (2009) Mice with altered myelin proteolipid protein gene expression display cognitive deficits accompanied by abnormal neuron-glia interactions and decreased conduction velocities. *J. Neurosci.* 29, 8363.

Tang, Y.P., Noda, Y., Hasegawa, T., Nabeshima, T. (1997a) A concussive-like brain injury model in mice (I): impairment in learning and memory. *J. Neurotrauma* 14, 851.

Tang, Y.P., Noda, Y., Hasegawa, T., Nabeshima, T. (1997b) A concussive-like brain injury model in mice (II): selective neuronal loss in the cortex and hippocampus. *J. Neurotrauma* 14, 863.

Targosz-Gajniak, M., Siuda, J., Ochudło, S., Opala, G., Targosz-Gajniak, M. (2009) Cerebral white matter lesions in patients with dementia - from MCI to severe Alzheimer's disease. *J. Neurol. Sci.* 283, 79.

Taylor, D.R., Hooper, N.M. (2007) Role of lipid rafts in the processing of the pathogenic prion and Alzheimer's amyloid-beta proteins. *Sem. Cell Dev. Biol.* 18, 638.

Teasdale, G., Jennett, B. (1974) Assessment of coma and impaired consciousness. A practical scale. *Lancet* 2, 81.

Teigler, A., Komljenovic, D., Draguhn, A., Gorgas, K., Just, W.W. (2009) Defects in myelination, paranode organization and Purkinje cell innervation in the ether lipid-deficient mouse cerebellum. *Hum. Mol. Genet.* 18, 1897.

Thal, D.R., Griffin, W.S.T., de Vos, R.A.I., Ghebremedhin, E. (2008) Cerebral amyloid angiopathy and its relationship to Alzheimer's disease. *Acta Neuropathol.* 115, 599.

Tiehuis, A.M., Vincken, K.L., van den Berg, E., Hendrikse, J., Manschot, S.M., Mali, W.P., Kappelle, L.J., Biessels, G.J. (2008) Cerebral perfusion in relation to cognitive function and type 2 diabetes. *Diabetologica* 51, 1321.

Tomic, J.L., Pensalfini, A., Head, E., Glabe, C.G. (2009) Soluble fibrillar oligomer levels are elevated in Alzheimer's disease brain and correlate with cognitive dysfunction. *Neurobiol. Dis.* 35; 352

Turner, P.R., O'Connor, K., Tate, W.P., Abraham, W.C. (2003) Roles of amyloid precursor protein and its fragments in regulating neural activity, plasticity and memory. *Prog. Neurobiol.* 70, 1.

Uno, H., Alsum, P.B., Dong, S., Richardson, R., Zimbric, M.L., Thieme, C.S., Houser, W.D. (1996) Cerebral amyloid angiopathy and plaques, and visceral amyloidosis in aged macaques. *Neurobiol. Aging* 17, 275.

Uryu, K., Laurer, H., McIntosh, T., Pratico, D., Martinez, D., Leight, S., Lee, V.M.Y., Trojanowski, J.Q. (2002) Repetitive mild brain trauma accelerates A beta deposition, lipid peroxidation, and cognitive impairment in a transgenic mouse model of Alzheimer amyloidosis. *J. Neurosci.* 22, 446.

Vernooij, M.W., Ikram, M.A., Vrooman, H.A., Wielopolski, P.A., Krestin, G.P., Hofman, A., Niessen, W.J., Van der Lugt, A., Breteler, M.M. (2009) White matter microstructural integrity and cognitive function in a general elderly population. *Arch. Gen. Psychiat.* 66, 545.

Vernooij, M.W., van der Lugt, A., Ikram, M.A., Wielopolski, P.A., Vrooman, H.A., Hofman, A., Krestin, G.P., Breteler, M.M. (2008) Total cerebral blood flow and total

brain perfusion in the general population: The Rotterdam Scan Study. *J. Cereb. Blood Flow Metab.* 28, 412.

Vicens, P., Redolat, R., Carrasco, M.C. (2002) Effects of early spatial training on water maze performance: a longitudinal study in mice. *Exp. Gerontol.* 37, 575.

Wakita, H., Tomimoto, H., Akiguchi, I., Matsuo, A., Lin, J.-X., Ihara, M., McGeer, P.-L. (2002) Axonal damage and demyelination in the white matter after chronic cerebral hypoperfusion in the rat. *Brain Res.* 924, 63.

Wang, J.-Z., Liu, F. (2008) Microtubule-associated protein tau in development, degeneration and protection of neurons. *Prog. Neurobiol.* 85, 148.

Wang, M.S., Davis, A.A., Culver, D.G., Wang, Q., Powers, J.C., Glass, J.D. (2004) Calpain inhibition protects against Taxol-induced sensory neuropathy. *Brain* 127, 671.

Warburton, E.C., Aggleton, J.P. (1999) Differential deficits in the Morris water maze following cytotoxic lesions of the anterior thalamus and fornix transection. *Behav. Brain Res.* 98, 27.

Warburton, E.C., Baird, A., Morgan, A., Muir, J.L., Aggleton, J.P. (2001) The conjoint importance of the hippocampus and anterior thalamic nuclei for allocentric spatial learning: evidence from a disconnection study in the rat. *J. Neurosci.* 21, 7323.

Wenk, G.L. (2003) Neuropathologic changes in Alzheimer's disease. *J. Clin. Psychiat.* 64 Suppl 9, 7.

Werner, C., Engelhard, K. (2007) Pathophysiology of traumatic brain injury. *Br. J. Anaesth.* 99, 4.

Wiig, K.A., Bilkey, D.K., Wiig, K.A. (1995) Lesions of rat perirhinal cortex exacerbate the memory deficit observed following damage to the fimbria-fornix. *Behav. Neurosci.* 109, 620.

Wilcock, D.M., Lewis, M.R., Van Nostrand, W.E., Davis, J., Previti, M.L., Gharkholonarehe, N., Vitek, M.P., Colton, C.A. (2008) Progression of amyloid pathology to Alzheimer's disease pathology in an amyloid precursor protein transgenic mouse model by removal of nitric oxide synthase 2. *J. Neurosci.* 28, 1537.

Willer, B., Leddy, J.J. (2006) Management of concussion and post-concussion syndrome. *Curr. Treat. Options Neurol.* 8, 415.

Wirths, O., Weis, J., Kayed, R., Saido, T.C., Bayer, T.A. (2007) Age-dependent axonal degeneration in an Alzheimer mouse model. *Neurobiol. Aging* 28, 1689.

Wood, E.R., Dudchenko, P.A., Eichenbaum, H. (1999) The global record of memory in hippocampal neuronal activity. *Nature* 397, 613.

Xu, H., Yang, H.J., Zhang, Y., Clough, R., Browning, R., Li, X.M. (2009) Behavioral and neurobiological changes in C57BL/6 mice exposed to cuprizone. *Behav. Neurosci.* 123, 418.

Yamakami, I., McIntosh, T.K. (1989) Effects of traumatic brain injury on regional cerebral blood flow in rats as measured with radiolabeled microspheres. *J. Cereb. Blood Flow Metab* 9, 117.

Yamakami, I., McIntosh, T.K. (1991) Alterations in regional cerebral blood flow following brain injury in the rat. *J. Cereb. Blood Flow Metab.* 11, 655.

Yamazaki, Y., Hozumi, Y., Kaneko, K., Sugihara, T., Fujii, S., Goto, K., Kato, H. (2007) Modulatory effects of oligodendrocytes on the conduction velocity of action potentials along axons in the alveus of the rat hippocampal CA1 region. *Neuron Glia Biology* 3, 325.

Yoshiyama, Y., Uryu, K., Higuchi, M., Longhi, L., Hoover, R., Fujimoto, S., McIntosh, T., Lee, V.M.Y., Trojanowski, J.Q. (2005) Enhanced neurofibrillary tangle formation, cerebral Atrophy, and cognitive deficits Induced by repetitive mild brain injury in a transgenic tauopathy mouse model. *J. Neurotrauma* 22, 1134.

Zempel, H., Thies, E., Mandelkow, E., Mandelkow, E.-M. (2010) Aβ oligomers cause localized $Ca^{2+}$ elevation, missorting of endogenous tau into dendrites, tau phosphorylation, and destruction of microtubules and spines. *J. Neurosci.* 30, 11938.

Zhiyou, C., Yong, Y., Shanquan, S., Jun, Z., Liangguo, H., Ling, Y., Jieying, L. (2009) Upregulation of BACE1 and β-amyloid protein mediated by chronic cerebral hypoperfusion contributes to cognitive impairment and pathogenesis of Alzheimer's disease. *Neurochem. Res.* 34, 1226

Zohar, O., Schreiber, S., Getslev, V., Schwartz, J.P., Mullins, P.G., Pick, C.G. (2003) Closed-head minimal traumatic brain injury produces long-term cognitive deficits in mice. *Neuroscience* 118, 949.

# Appendix A Additional behaviour and pathology results following mild fluid percussion injury in wild-type mice

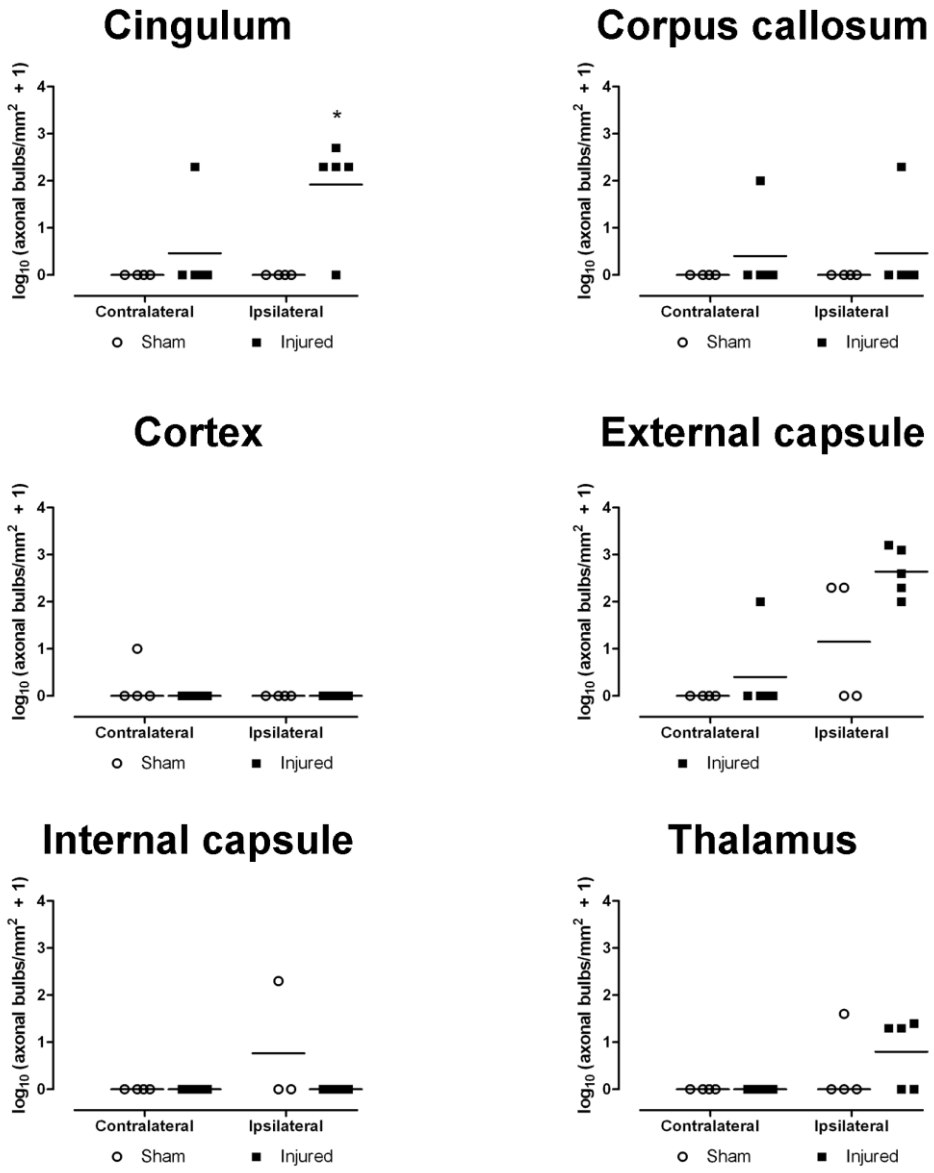


**A.1: Axonal damage 4 hours after mild TBI**

Analysis of APP staining at 4 hours after mild TBI. Injured animals showed significantly more axonal bulbs in the ipsilateral cingulum than controls. * = $p < 0.05$ vs sham. Line shows mean value.

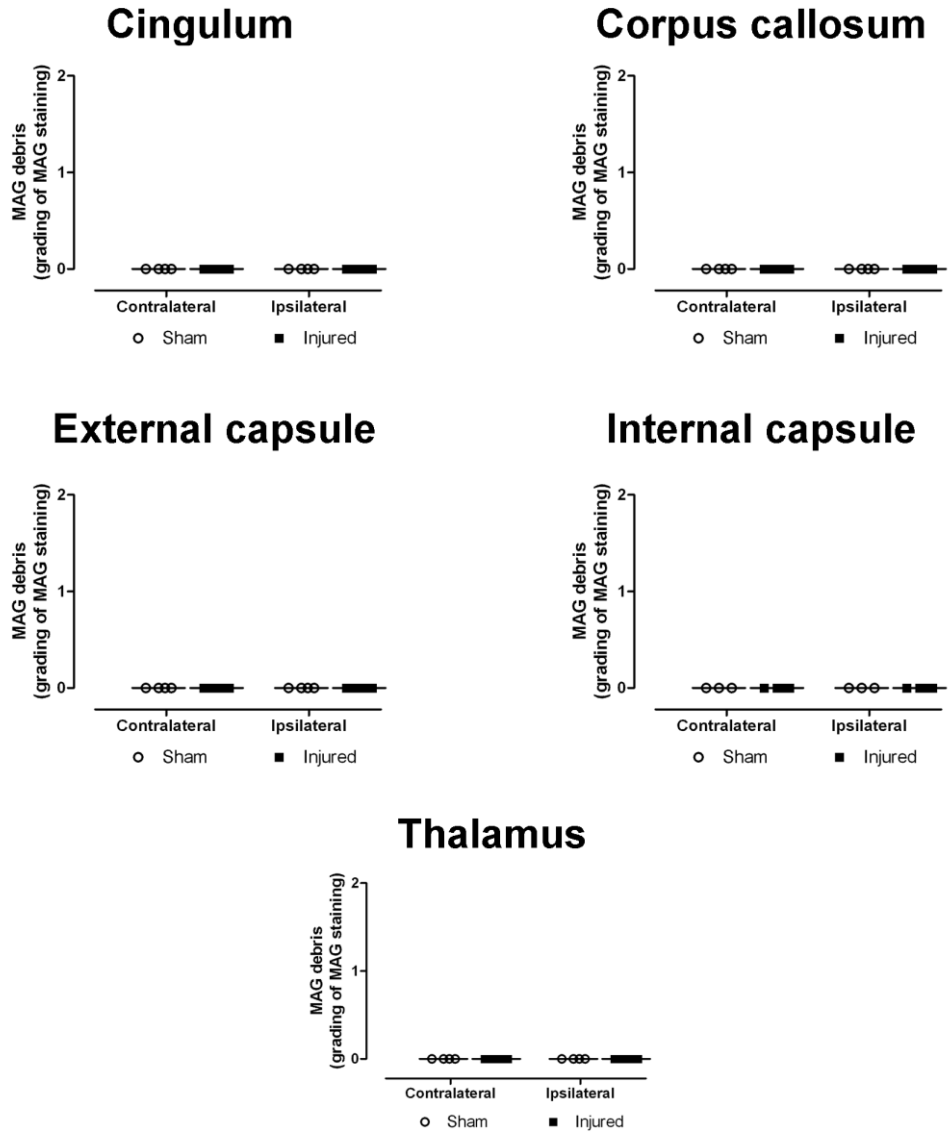


**A.2: Myelin debris 4 hours after mild TBI**

Analysis of MAG staining 4 hours after mild TBI. There were no differences between the groups in grading of MAG debris. Line shows median value.

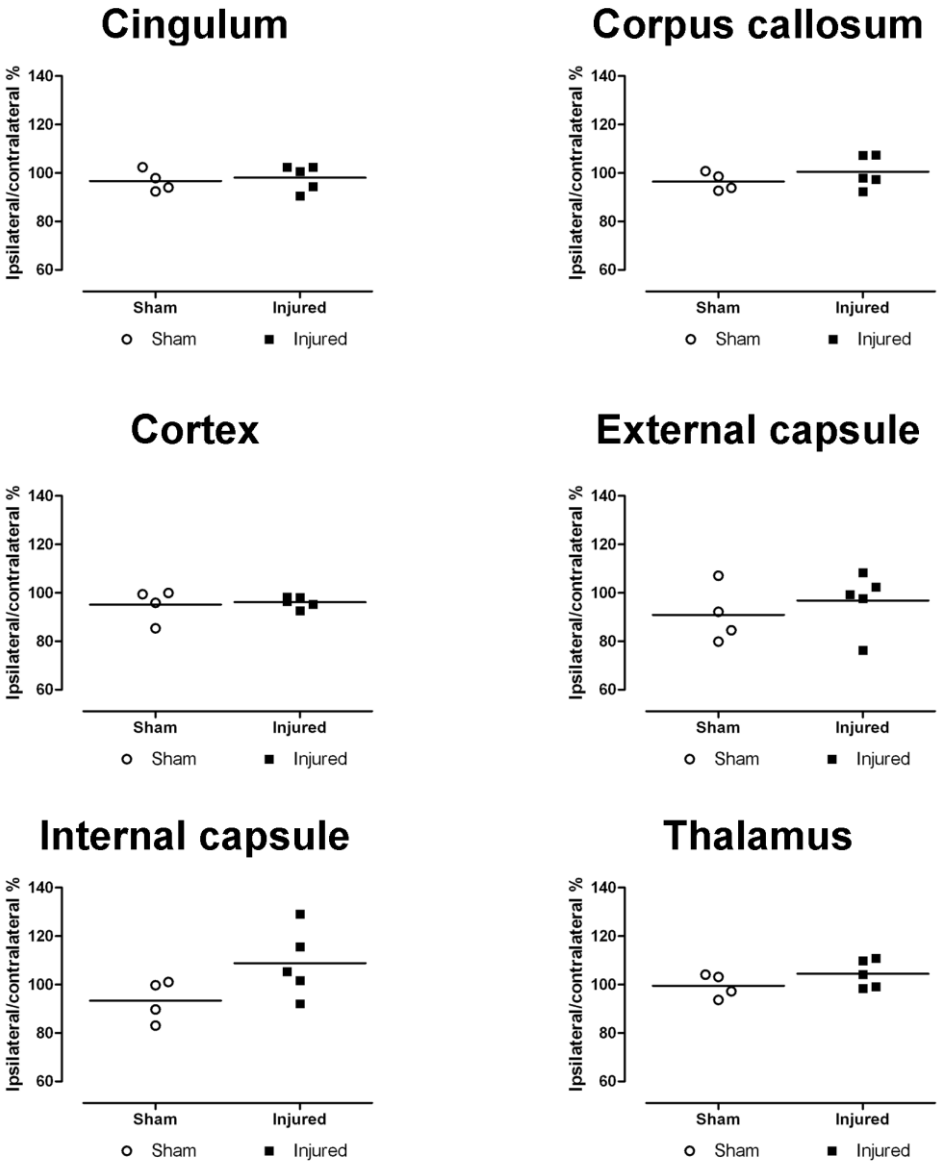


**A.3: Myelin integrity 4 hours after mild TBI**

Analysis of MBP staining at 4 hours after mild TBI. There were no differences between the groups in relative optical density of MBP staining. Line shows mean value.

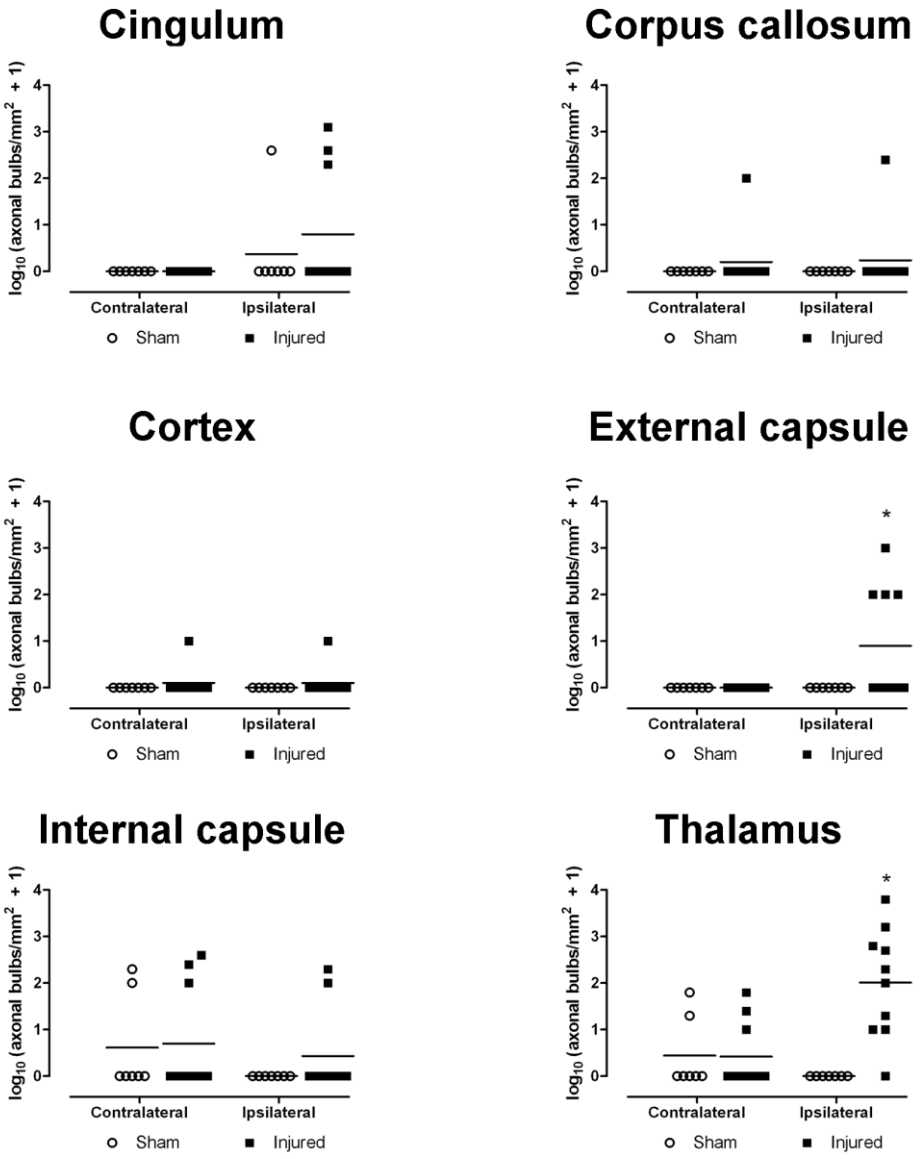


**A.4: Axonal damage 6 weeks after mild TBI**

Analysis of APP staining at 6 weeks after mild TBI. Injured animals showed significantly more axonal bulbs in the ipsilateral external capsule and thalamus than controls. * = $p < 0.05$ vs sham. Line shows mean value.

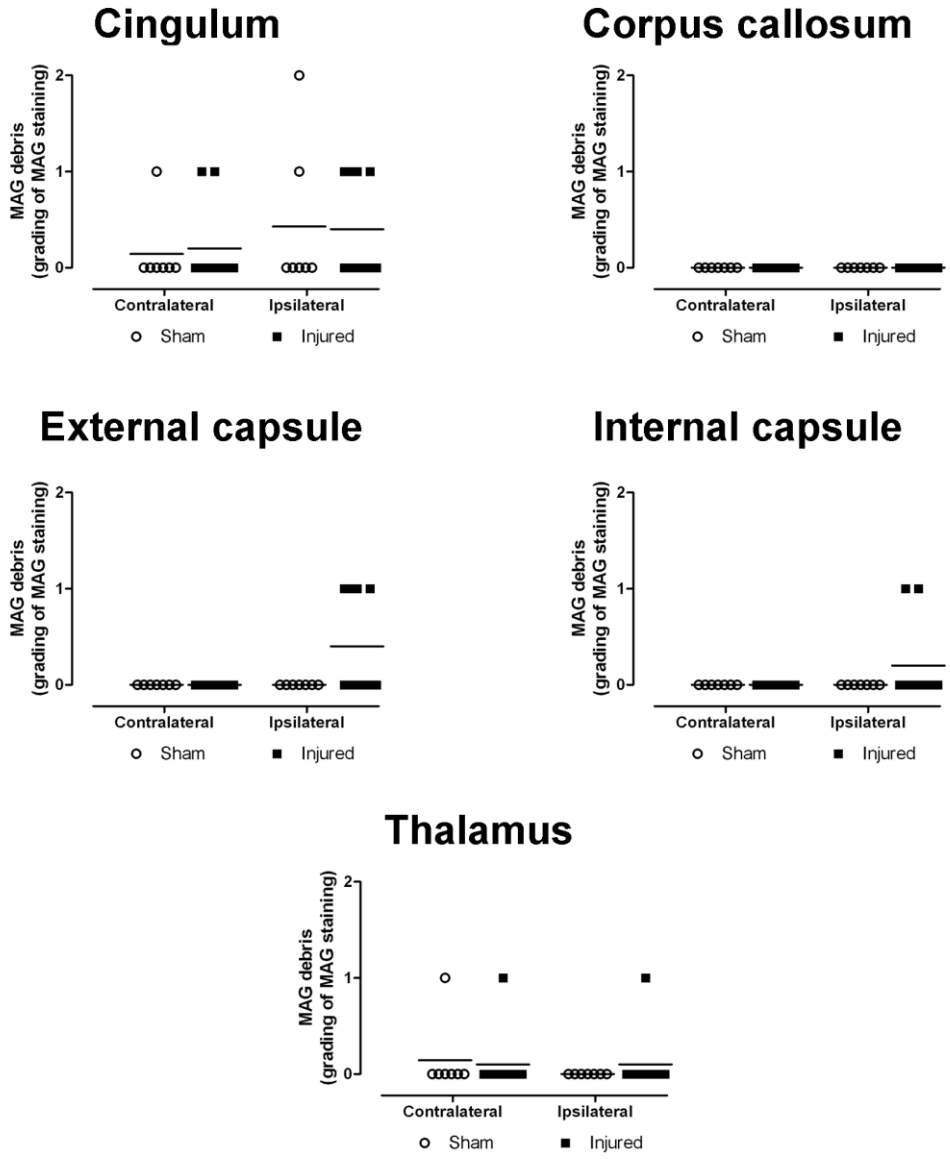


**A.5: Myelin debris 6 weeks after mild TBI**

Analysis of MAG staining at 6 weeks after mild TBI. There were no differences between the groups in grading of MAG debris. Line shows median value.

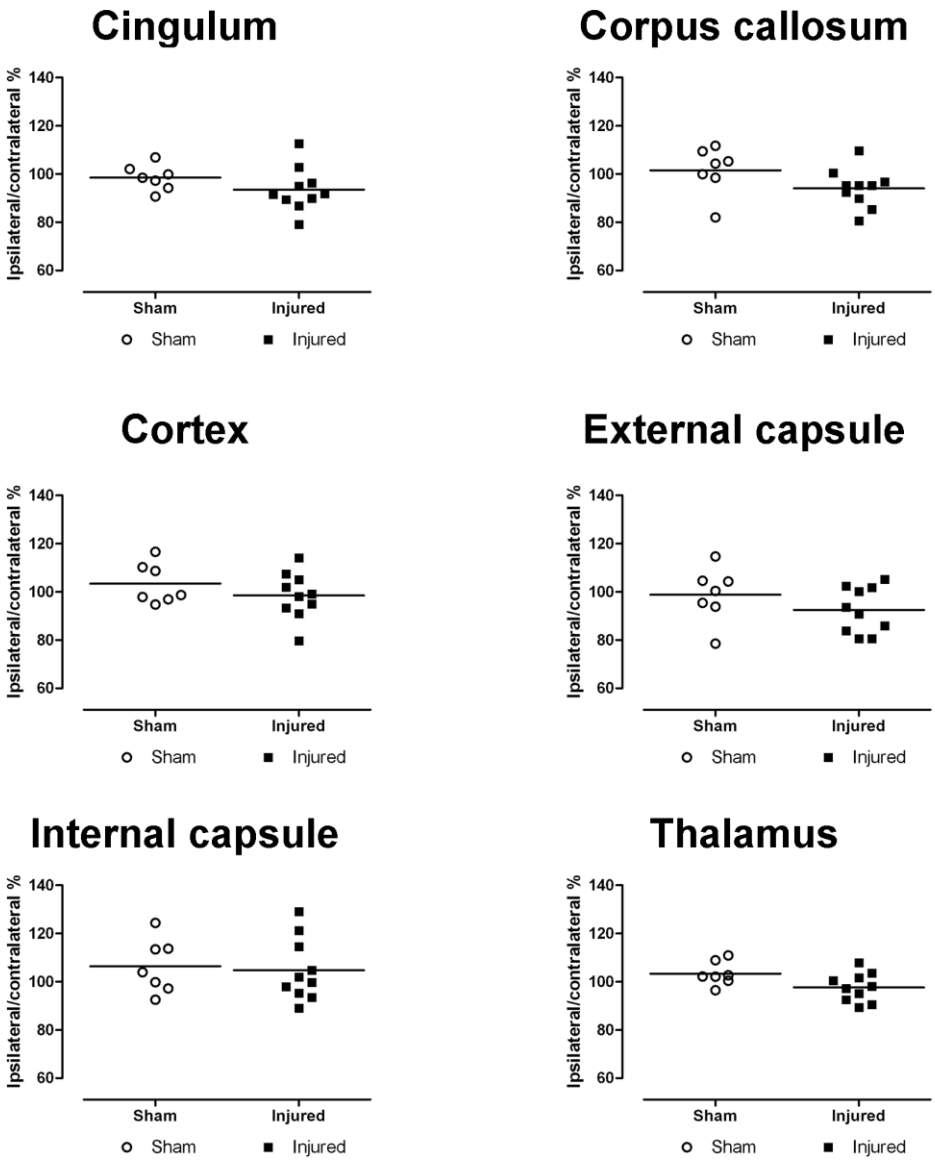


**A.6: Myelin integrity 6 weeks after mild TBI**

Analysis of MBP staining at 6 weeks after mild TBI. There were no differences between the groups in relative optical density of MBP staining. Line shows mean value.

| | | 4 hours | | 24 hours | | 72 hours | | 4 weeks | | 6 weeks | |
|---|---|---|---|---|---|---|---|---|---|---|---|
| | | *Sham* | *Injured* | *Sham* | *Injured* | *Sham* | *Injured* | *Sham* | *Injured* | *Sham* | *Injured* |
| **Haematoxilyn and eosin** | | | | | | | | | | | |
| Cortex | | | | | | | | | | | |
| | *Ipsilateral* | 2/4 | 4/5 | 3/4 | 4/5 | 2/3 | 1/4 | 0/5 | 1/5 | 0/7 | 0/10 |
| | *Contralateral* | 0/4 | 0/5 | 1/4 | 0/5 | 0/3 | 0/4 | 0/5 | 0/5 | 0/7 | 0/10 |
| Hippocampus | | | | | | | | | | | |
| | *Ipsilateral* | 1/4 | 1/5 | 1/4 | 0/5 | 1/3 | 0/4 | 0/5 | 0/5 | 0/7 | 3/10 |
| | *Contralateral* | 0/4 | 0/5 | 1/4 | 0/5 | 0/3 | 0/4 | 0/5 | 0/5 | 0/7 | 0/10 |
| Thalamus | | | | | | | | | | | |
| | *Ipsilateral* | 0/4 | 0/5 | 0/4 | 0/5 | 0/3 | 0/4 | 0/5 | 0/5 | 0/7 | 0/10 |
| | *Contralateral* | 0/4 | 0/5 | 0/4 | 0/5 | 0/3 | 0/4 | 0/5 | 0/5 | 0/7 | 0/10 |
| **Fluoro-jade C** | | | | | | | | | | | |
| Cortex | | | | | | | | | | | |
| | *Ipsilateral* | 1/4 | 0/5 | 4/4 | 3/5 | 2/3 | 2/4 | 1/5 | 2/5 | 0/7 | 1/10 |
| | *Contralateral* | 0/4 | 0/5 | 0/4 | 0/5 | 0/3 | 1/4 | 0/5 | 0/5 | 0/7 | 0/10 |
| Hippocampus | | | | | | | | | | | |
| | *Ipsilateral* | 0/4 | 0/5 | 0/4 | 0/5 | 0/3 | 0/4 | 0/5 | 0/5 | 0/7 | 0/10 |
| | *Contralateral* | 0/4 | 0/5 | 0/4 | 0/5 | 0/3 | 0/4 | 0/5 | 0/5 | 0/7 | 0/10 |
| Thalamus | | | | | | | | | | | |
| | *Ipsilateral* | 0/4 | 0/5 | 0/4 | 0/5 | 0/3 | 0/4 | 0/5 | 0/5 | 0/7 | 0/10 |
| | *Contralateral* | 0/4 | 0/5 | 0/4 | 0/5 | 0/3 | 0/4 | 0/5 | 0/5 | 0/7 | 0/10 |

### A.7: Cell death following mild TBI using H&E and FJC staining

Numbers of animals showing damaged neurons at each time point measured after injury using H&E and FJC staining. Cell death was observed in regions close to the craniotomy site in both sham and injured animals and was most prominent in the hours after injury. Data are expressed as number of animals showing damaged neurons/number of animals in the group.

# Appendix B Additional pathology results following mild fluid percussion injury in a transgenic model of Alzheimer's disease

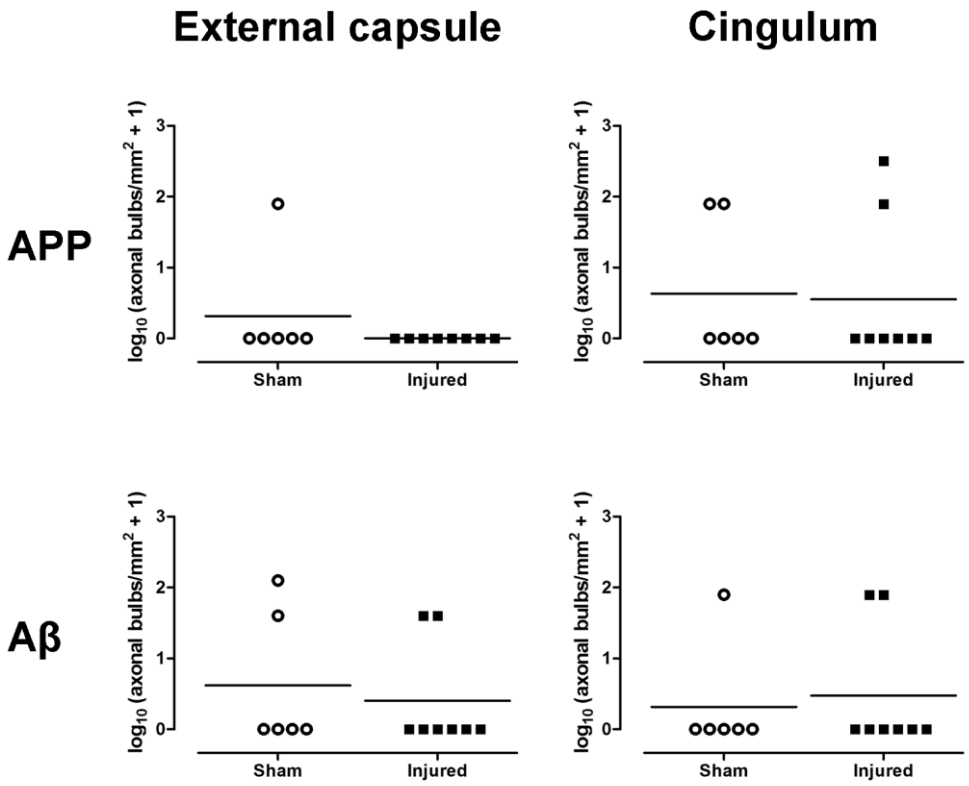


**B.1: No significant accumulation of APP or Aβ in the contralateral external capsule and cingulum 24 hours after mild TBI** Accumulation of APP and Aβ in the contralateral external capsule and cingulum at 24 hours after injury was minimal and did not differ between injured and sham groups. Line represents the mean value

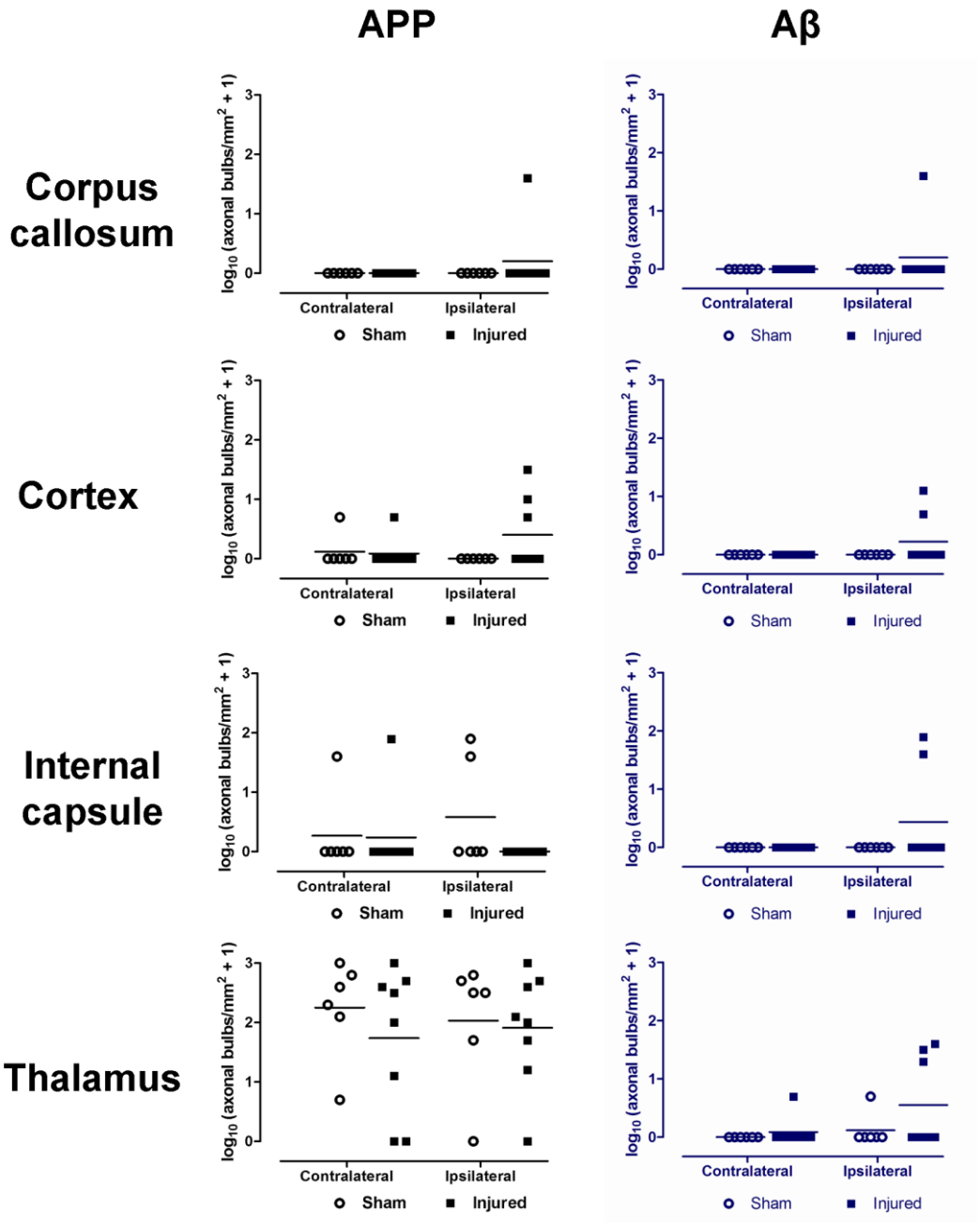


**B.2: Regions where APP and Aβ accumulations are unaffected by mild TBI**

APP and Aβ accumulations were unaltered 24 hours after mild FPI in the corpus callosum, cortex, internal capsule and thalamus bilaterally. Line represents the mean value

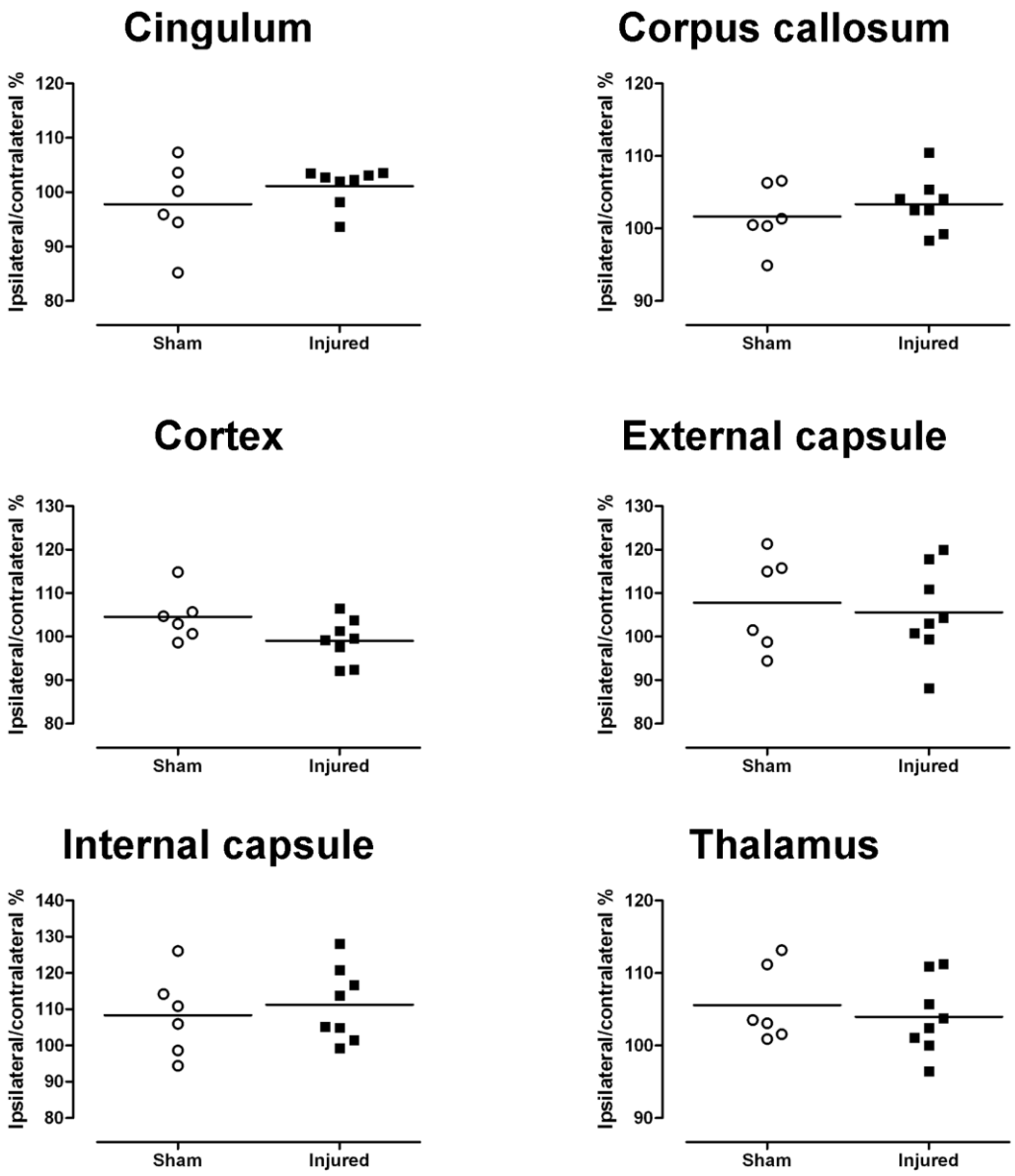


**B.3: No effect of mild TBI on relative optical density of MBP staining at 24 hours after injury**

There was no difference between injured and sham animals in density of MBP staining in any region examined 24 hours after mild FPI. Values are expressed as relative optical density of the ipsilateral hemisphere normalised to the contralateral hemisphere. Line represents the mean value.

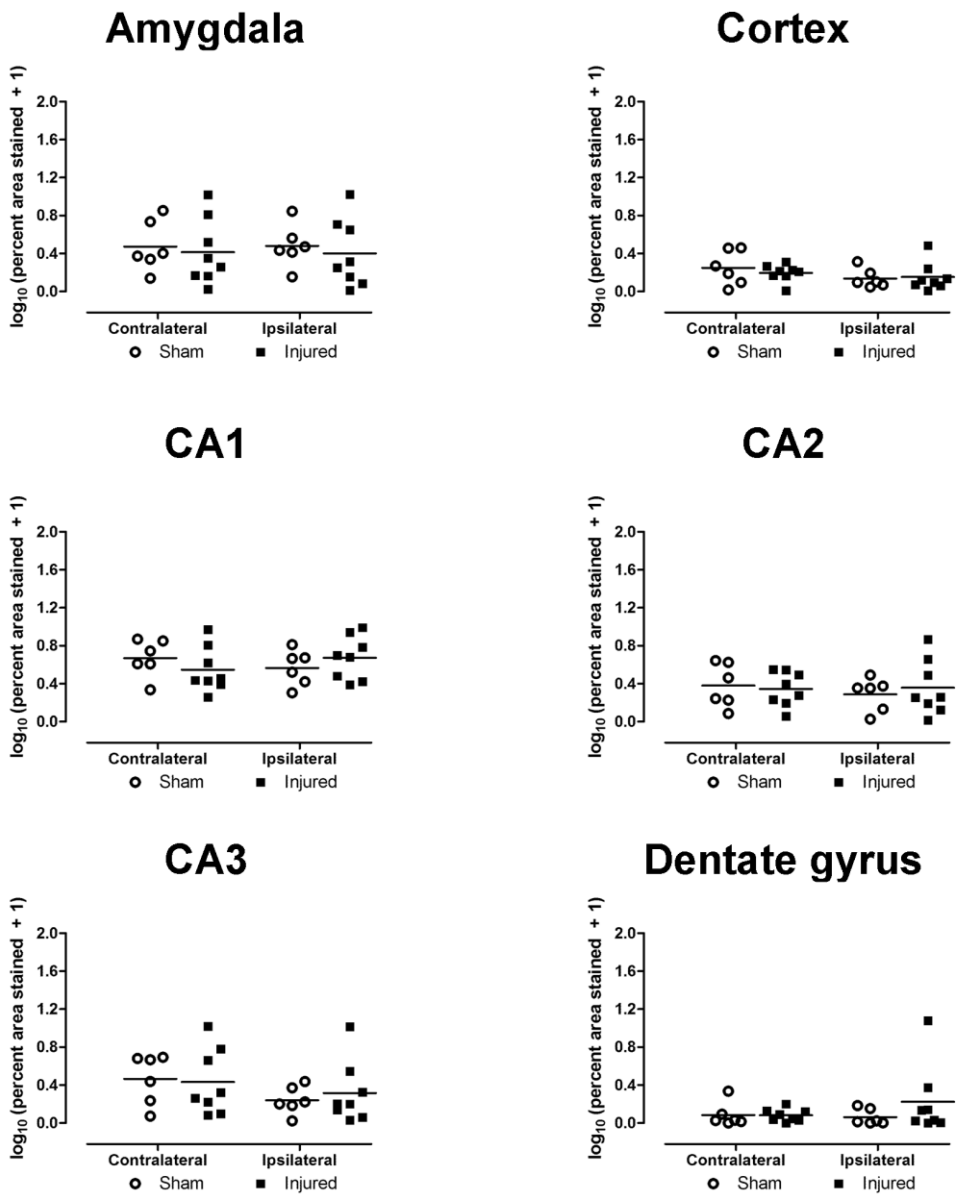


**B.4: Intracellular Aβ is unaffected by mild TBI at 24 hours after injury** Injured and sham animals showed the same levels of Aβ staining intracellularly in any regions examined at 24 hours after injury. Line represents the mean value.

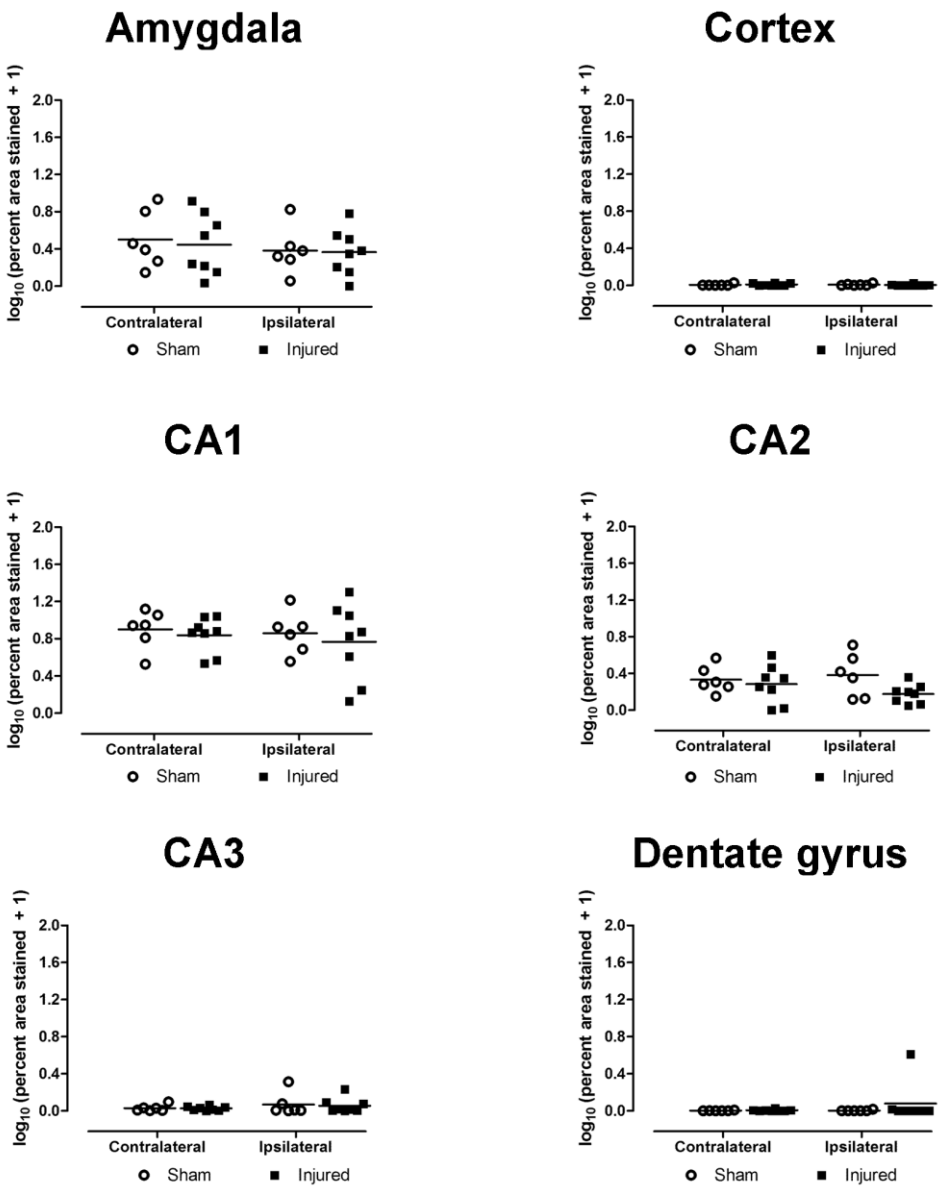


**B.5: Intracellular levels of normal tau are unaffected at 24 hours after mild TBI**

Injured animals showed the same level of staining for normal tau in all regions examined as sham animals. Line represents the mean value

# Appendix C Publications

## Papers

Spain A, Daumas S, Lifshitz J, Rhodes J, Andrews PJ, Horsburgh K and Fowler JH. (2010). Mild fluid percussion injury in mice produces evolving selective axonal pathology and cognitive deficits relevant to human brain injury. *J. Neurotrauma*. 27, 1429.

Coltman R*, Spain A*, Tsenkina Y*, Fowler JH, Smith J, Scullion G, Allerhand M, Scott F, Kalaria RN, Ihara M, Daumas S, Deary IJ, Wood E, McCulloch J, Horsburgh K. (In press). Selective white matter pathology induces a specific impairment in spatial working memory. *Neurobiol. Aging.* (* Joint first authors).

## Abstracts

Spain A, Daumas S, Lifshitz J, Rhodes J, Andrews PJ, Horsburgh K and Fowler JH. (2010). Selective axonal damage and short-term spatial reference memory deficits after mild fluid percussion injury in mice. *International Conference on Alzheimer's Disease*

Coltman R, Spain A, Tsenkina Y, Smith J, Fowler JH, Ihara M, Kalaria RN, Daumas S, Kelly P, Deary IJ, Wood E, McCulloch J, Horsburgh K. (2010). Chronic cerebral hypoperfusion causes myelin damage and is associated with a selective impairment in working memory. *International Conference on Alzheimer's Disease*

Spain A, Daumas S, Lifshitz J, Rhodes J, Andrews PJ, Horsburgh K and Fowler JH. (2009). A model of traumatic brain injury in mice demonstrating evolving axonal pathology and spatial learning and memory deficits. *6th Annual Scottish Neuroscience Group Meeting*

Spain A, Horsburgh K, Daumas S, Lifshitz J, Andrews PJ, Rhodes J, Fowler JH. (2008). Axonal damage and cognitive deficits after fluid percussion injury in mice. *5th Annual Scottish Neuroscience Group Meeting*